TECHNISCHE UNIVERSITÄT MÜNCHEN

Lehrstuhl für Entwicklungsgenetik

Establishment of mouse disease models by using sequence specific nucleases

Sudeepta Kumar Panda

Vollständiger Abdruck der von der Fakultät Wissenschaftszentrum Weihenste-phan für Ernährung, Landnutzung und Umwelt der Technischen Universität München zur Erlangung des akademischen Grades eines

Doktors der Naturwissenschaften

genehmigten Dissertation

Vorsitzender: Univ.-Prof. Dr.rer.nat. Erwin Grill

Prüfer der Dissertation:

1 Univ.-Prof. Dr.rer.nat. Wolfgang Wurst

2 Univ.- Prof. Dr. Kay Heinrich Schneitz

Die Dissertation wurde am 07.04.2014 bei der Technischen Universität München eingereicht und durch die Fakultät Wissenschaftszentrum Weihenstephan für Ernährung, Landnutzung und Umwelt am 14.08.2014 angenommen.

Erklärung

Ich erkläre hiermit an Eides statt, dass ich die vorliegende Arbeit ohne unzulässige Hilfe Dritter und ohne Benutzung anderer als der angegebenen Hilfsmittel angefertigt habe. Die aus anderen Quellen direkt oder indirekt übernommenen Daten und Konzepte sind unter Angabe des Literaturzitates gekennzeichnet.

कर्मण्येवाधिकारस्ते मा फलेषु कदाचन।
मा कर्मफलहेतुर्भूर्मा ते सङ्गोऽस्त्वकर्मणि॥२-४७॥

Source: Shreemad Bhagavad Gita, Chapter 2, Verse 47

Translation:

English: Your right is only to perform your duty, but never to its results. Let not the results be your motive, nor you be indolent

German: Ihr Recht ist nur Ihre Pflicht zu erfüllen, aber nie, um der Ergebnisse willen. Lassen Sie nicht die Ergebnisse Ihr Motivation sein, noch seien sie arbeitsscheu

Dedicated
To my Beloved
Parents

Acknowledgment

I also thank all other members of the IDG for the friendly working atmosphere, the helpfulness, and the steady support, which have made the work here at the Institute so pleasant.

Life in Germany would not have been as much fun if without my best buddies, Rajesh Rathore and Ayush Pranshu. Special thanks go to them for being greatest help whenever I need help and cheering me up during the tough times. Their perpetual welcoming hands and the willingness to share the knowledge on social, computer and software skills have made my life a lot easier. I would also like to thank all of my friends: Vinaya, Rahul, Nasir, Anil, Vidya, Sailesh, Nitu, Krish, and Subhamoy for their help and support. Their existence has brought much laughter during my PhD life.

I would deeply grateful to my funding organisation, Indian Council of Agricultural Research (ICAR) for financial support throughout my PhD work, without which this thesis work would not have been possible.

Finally, outside of scientific community, family members: Supriya, Lily (sister-in-law), Sangram, Ranjan (brother), and especially my parents are undoubtedly the greatest pillars of support. Their financial support to start my PhD has made me 5,000 miles away from home, but their unconditional loves and affections have made this distance non-existence. None of my achievements would have been possible without sacrifices and unconditional support of my parents. They have always believed in me and supported my choices, however unconventional they were to them. I thank them for dedicating their lives to see me succeed. I would also like to thank my fiancée Shree for being there for me always.

In the end, I solemnly bow my head to the lotus feet of Bhagwan Sri Sathya Sai Baba; without Swami's grace and divine guidance, I would not be where I am today.

Contents

1 Abstract

1.1 Abstract

Genetic engineered mice serve as indispensable tool for understanding gene function in development and disease. Because conventional gene targeting, which relies on embryonic stem (ES) cells for the generation of chimeric mice, is a time-consuming, labor-intensive, and expensive procedure, I tested transcription activator-like effector nucleases (TALENs) or the CRISPR/Cas system for mutagenesis of the mouse genome directly in one-cell embryos. Here I report a routine method for the efficient generation of mouse disease models by microinjection of TALENs or Cas9 mRNAs by adding a plasmid-coded poly(A) tail (TALEN-95A or Cas9-95/166A), circumventing the *in vitro* polyadenylation step. Within two days of pronuclear microinjection, TALEN-95A mRNAs induced sequence deletions in the *C9orf72* gene in 41% of pups, as a model for frontotemporal lobar degeneration. Co-injection of TALEN-95A together with mutagenic oligodeoxynucleotides (ODNs), patient-derived amyotrophic lateral sclerosis missense mutations were introduced into the fused in sarcoma (*Fus*) gene at the rate of 6.8%. Efficient germline transmission was achieved, as the F_0 mutants transmitted the disease alleles to their F_1 progeny. In response to oxidative stress, cells expressing the *Fus* mutants exhibited perinuclear stress granule formation, which is a pathological hallmark of amyotrophic lateral sclerosis (ALS). Similarly, pronuclear injection of Cas9/sgRNA with or without oligodeoxynucleotides in one-cell embryos was efficient to generate knockin or knockout mutations in the *Rab 38* or *Fus* gene with an efficiency of 14 or 12%, respectively. In addition, using sgRNAs targeting two distinct sites in *Fus*, I could generate mice harbouring a deletion of 2.6 kb in both alleles within a seven weeks. Taken together, these results demonstrate that TALENs and/or CRISPR/Cas represent highly efficient and versatile genome editing tools, enabling the accelerated production of new disease models for studying genetic disease mechanisms and interventions.

1.2 Zusammenfassung

Genetisch veränderte Mäuse gelten als unverzichtbare Werkzeuge um die Rolle von Genen in der Entstehung und Entwicklung von Krankheiten nachvollziehen zu können. Das herkömmliche Gen-Targeting, welches auf der Erzeugung von chimären Mäusen durch embryonale Stammzellen beruht, stellt allerdings eine zeitraubende, arbeitsintensive und kostspielige Prozedur dar. Aus diesem Grund habe ich als Alternativen für die gezielte Mutagenese im Mausgenom die Verwendung von TALENs (transcription activator-like effector nucleases) und des CRISPR/CAS-Systems direkt in Ein-Zell-Embryonen getestet. Im Rahmen dieser Arbeit beschreibe ich eine Routinemethode für die effiziente Erzeugung von Krankheitsmodellen mittels Mikroinjektion von TALENs oder Cas9 mRNAs durch die Verwendung eines plasmidkodierten Poly(A)-Schwanzes (TALEN-95A oder Cas9-95/166A), wodurch der *in vitro*-Polyadenylierungsschritt umgangen werden kann. Die Mikroinjektion von TALEN-95A mRNA in den Pronukleus induzierte in 41% der Nachkommen Sequenzdeletionen im *C9orf72*-Gen, welche als Modell für die frontotemporale Lobärdegeneration dienen kann. Durch die gemeinsame Injektion von TALEN-95A mRNA und mutagenen Oligodesoxynukleotiden (ODNs) wurden mit einer Rate von 6,8% Mismatchmutationen in das *Fus* (fused in sarcoma)-Gen eingeführt, welche auch in Patienten mit amyotropher Lateralsklerose (ALS) beobachtet wurden. Die erfolgreiche Keimbahntransmission der Krankheitsallele wurde durch die Übertragung der Allele von den F_0-Mutanten an die F_1-Nachkommen gezeigt. Zellen, welche die *Fus*-Krankheitsmutationen tragen, reagieren auf oxidativen Stress mit der Bildung von perinukleären Stressgranula, was ein pathologisches Merkmal der ALS darstellt. Auf ähnliche Weise konnten durch die pronukleäre Injektion von Cas9/sgRNA mit oder ohne Oligodesoxynukleotiden in Ein-Zell-Embryonen effizient Knockin- bzw. Knockout-Mutationen in das *Rab38*-Gen (mit einer Rate von 14%) bzw. in das *Fus*-Gen (mit einer Rate von 12%) eingebracht werden. Darüber hinaus konnte ich innerhalb von sieben Wochen durch die Verwendung von zwei sgRNAs, welche unterschiedliche Bindestellen im *Fus*-Gen besitzen, mutante Mäuse mit einer 2,6 kb-Deletion in beiden Allelen erzeugen. Zusammenfassend zeigen diese Ergebnisse, dass sowohl TALENS als auch das CRISPR/Cas-System als hocheffiziente und vielseitige Genom-Editing-Tools einsetzbar sind, was eine schnellere Erzeugung von neuen Krankheitsmodellen für die Untersuchung genetischer Krankheitsmechanismen ermöglicht.

2 Introduction

Targeted gene modification is a powerful tool to analyse gene functions and disease mechanisms by generating animal models of human disease and to produce superior livestock having desired genetic traits. Conventional gene targeting through embryonic stem (ES) cells have been used extensively for generating mouse mutants by the process of homologous recombination that involves the steps of vector construction, chimaera production, and germline transmission. Nevertheless, ES cell-mediated gene targeting is an inefficient (10^{-6} to 10^{-5}), laborious, and time consuming process (Capecchi, 2005). Other known drawbacks of this method are the limited rate of germline transmission (Ledermann, 2000) and failure to culture truly functional ES cell in most species except for mice (Mishina and Sakimura, 2007), which greatly restricts the wide application of this approach. This barrier has been eventually overcome by the transfer of nuclei from cultured somatic cells, as an alternative for the engineering of livestock species, but remains a difficult task (McCreath et al., 2000). In contrast, it has been demonstrated that the introduction of double-strand breaks (DSBs) into chromosomal DNA can significantly stimulate homologous recombination (Rouet et al., 1994). In eukaryotic cells, DSBs are repaired by the two major pathways of non-homologous end joining (NHEJ) and homologous recombination (HR). NHEJ is the predominant repair pathway in mammalian cells, occurring in the G_0 (quiescent) and G_1 phase of the cell cycle, in which the open ends of the DSB are bound by Ku70/Ku80 heterodimers recruiting DNA-dependent protein kinase catalytic subunits (DNA-PKcs) and the XRCC4–DNA ligase IV complex. This type of repair frequently causes a spectrum of indel mutations resulting into knockout alleles (Calsou et al., 2003). In the presence of sister chromosomes or chromatids, DSBs can be repaired in the S and G2 phases of the cell cycle by the more rare homologous recombination process. Here 5´-3' end resection of DNA ends occurs by the MRE11-RAD50-NBS1 (MRN) complex, promoting homology directed repair (HDR) in conjunction with the ataxia telangiectasia mutated (ATM) and RAD51 proteins (Hashimoto et al., 2010), resulting into knockin alleles if a gene targeting vector is provided. To harness the stimulatory power of targeted DSBs, various types of site-specific nucleases were developed to widen the application of gene targeting in prokaryotes and eukaryotes.

2.1 Homing endonucleases

Homologous recombination could be significantly enhanced by several orders of magnitude by creating DSBs at specific genomic sites using the yeast-derived homing endonuclease I-SceI (Jasin, 1996; Rouet et al., 1994). Sce-I is a member of LAGLIDADG family of homing endonucleases that catalyze their own duplication into new loci by creating

site-specific DSBs at an 18 bp non-palindromic recognition sequence, initiating their transfer through homologous recombination. The stimulation of gene targeting by *SceI* has been shown in various mammalian cell lines including mouse ES cells, demonstrating that DSB-induced homologous recombination is a widespread, if not universal phenomenon (Choulika et al., 1995; Donoho et al., 1998; Sargent et al., 1997). Nevertheless, the use of I-SceI-mediated gene targeting in mammalian species are impeded by its specific recognition site that does not occur in the genome and by its complex protein-DNA interaction that prevents the simple reprogramming of this enzyme towards new target sites.

2.2 Zinc finger nucleases

The Cys_2-His_2 zinc finger domain represents the most common type of DNA-binding motifs found in eukaryotes. Each finger motif is composed of 30 amino acids, folding into a ßßα configuration coordinated by a Zn^{2+} ion and two pairs of cysteine and histidine residues. Several amino acids on the surface of the α-helix typically contact a sequence of 3 bp within the major groove of the DNA helix having a sequence motif of 5'-NGG-3' (Pavletich and Pabo, 1991). The combination of 3-6 zinc finger motifs can recognise target DNA sequences of 9-18 bp (Figure 1). The DNA binding domain of zinc finger proteins can be fused with the non-specific cleavage domain of the restriction endonuclease FokI (Fn domain) derived from *Flavobacterium okeanokoites* to create target specific zinc finger nucleases (ZFNs) (Bibikova et al., 2002; Chandrasegaran and Smith, 1999; Porteus and Carroll, 2005).

By placing two arrays of 3-6 zinc finger motifs at opposite DNA strands located on either side of an intervening 5-6 bp spacer sequence, two FokI nuclease domains dimerize and induce a DSB at the target sequence (Smith et al., 2000) (Figure 1). Several approaches were developed to engineer zinc finger proteins having optimised DNA binding specificities such as the modular assembly (Bhakta and Segal, 2010), the oligomerised pool engineering (OPEN) (Maeder et al., 2008), the context-dependent assembly (CODA) (Sander et al., 2011), and the optimised two finger archive (Gupta et al., 2012) protocol. Artificially designed ZFNs can be utilised to create loss-of-function or gain-of-function mutations at the target genomic location via exploiting the NHEJ or HR DNA repair pathway in the presence or absence of a gene targeting vector or single-stranded deoxyoligonucleotides. Indeed, ZFNs-mediated targeted mutagenesis was demonstrated in fruit flies (Bibikova et al., 2002), *C. elegans* (Morton et al., 2006), and cultured mammalian cells (Hockemeyer et al., 2009; Porteus and Carroll, 2005; Santiago et al., 2008) by induction and repair of DSBs
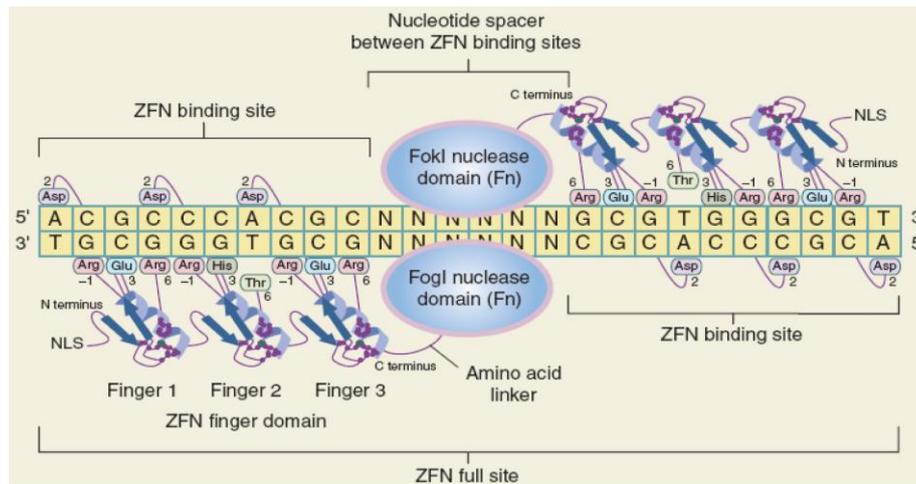
Figure 1: Structure of zinc finger nucleases. A ZFN array encompasses an N-terminal zinc finger DNA-binding domain, a variable peptide linker, and a C-terminal Fn domain. Each zinc finger unit binds to a DNA triplet having a 5´-NGG-3´ recognition sequence. Inverted positioning of individual zinc finger nuclease proteins allows FokI dimerization to induce a double-strand break witin the 5-6 bp spacer sequence. Adopted from Porteus and Carroll (2005).

Moreover, ZFNs were successfully applied in one-cell embryos to generate knockout and knockin mutations in the germline of zebrafish (Doyon et al., 2008; Meng et al., 2008), rat (Geurts et al., 2009; Mashimo et al., 2010; Cui et al., 2011), mouse (Carbery et al., 2010; Meyer et al., 2010, 2012), rabbit (Flisikowska et al., 2011), and pig (Lillico et al., 2013) by the expression of the ZFN protein in early zygotes. Despite the initial success in mutagenesis using ZFNs, the further expansion of zinc finger based applications are hindered by the lack of known fingers for various nucleotide triplets and the problematic context-dependent effects of individual fingers in the array.

2.3 Transcription activator-like effector nucleases

The recent discovery of transcription activator-like effector (TALE) proteins having DNA-binding capability (Boch et al., 2009; Moscou and Bogdanove, 2009) provides an alternative platform for engineering the mammalian genome. Unlike zinc fingers, TALE are naturally occurring proteins found in then plant pathogen *Xanthomonas*, which are injected and imported into the plant cell nucleus through the type-III secretory pathway, and targeted to the effector-specific gene promoter (Kay et al., 2007). Natural TALE proteins encompass central tandem repeats that mediate the DNA-binding specificity, which are flanked by N-terminal sequences required for the bacterial type-III secretion and C-terminal sequences encoding for nuclear localisation and transcriptional activation (Figure 2).
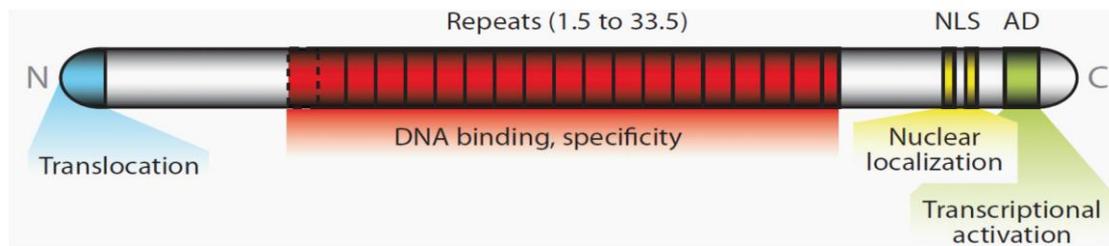
Figure 2: Natural TALE protein from *Xanthomonas*. The number of tandem repeats in TALE varies in between 1.5 to 33.5. The N-terminal region encodes the type-III translocation domain and the C-terminal region encodes the nuclear localisation sequences (NLS) and transcriptional activation domain (AD). Adopted from Boch and Bonas (2010).

The central repeat domain of most TALE proteins consists of 13 to 28 repeats (Boch and Bonas, 2010). Like zinc finger elements, each TALE repeat consists of highly conserved 33 to 35 amino acids (mostly 34 amino acids) except for the two hypervariable amino acids at position 12 and 13, known as repeat variable di-residues (RVDs) that mediate specific recognition of one base pair of the target DNA sequence (Boch et al., 2009). Although many RVDs are found in nature, the strongest RVD-base relationships are histidine/aspartic acid (HD), asparagine/glycine (NG), asparagine/isoleucine (NI), and asparagine/asparagine (NN) that recognise cytosine (C), thymine (T), adenine (A), and guanine (G) or adenine (A), respectively. This simple one to one relation between the RVDs of individual TALE repeats with individual nucleotides of the target sequence enables the easy construction of the new DNA-binding domains with unprecedented freedom (Moscou and Bogdanove, 2009). In addition to the nucleotide sequence specified by RVDs, naturally occurring TALE binding sites always start with a T nucleotide, which is a prerequisite for TALE activity (Boch et al., 2009). The individual repeats of TALE arrays form a left handed, two helix bundles that represent the RVDs containing loop to the specific nucleotide of target DNA sequence. The each TALE repeat self-associates to form a right-handed superhelix structure that wraps around the DNA helix. The 12th RVD residue forms a stabilizing contact within the protein backbone, whereas the 13th RVD residue makes a base-specific contact to the DNA sense strand by weak or strong van der Waals interaction (Deng et al., 2012a; Mak et al., 2012) (Figure 3). Following a specific target sequence, individual TALE repeats can be assembled in the appropriate order and fused with the FokI nuclease domain to function as sequence-specific TALE nucleases (TALENs) (Li et al., 2011). A typical TALEN architecture encompasses two TALE-FokI fusion proteins, which specifically target 14-18 bp of DNA sequence that are each preceded by a T nucleotide, and separated by a 14-16 bp spacer region (Christian et al., 2010; Miller et al., 2011). For the construction of TALEN repeat

arrays, the Golden gate cloning method was initially developed to assemble multiple DNA fragments from a TALE element library in an ordered fashion by the use of type-IIS restriction enzymes (Cermak et al., 2011; Morbitzer et al., 2011). For high throughput productions of TALEN, fast ligation-based automatable solid-phase high throughput (FLASH) (Reyon et al., 2012) and the iterative cap assembly (ICA) (Briggs et al., 2012) methods were developed. The FLASH method relies on the preassemble arrays of three or four TALE repeats, so that subsequent assemblies require only a few ligation steps, enabling the fast tract production of TALEN. The ICA method relies on the rapid assembly of DNA repeat modules by sequential ligation of monomers on a solid support together with capping oligonucleotides to increase the fraction of full-length TALEN products. In order to generate cellular and mouse disease models, different TALEN pairs were constructed to target endogenous genomic loci of human and mouse genes associated with disease phenotypes.
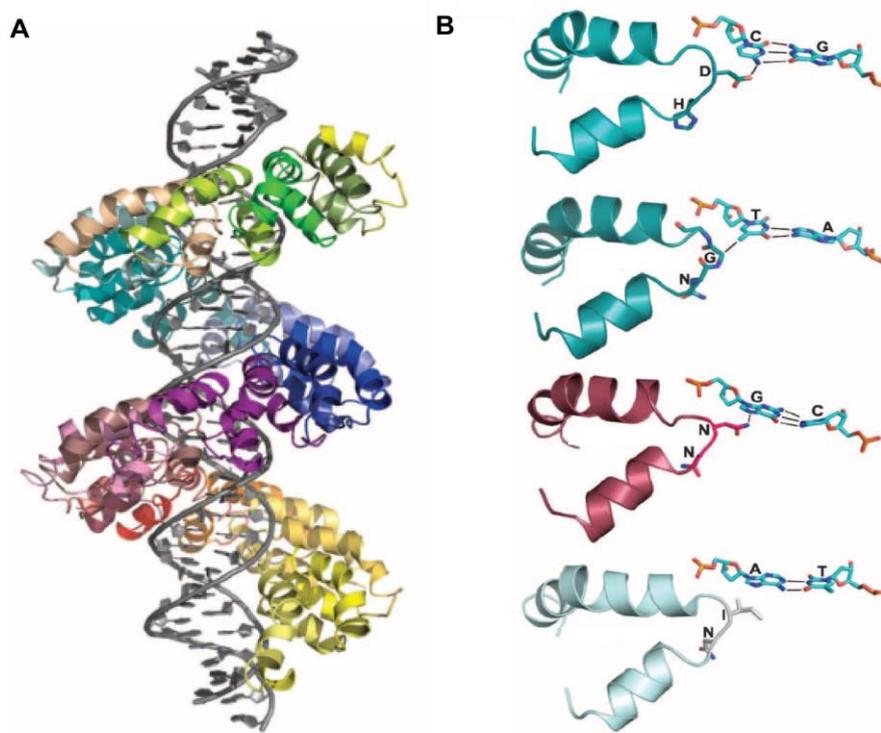
Figure 3: Structure of TALE binding region complex with its target site of DNA. (**A**) Each TALE repeat self-associates to form the right handed superhelix that wraps around the major groove of DNA. (**B**) Showing the interaction of TALE repeats to DNA bases. Aspartic acid of HD forms the steric electrostatic contact with the cytosine base. The α-carbon atom of glycine of NG forms the nonpolar interaction with the methyl group of thymine. NN interact with the N7 nitrogen of guanine or adenine. NI forms the desolvating interface with the adenine. Adopted and modified from Mak et al., (2012).

2.3.1 TALE-Nickases

The creation of a double-strand break (DSB) requires the dimerization of one FokI monomer with a second one which is recruited either from solution (Bitinaite et al., 1998) or bound to a second recognition site (Vanamee et al., 2001). As pointed out by Halford et al., (2011), the catalytic domain of FokI can dimerize across distance sites or even at solitary sites that elicit off-target activity. Indeed, two recent studies have identified off-site activity of ZFNs targeted *in vivo* to the *CCR5* or *IL2RG* genes (Gabriel et al., 2011), and to the *CCR5* and *VEGF-A* genes in human cell lines (Pattanayak et al., 2011). One potential strategy for enforcing the DNA repair pathway bias would be targeted introduction of a DNA single strand break (SSB). Proof of the SSB mediates homology directed repair (HDR) was reported previously, in which nicks created by derivatives of RAG protein (Lee et al., 2004) and I-Anil LAGLIDADG homing endonuclease (Smith et al., 2000) were efficiently enhancing the frequency of homologous recombination events. Furthermore, zinc finger nickases were created by introducing point mutations in one of the cleavage domains of FokI, enabling HDR with reduced mutagenic effect (Kim et al., 1996; Ramirez et al., 2012; Wang et al., 2012). To promote the homology directed repair by creating SSBs, the D450A (Asp450 to Ala) mutation (Waugh and Sauer, 1993) was introduced into one FokI monomer of TALEN pairs to induce cleavage at only one strand of the target DNA.

2.3.2 TALE-CND nuclease

In order to reduce the FokI off-site activity, another rational approach is to create chimaeric nucleases by substituting the non-specific FokI catalytic domain with other nucleases. Indeed, a number of programmable nucleases were developed, in which PvuII cleavage domain was successfully combined with a variety of DNA binding domains like triple-helix form oligonucleotides (Eisenschmidt et al., 2005), inactive I-SceI (Fonfara et al., 2012), zinc finger modules (Schierling et al., 2012), and TALEN modules (Yanik et al., 2013). Furthermore, the non-specific FokI cleavage domain in ZFN or TALEN was successfully exchanged with TevI GLY-GLY homing endonuclease (Kleinstiver et al., 2012; Beurdeley et al., 2013) and Gin recombinase (Gaj et al., 2013; Mercer et al., 2012) to induce DSBs or with MutH, a site specific DNA nicking enzyme to create the TALE-MutH programmable nickases to reduce the risk of genotoxicity (Gabsalilow et al., 2013). By searching the relatives of FokI endonuclease in the publicly available REBASE restriction enzyme database (from Neo England Biolabs), FokI sequence homology regions are found in *Clostridium* species termed as *Clostridium* nuclease domain (CND). Irion et al., (2007) reported the human *ROSA26* locus, a sequence homolog of the mouse *Rosa26*, which serve as a safe harbor for

integration of reporter construct as well as transgenes because of easy targeting and strong ubiquitous expression of inserted sequences without any gene silencing effects. To circumvent the potential limitation of FokI off-site activity, a new programmable TALE nuclease was created by combining the *Clostridium* nuclease domain to TALE repeat array to induce efficient site specific DSB.

2.3.3 Optimisation of TALEN mRNA

TALEN binding sites are found in the mouse genome at an average distance of 14 bp (Wefers et al., 2013a), supporting genome-wide targeted mutagenesis. Pronuclear microinjection of TALENs together with single-stranded oligonucleotides (ODN) into one-cell embryos provided a first proof-of-principle for generating precise targeted mutations by creating and correcting the chocolate missense mutation in the *Rab38* gene. The rate of HR and NHEJ were found to be 2% and 8% respectively (Wefers et al., 2013a), using experimental conditions that were not yet optimised. Recently two groups demonstrated higher rates of NHEJ-mediated nucleotide deletions (> 40%) upon microinjection of TALEN mRNAs (40 ng/µl, 50 ng/µl) directly into the cytoplasm of one-cell embryos suggesting the tolerance of zygotes to larger injection volumes (Qiu et al., 2013; Sung et al., 2013). Nevertheless for the generation of targeted precise mutations in endogenous locus, it seems instrumental to deliver the DNA templates with the TALEN mRNA into the pronucleus of one-cell embryos, required only minimal injection volumes. However, the production of mRNA from TALEN expression vectors is a tricky procedure that often yields inadequate amounts of full-length TALEN mRNA resulting in lower efficiency of TALEN mutagenesis. To set up an efficient routine procedure for *in vivo* mutagenesis, production of TALEN mRNA was enhanced by optimising nuclease expression upon pronuclear injection, such that more than one knockin or knockout alleles can be produced by single day of microinjection.

2.4 Generation of cellular model

Creating cellular model has been a challenging task of a genetic engineer. However, cellular model became a favorite model for biologists due to its inexpensive in generation and maintenance of culture, avoid risk of losing any precious biological material and expedite the various inherent intriguing biological mechanisms at first instance before testing for the *in vivo* application. Cellular models also provide a great avenue for studying the disease mechanism and drug discovery. To generate the cellular genetic model, TALENs with the reporters are transfected in human cell line to induce targeted genome modification.

2.5 Generation of disease mouse models

Genetically modified mammals can serve as valuable models of human genetic disorders, but the majority of disease-associated alleles represent single-nucleotide replacement that lead to missense, nonsense, and silent mutations (Sauna and Kimchi-Sarfaty, 2011). Compared with other animal models, mice are preferred because of their small body size, their fertilization cycle, and genetically close relationship to human genome. To unravel the function of disease-related genes and to understand the mechanism of disease progression, mouse mutants were generated by pronuclear microinjection of TALEN mRNA targeted to the mouse homologs of human disease genes into one-cell embryos to generate novel Knockout and Knockin mutants.

2.5.1 Frontotemporal lobar degeneration

Frontotemporal lobar degeneration (FTLD) is a common cause of presenile dementia caused by the degeneration of neurons in frontal and temporal lobes, which results in changes of personality, language, and behavior (Rademakers et al., 2012). Approximately 15% FTLD patients shows the symptoms of amyotrophic lateral sclerosis (ALS) and 50% of ALS patients also experience the symptoms of FTLD, including brain atrophy and cognitive changes. Remarkably both of these disease conditions are characterised by proteinaceous inclusions of the TAR DNA binding protein of 43 kDa (TDP-43) (Neumann et al., 2006). This significant overlap in the disease proteinopathy indicates that both ALS and FTLD are phenotypic variants of common pathological processes at opposite ends of the disease continuum. Linkage analysis of single kindreds as well as genome wide association studies in ALS and FTLD identified a locus on chromosome 9p21 (C9p21) as a potential common cause of ALS and FTLD (Laaksovirta et al., 2010; Vance et al., 2006). Further analysis of the C9p21 locus identified a massive expansion of a GGGGCC (G_4C_2) repeat in the first intron of chromosome 9 open reading frame 72 (*C9orf72)* (DeJesus-Hernandez et al., 2011; Renton et al., 2011; Gijselinck et al., 2012; Smith et al., 2013), which accounts for 20-80% of familial and 5-15% of sporadic ALS and FTLD cases (DeJesus-Hernandez et al., 2011; Renton et al., 2011)

2.5.1.1 *C9orf72*

The *C9orf72* gene comprises 11 exons, including two non-coding exons (1a, 1b). Based on the exon-intron structure, it is predicted to produce three alternative mRNA transcript variants by alternative splicing, with exons 1a and 1b to be differentially incorporated into RNA. The functions of the resulting protein isoforms are presently

unknown. *C9orf72 e*xpression is highest in CNS, especially in the cerebellum and also observed in the frontal cortex, hippocampus, hypothalamus, and spinal cord (Renton et al., 2011).

Sequence homology identifies C9ORF72 as a member of the highly conserved family of DENN (differentially expressed in normal and neoplastic cell) proteins, which is a GDP/GTP exchange factor (GEF) that activates Rab-GTPases (Levine et al., 2013). GTPases function in the vesicular formation and membrane trafficking, which is crucial for synapse formation and function. G_4C_2 hexanucleotide repeat expansions are found in FTLD and ALS cases within the first intron of *C9orf72*, just upstream, or within the promoter region of the noncoding exon 1b (Figure 4).
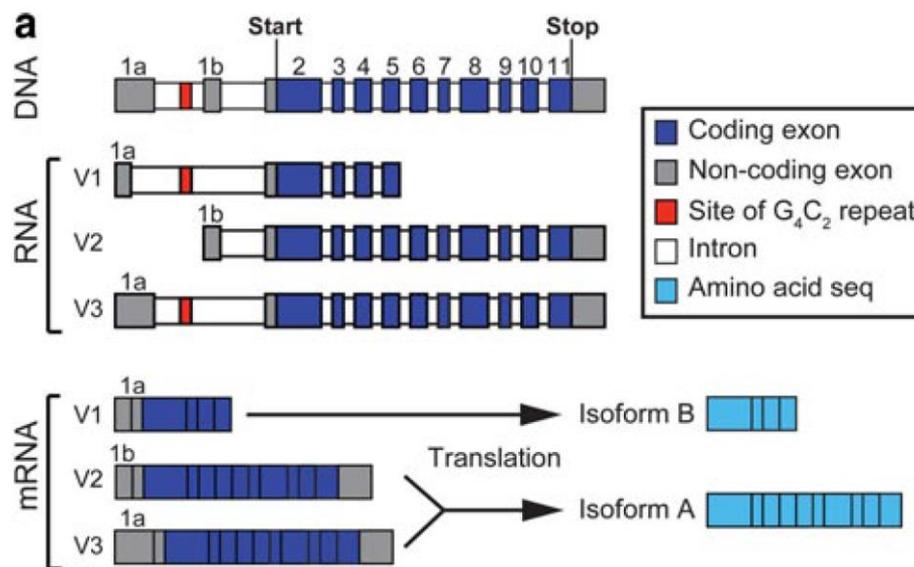
Figure 4: Showing the alternative splicing variants of *C9orf72* gene. *C9orf72* comprises two non-coding exons (1a, 1b) (grey) and coding exons 2-11 (blue). It transcribed into three variant pre mRNA (V1, V2, V3). V1 encodes shorter isoform B, whereas V2 and V3 encoded longer isoform A. Adapted from Stepto et al., (2014).

As shown by genome sequencing, healthy controls harbor less than 30 G_4C_2 hexanucleotide repeats, whereas in FTLD and ALS patients the repeat domain is expanded to 600 to 2,000 copies (DeJesus-Hernandez et al., 2011). Three common hypothesis are emerging about the underlying disease mechanism that's lead to cellular cytotoxicity: i) reduced or loss-of-function of the *C9orf72* encoded protein, ii) a RNA gain-of mechanism (Cruts et al., 2013; Ling et al., 2013), iii) repeat associated non-ATG translation causing the production and aggregation of dipeptide repeat proteins (Ash et al., 2013; Mori et al., 2013). To further understand the disease mechanism, whether *C9orf72* loss-of-function also contribute to the FTLD phenotype and to decipher its cellular function, the mouse homolog of

the *C9orf72* gene (*3110043O21Rik*) was disrupted by the generation of TALEN induced mutations close to the translational start site.

2.5.2 Amyotrophic lateral sclerosis

Amyotrophic lateral sclerosis (ALS) is characterised by the degeneration of the upper motor neurons in the motor cortex and lower motor neurons of the brainstem and spinal cord, resulted in muscle wasting, weakness, and fatality (Robberecht and Philips, 2013). The majority of ALS patients die within 1-5 years after disease onset, typically due to respiratory failure. The abnormal cytoplasmic aggregation of FUS in neuron and glial cells is a pathological hallmark of ALS and some cases of FTLD (Kwiatkowski et al., 2009; Vance et al., 2006;). Although the majority of ALS cases are sporadic (sALS), about 10% are inherited in a dominant manner (Boillée et al., 2006). Of these, 5-10% are caused by TAR DNA binding protein 43 (TDP-43) (Gitcho et al., 2008) or the *FUS* gene (Kwiatkowski et al., 2009). Moreover, *FUS* gene mutations are the second most frequent cause of familial ALS (fALS) (Syriani et al., 2011).

2.5.2 1 Fused in sarcoma

Fused in sarcoma (FUS) is a DNA and RNA binding protein that shuttles continuously in between the nucleus and cytoplasm (Ayala et al., 2008), and is involved in multiple steps such as transcriptional regulation, pre-mRNA splicing, and microRNA processing (Lagier-Tourenne and Cleveland, 2009). FUS has also been associated with mRNA transport and export to neuronal dendrites (Fujii et al., 2005). Although FUS predominately locates in the nucleus, cytosolic FUS inclusions with reduction of nuclear staining were found most predominantly in fALS patients. Twelve fALS-associated mutations were found clustered in the C-terminal region of *Fus* leading to the accumulation of FUS in the cytosol, accounting for 4% of fALS cases (Kwiatkowski et al., 2009). FUS is a member of the TET family of proteins that includes EWS (Ewing´s sarcoma) and TAF15 (TATA-binding protein-associated factor 15), which originated from a common ancestor (Law et al., 2006). All three proteins share common amino terminus region enriched in serine, tyrosine, glutamine, and glycine residues (SYQG rich), a conserved RNA-recognition motif flanked with glycine rich region, a zinc finger motif, and multiple arginine/glycine/glycine (RGG)-rich regions that may be important for RNA binding (Figure 5A). Strikingly most of the mutations are clustered in the C-terminus with evidence that five terminal arginine residues present in this site. Further, the C-terminal motif is highly conserved throughout the evolution (Figure 5B). The non-classical PY nuclear localisation signal (NLS) was identified in the C-terminus of *Fus*, which is necessary for its nuclear import (Dormann et al., 2010).

A

C
G   T
SC   QK   HG   SL
⊥ | | | | | |
514   RGEHRQDRRERPY   526

insGG, delGG   R244C

| S,Y,Q,G rich | G rich | | RNA binding | G rich | ZnF | RGG rich | |

1 2   3   4   5   6   7 8 9   10   11   12   13   14   15

B

514   526

Human (Homo sapiens)   - RG-EHRQD--RRERPY
Chimpanzee (Pan troglodytes)   - RG-EHRQD--RRERPY
Mouse (Mus musculus)   - RG-EHRQD--RRERPY
Rat (Rattus norvegicus)   - RG-EHRQD--RRERPY
African clawed frog (Xenopus laevis)   - RG-EHRQD--RRDRPY
Zebrafish (Danio rerio)   - RG-EHRQD--RRDRPY
Roundworm (Caenorhabditis elegans)   - RGGPPGGD---RYRPY
Fruit fly (Drosophila melanogaster)   - DGGPMRNDGGMRSRPY

Figure 5: Schematic structure of the FUS protein. (**A**) FUS is encoded by 15 exons having N-terminal rich SYQG (serine, tyrosine, glutamine and glycine), G rich, and RGG rich regions enriched with glycine or arginine-glycine-glycine motif respectively. All missense mutations (12 out of known 22 mutations) identified in familial ALS patients, are clustered in the C-terminal PY motif of *Fus*. Also insertion (ins) GG, deletion (del) GG and R244C point mutation were located in G rich domain. Adopted from Kwiatkowski et al., (2009). (**B**) Amino acid alignment of the C-termini of FUS among a variety of species showed that the sequence of this domain is well conserved during evolution (identical residues are highlighted in yellow, homologous residues in light grey). Adopted from Dormann et al., (2010).

The majority of fALS-mutations occur within NLS that disrupts the nuclear import of FUS leading to its cytoplasmic deposition in the brain and spinal cord of patients (Bosco et al., 2010; Dormann and Haass, 2013; Gal et al., 2011; Ito et al., 2011; Kino et al., 2011). The extend of cytosolic mislocalisation due to impairment of nuclear import correlates with the age of disease onset, such as the P525L (proline to leucine) replacement leads to an early onset and rapid progression of the disease with high severity, whereas the R521G (arginine

to glycine) replacement lead to a late disease onset of less severity. However, it is still unclear whether the neurodegeneration that occurs in ALS is caused by the loss of FUS nuclear function, or by the gain of a toxic function due to cytoplasmic FUS aggregation.

Expression of ALS-linked FUS mutants in zebrafish (Kabashi et al., 2011), fruit flies (Sasayama et al., 2012), *C. elegans* (Murakami et al., 2012), and in rat (Huang et al., 2011) can lead to motor neuron dysfunction and neurodegeneration but is perinatal lethal in mice (Hicks et al., 2000). To understand the normal function of FUS in RNA processing, it is essential to create mouse models harboring patient derived missense mutations to unravel the disease mechanism. To faithfully mimic the human codon replacements R521G and P525L, the analogous positions R513 and P517 of the mouse *Fus* gene were targeted using TALENs and oligodeoxynucleotides.

2.6 HRMA

Careful screening of the pups generated from TALEN microinjection is a very tedious job to discriminate the positive mutants. Mostly used PCR-based restriction fragment length polymorphism assay relied upon the digestion of the PCR products and gel electrophoresis for the detection of mutants having subtle mutation from the wild-type control. In the past, High Resolution Melt Analysis (HRMA) has been used to detect sequence polymorphism in zebrafish (Parant et al., 2009) by determining their specific denatured profile of PCR products in the presence of an intercalating dye (Liew et al., 2004). HRMA is a highly sensitive automated close tube genotyping method that does not require agarose gel electrophoresis containing the harmful ethidium bromide dye, restriction digestion, and size separation of PCR products. To minimize the time consuming genotyping efforts, PCR products derived from the tail DNA of mice were examined by HRMA to detect nuclease induced sequence alteration at the targeted loci.

2.7 CRISPR/Cas

Bacteria and archaea have evolved an RNA mediated adaptive immune system termed as clustered regularly interspaced short palindromic repeats (CRISPR)/Cas (CRISPR-associated) to combat foreign invaders such as viruses and plasmids (Horvath and Barrangou, 2010; Wiedenheft et al., 2012). Each CRISPR locus consists of identical repeated DNA sequences (repeats) of similar size, interspaced by highly variable sequences referred as spacers. Spacer originated from the invading phages or plasmids and comprising the prokaryotic "immunogenic memory". CRISPR-associated (Cas) genes encode the conserved proteins that together with CRISPR makes the CRISPR/Cas system, defending

the prokaryotic cells against invaders. Cas genes encode a large and heterogeneous family of proteins that carry functional domains typical of nucleases, helicases, polymerases, and polynucleotide-binding proteins (Haft et al., 2005).
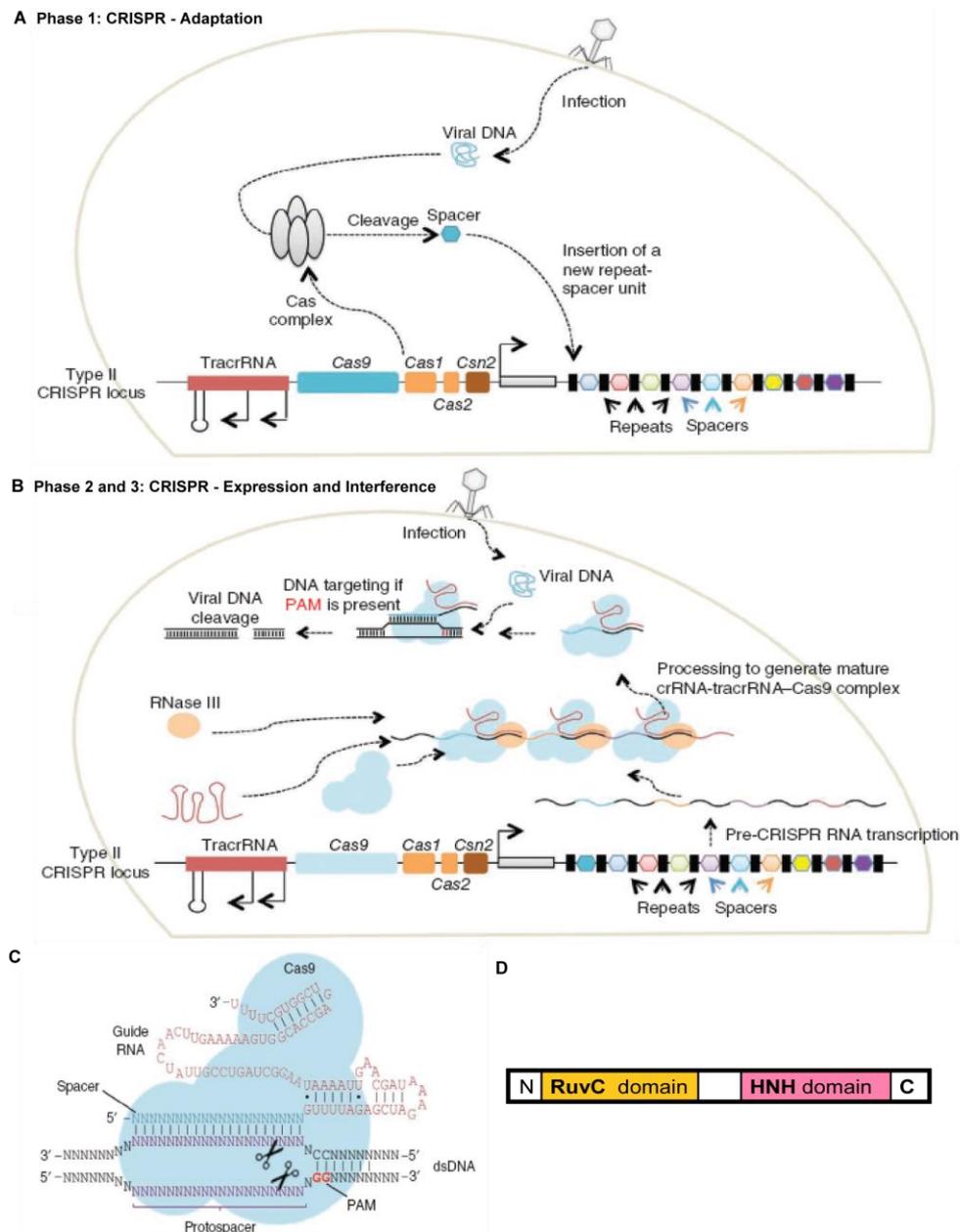
Figure 6: Functionality of type II CRISPR/Cas system in bacteria and eukaryotes. (**A**) Phase 1: in the adaption phase, CRISPR system stores the memory of the previous infection by integrating the fragments of the invading DNA into the CRISPR locus as 'spacers'. (**B**) Phase 2 and 3: on subsequent invader attack, bacterium uses the stored information to defend against the pathogens by transcribing the locus as pre-crRNA. Subsequently tracrRNA hybridizes to the repeat regions of the pre-crRNA, which recruited endogenous RNase III that cleave the hybridized crRNA-tracrRNA, and removes the 5′ end of the spacer, yielding mature crRNAs that remain associated with the tracrRNA and Cas9. The

ternary complex cleaves the target invading DNA by complementary base pairing with protospacer sequence only if PAM sequence is present. (**C**) The sgRNA guided Cas9 nuclease complex for eukaryotic genome engineering. Target recognition and cleavage require the protospacer sequence complementary to the spacer and requirement of the appropriate NGG PAM sequence motif at the 3' end of the protospacer. (**D**) The Cas9 nuclease encompasses RuvC catalytically active domain at N-terminal end which cleaves the non-complementary strand, whereas the C-terminal HNH domain cleaves the complementary DNA strand. Adopted from Mali et al., 2013.

CRISPR/Cas mediated resistance occurs in three different phases: (i) CRISPR-Adaptation, in which the alien DNA is encountered by the CRISPR/Cas machinery and invader derived short DNA fragments are generated and integrated as new spacers into the CRISPR repeat array (Figure 6A). (ii) CRISPR-Expression is a multiple step (Deltcheva et al., 2011), in which the spacer-repeat CRISPR array is first transcribed into a long pre-crRNA. Second, *trans*-activating crRNA (tracrRNA) hybridize to the repeat regions of the pre-crRNA. Third, RNAase III removes the 5' end of each spacer to yield mature crRNA that remains associated with both the tracrRNA and Cas9. (iii) CRISPR-Interference, invaders nucleic acid is recognised by complementarity to the crRNA and degraded (Figure 6B) (For review see, van der Oost et al., 2009). Target recognition and subsequent cleavage by the crRNA-tracrRNA-Cas9 requires the sequence complementarity in between the spacer and the target protospacer sequence as well as the presence of the appropriate protospacer adjacent motif (PAM) sequence at the 3´end of the protospacer sequence (Figure 6C). The most commonly used Cas9 system of *Streptococcus pyogenes*, requires a PAM sequence of NGG, where N is any nucleotide (Jinek et al., 2012).

Cas9 generates blunt ended DSBs, three base pairs upstream of the 3' end of protospacer mediated by an HNH nuclease domain that cleave the complementary strand, whereas the RuvC-like nuclease domain cleaves the non-complementary strand (Figure 6D). The crRNA-tracrRNA-Cas9 system was successfully used as efficient gene-editing tool in human cells (Cong et al., 2013; Jinek et al., 2013; Mali et al., 2013), zebrafish (Chang et al., 2013; Hwang et al., 2013), drosophila (Bassett et al., 2013; Gratz et al., 2013), and *C. elegans* (Dickinson et al., 2013; Friedland et al., 2013) by expressing codon-optimised version of the Cas9 protein with the appropriate nuclear localisation signal, and the crRNA and tracrRNA expressed either individually or as chimaera (sgRNA; Jinek et al., 2013) via expression from a RNA Polymerase III promoter. Moreover, by using multiple guide sequences, Cas9 can be programmed to simultaneous editing of several sites in mammalian genomes (Cong et al., 2013). Simplicity of sgRNA design and delivery suggest that the CRISPR/Cas system is most advanced for the production of mouse mutants. To expedite the generation of small or large scale genome-modified mice, one or two sgRNAs along with Cas9 mRNA were pronuclear microinjected into mouse one-cell embryos to create targeted knockout or homologous recombined mice by modifying single or two loci in the same chromosome.

2.8 Aim of the thesis

Sequence specific nucleases like ZFNs and TALENs are widely used for gene targeting in many species and provide an alternative tool to embryonic stem cell technology. However, TALENs are superior to ZFNs because of the abundance of genomic target sites and the simple one to one relation of specific TALE repeats to individual nucleotides of the target sequence. In fact, the first evidence of TALEN mediated mouse mutagenesis was established by pronuclear microinjection of TALEN mRNA into one-cell embryos (Wefers et al., 2013a). Nevertheless, in this study the efficiency of gene targeting achieved at rates of 8% and 2% for NHEJ and HR events, which was not yet optimised. Therefore, several aspects of TALEN mediated mutagenesis can be further improved to increase its efficiency and versatility.

The efficiency of genome editing is directly correlated to the induced cleavage frequency at the target sequence with a higher specificity. Meanwhile, the finding of the previous report shows that FokI nuclease domain elicits off-target activity by dimerisation at distant or solitary sites (Halford et al., 2011). However, in order to reduce such off-site activity, a nickase strategy is developed to inactivate the monomer of ZF-FokI array that basically lower the FokI-homodimerisation at unintended sites. Consequently, nickases directs DSBs repair bias towards the HR over the NHEJ event (Sanders et al., 2009). Hence, the question arises, whether a nickase strategy can be adopted in the TALEN platform for enhancing nuclease precision, and whether any other novel nuclease domain can be replaced FokI by improving cleavage efficacy of the TALEN scaffold.

In order to generate the targeted mutants, TALEN mRNAs together with or without the targeting molecules are microinjected into the pronucleus of one-cell mouse embryos. Nonetheless, upon the *in vitro* transcription of the TALEN coding regions, smeared appearance of the transcripts are repeatedly observed, which reveal the presence of the full-length TALEN mRNAs associated with different truncated variants, perhaps due to faulty polyadenylation step of *in vitro* transcription. For achieving the high efficient nuclease mutagenesis, the production of robust full-length TALEN mRNA is an indispensable step of pronuclear microinjection, however its production is always painstaking and face great challenge in most of the laboratories, which has to be addressed.

Genetic disease models serve as tool for understanding the pathogenesis and mechanism of disease. Expanded hexanucleotide (GGGGCC) repeats in the promoter region of first intron of chromosome 9 open reading frame 72 (*C9orf72*) are the most common cause of frontotemporal lobar degeneration (FTLD) and amyotrophic lateral sclerosis (ALS). However, the mechanism by which repeat expansion caused the disease

are not clearly understood, but the leading candidate mechanisms are toxic RNA gain-of-function or loss-of *C9orf72* gene function or combination of a both. Missense mutations in the fused in sarcoma (*Fus*) gene are identified as a common cause of chromosome 16p-linked amyotrophic lateral sclerosis (ALS) (Kwiatkowski et al., 2009). Interestingly, the majority of familial ALS mutations occur within the NLS that disrupt the nuclear import of FUS leading to its cytoplasmic deposition in brain and spinal cord of patients. Notably, most frequent missense mutations found in fALS patients are R521G and P525L, in which the severity of pathogenesis correlated to their age related disease onset. However, the causative mechanisms of the ALS pathogenesis is still unknown, whether the neurodegeneration is caused due to the loss of the FUS nuclear function, or by the toxic gain-of-function due to cytoplasmic FUS aggregation. Therefore, a *C9orf72* knockout mouse model and patient derived codon replacement *Fus* mouse models are a prerequisite to unravel the unknowing disease mechanism.

The recent emergence of the CRISPR/Cas further expands the era of gene targeting beyond TALENs and ZFNs due to its simple design and wide adaptability. In fact, gene targeting by the CRISPR/Cas system is enabled by sgRNA sequences that drive the Cas9 nuclease to induce cleavage at specific genomic target loci that are complementary to the crRNA preceded by a NGG PAM sequence. Moreover, the bacterial CRISPR/Cas system was successfully applied in human and mouse cells to induce cleavage at endogenous genomic loci (Cong et al., 2013; Mali et al., 2013). Furthermore, targeted double deletion is created by inducing concurrent DSBs by using two different sgRNA separated by 119 bp in between two genomic target sequence (Cong et al., 2013). Hence, the question arises whether the CRISPR/Cas tool can be applied in mouse zygotes for the expedite generation of disease models.

In light of this background, the objectives of my thesis were:

1. Generation, functional characterisation, and optimisation of TALENs to improve their efficiency and versatility.
2. Creation of *C9orf72* and *Fus* mouse mutants by TALENs as disease models for frontotemporal lobar degeneration and amyotrophic lateral sclerosis.
3. Establishment of the CRISPR/Cas system as a versatile tool for highly efficient mouse mutagenesis.

With these objectives, I intend to unravel novel molecular mechanisms of neurodegenerative disorders that ultimately may contribute to develop new strategies for therapeutic interventions.

3 Results

3.1 Construction and optimisation of TALEN for the efficient genome editing

3.1.1 Design, assembly and functional validation of TALEN

To access the ability and efficiency of TALENs for generating mutant mice through microinjection into zygotes, TALEN pairs were selected to target six mouse genes (*Psen2*, *Pink1*, *Hist2h3c1*, *3110043O21Rik*, *Fus,* and *CdK1*) located at five chromosomes. To access in addition the utility of TALENs for creation of human cellular models, six TALENs were selected to target the human genes *CDK1*, *ROSA26*, *APP,* and *SPAST*.
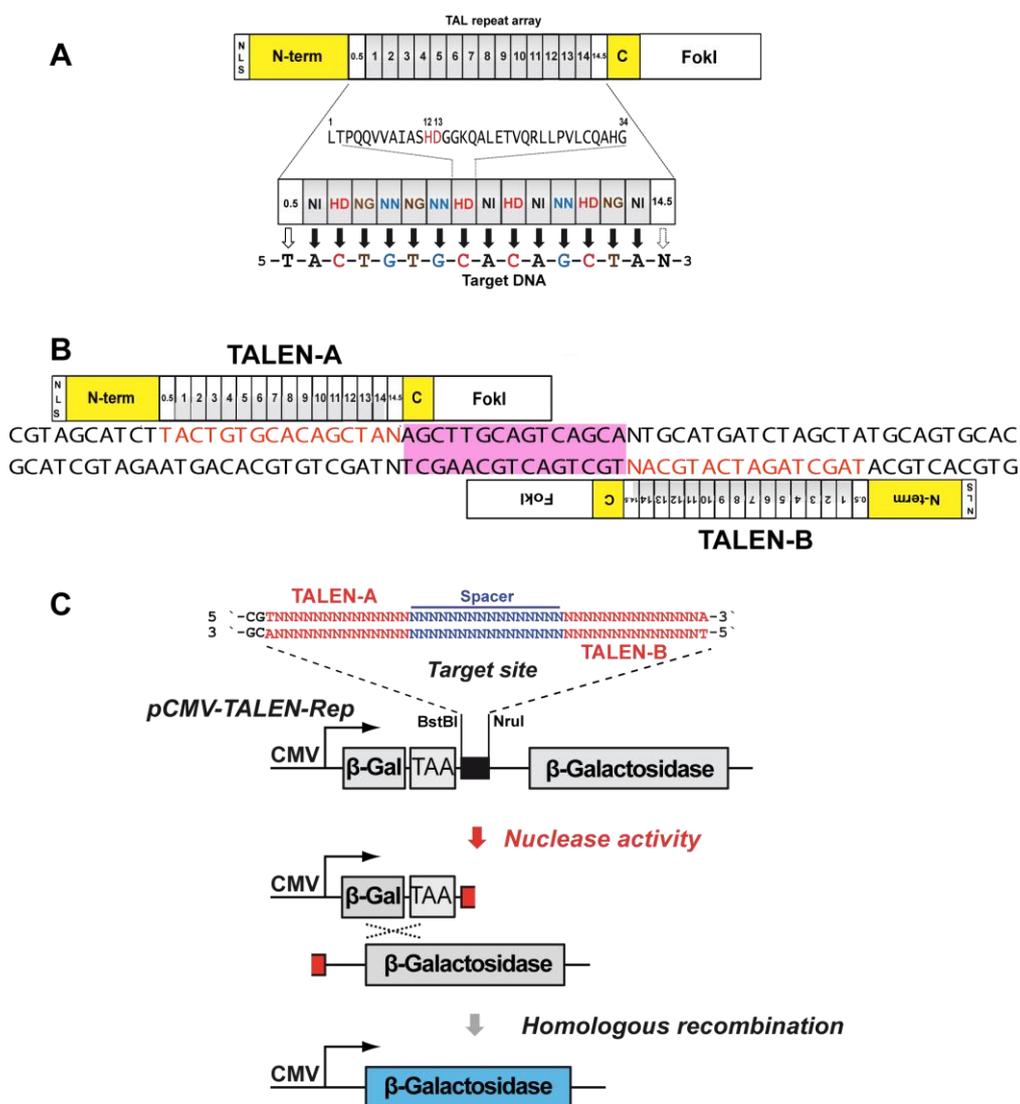
Figure 7: Modular assembly and functional validation of TAL effector nucleases. (**A**) A natural TALE (transcriptional activator-like effector) protein derived from

Xanthomonas plant pathogens consists of the nuclear localisation sequence (NLS), N-terminal translocation domain and flanking sequences (N-term, marked in yellow background), a central repeat domain of 14 repeats flanked by the invariable first (0.5) and last (14.5) half conserved repeats and C-terminal flanking sequences (C, marked in yellow background) attributed to the trans-activating effector domain. TALE proteins can be fused with the FokI nuclease domain for genetic engineering experiments. A thymidine (T) nucleotide invariably represents the first position of the target sequence, recognised by the 0.5 TALE repeat, whereas the last C-terminal half repeat does not contribute to the sequence specificity (N). Each TALE module encompasses a conserved sequence of 34 amino acids (aa) except for the position 12 and 13, as the so called repeat variable di-residues, which mediate of the contact to specific nucleotides. The RVDs-DNA recognition code follows a simple principle, such that NI binds to adenine (A), HD binds to cytosine (C), NG binds to thymidine (T), and NN binds to guanine (G) and adenine (A). (**B**) Schematic drawing of the configuration of a TALEN nuclease pair binding to a target DNA site. Sketch of the designed TALENs, in which the catalytic domain of the FokI endonuclease is fused to the C-terminal end of the TALE coding region. Typical structure of bipartite target sequences for binding of a pair of TALEN fusion proteins. The upstream (left) and downstream (right) target sequence consists of 15-18 bp (here 16 bp), in all cases starting with the invariable thymidine (T) which is recognised by the first half repeat (0.5) of each TALE protein. Target sequences are separated by spacer regions of 14-16 bp (pink background) which enables the dimerisation of both FokI domains in order to create a double-strand break. (**C**) The nuclease reporter vector pCMV-TALEN-Rep contains a truncated ß-galactosidase coding sequence (1 to 450 aa) followed by a translation stop codon (TAA), BstBI and NruI restriction sites for cloning of the defined TALEN target specific nucleotide sequences (pink letters) flanking the spacer region, followed by the entire but inactive ß-galactosidase coding sequence, except for the translational start codon. Upon co-transfection of a pair of TALEN expression vectors and the respective reporter plasmid into HEK293 cells, nuclease induced double-strand breaks (DSBs) occur at the target site of the reporter vector. A functional ß-galactosidase coding region is reconstituted through homologous recombination between identical sequences flanking the DSB site. The nuclease activity of TALEN is determined by comparing the levels of ß-galactosidase activity obtained from the transfection of reporter plasmid alone or together with the TALEN expression vectors.

Specific recognition sequences within the target genes, including presenilin 2 (*Psen2*), PTEN induced putative kinase 1 (*Pink1*), histone cluster 2, H3c1 (*Hist2h3c1*), RIKEN cDNA 3110043O21 (*3110043O21Rik*), fused in sarcoma (*Fus*), cyclin-dependent kinase 1 (*CdK1*), *ROSA26,* amyloid beta (A4) precursor protein (*APP*), and spastin (*SPAST*) were identified by using the TALEN*designer* webpage (http://www.talen-design.de/) such that each target site was uniquely represented within the genome (Wefers et al., 2013a) Two independent TALEN pairs (TALEN-A and TALEN-B) for each target site were constructed by golden gate cloning using TALE (RVD) modules specific for each individual nucleotide of the target sequence (Table S1). Complete coding regions for TALEN proteins were obtained by the insertion of the full-length ligation products into the mammalian expression vector pCAG-

TALEN-pA (Figure 7A). All TALEN pairs were constructed using the + 176/+44 TALEN scaffold such that each pair binds to opposing DNA strands of the target sequence, allowing the dimerization of their FokI domains in the spacer region (Figure 7B). Since the activity of TALENs can vary by one order of magnitude (Cermak et al., 2011), the quality control of the activity of TALEN pairs are essential to select highly effective nucleases for the subsequent application in one-cell mouse embryos or cell lines. For this purpose, TALEN target regions were cloned into the pCMV-TALEN-Rep vector in between a partly duplicated, non-functional ß-galactosidase gene.
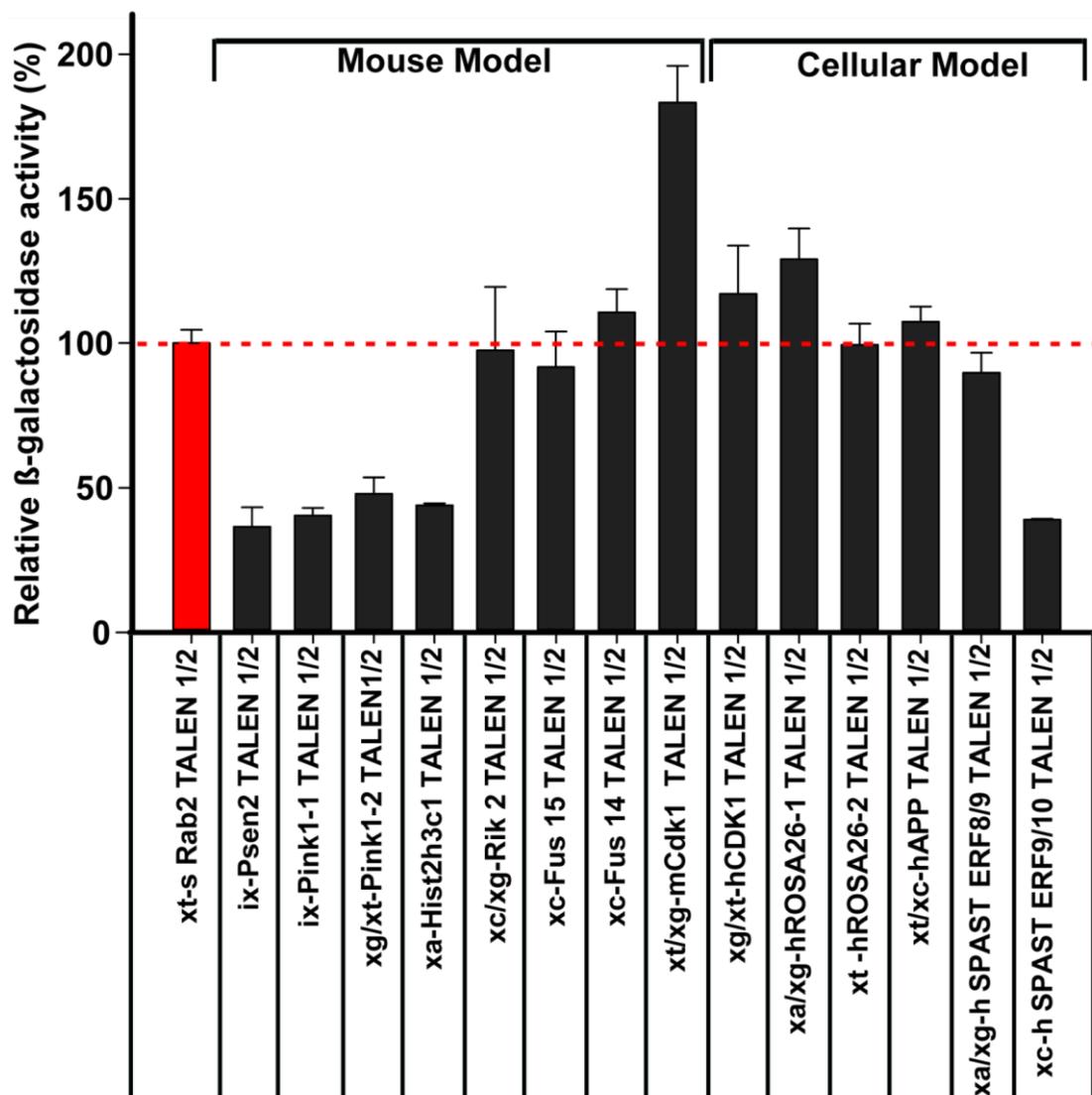
Figure 8: Functional validation of the TALEN pairs. The constructed 14 TALEN pairs specific to the target sequences were tested by the HEK293 reporter assay for evaluating the nuclease activity against their target DNA sequence, cloned into the pCMV-TALEN-Rep vector. Upon co-transfection into HEK293 cells, the activity of the reporter in presence or absence of the TALEN expression vectors were compared and expressed as an index of the nuclease activity. The black

bars indicated the nuclease efficiency of each constructed TALEN pair in comparison to the red column indicating the activity of RAB2-TALEN as positive control.

Upon co-transfection of the reporter and TALEN expression vector into HEK293 cells, nuclease mediated double-strand break of the reporter plasmid DNA promotes the repair of the gene segments by homologous recombination (Figure 7C), the activity of which is determined in cell lysates. Here Rab2-TALEN was used as positive control for the experiments. All of the newly constructed TALENs showed nuclease activity and 64% of these TALENs (nine of 14 pairs) exhibited comparable or superior nuclease activity as compared to the Rab2-TALEN positive control (Figure 8). Fus 15-TALEN and Rik2-TALEN, recognizing target sequences within exon 15 of *Fus* or exon 2 of *Rik* respectively, showed nuclease activity comparable to the positive control and were chosen for the application in one-cell mouse embryos to create targeted genome modification. Similarly, ROSA26-1 TALEN showed superior nuclease activity to the Rab2-TALEN control, and was used for creating cellular model.

3.1.2 Mutation of the FokI domain to generate TALEN nickases

To generate TALEN with strand-specific nuclease activity, the FokI catalytic domain was mutated in one the two TALENs required for their dimerization, which subsequently caused the DNA cleavage (Bitinaite et al., 1998). Specifically, the introduction of the D450A point mutation into the FokI catalytic domain results into nuclease inactivity (Sanders et al., 2009). The amino acid alignment of the *Clostridium* nuclease domain (CND) and FokI nuclease domains indicates the presence of D450 (GAT) amino acid at same position. The D450A (GAT>GCC) mutation was incorporated into both pairs of TALE-FokI and TALE-CND constructs targeting a sequence derived from the *ROSA26* gene. To test whether the introduction of the D450A point mutation in TALE-FokI or TALE-CND results into active nickases, three combinations (wt/wt, wt/D450A, and D450A/D450A) of TALE-FokI and TALE-CND plasmids were cotransfected into HEK293 cells. The *in vitro* reporter assay showed that the heterodimeric nickase pair (wt/D450A) of TALE-FokI and TALE-CND revealed a reduced (55-60%) nuclease activity as compared to the wild-type control (wt/wt) (Figure 9).

This result was consistent with a recent report describing the construction of nickases using the FokI domain including the D450A mutation (Liu et al., 2014; Wu et al., 2014). In contrast, the homodimeric nickase pairs (D450A/D450A) of TALE-FokI and TALE-CND showed the complete absence of nuclease activity as compared to the wild-type control. Taken together, these data demonstrate that the elimination of the cleavage activity in one of

the TALE-FokI or TALE-CND protein pairs by the D450A mutation results into a potent, strand-specific nickases.
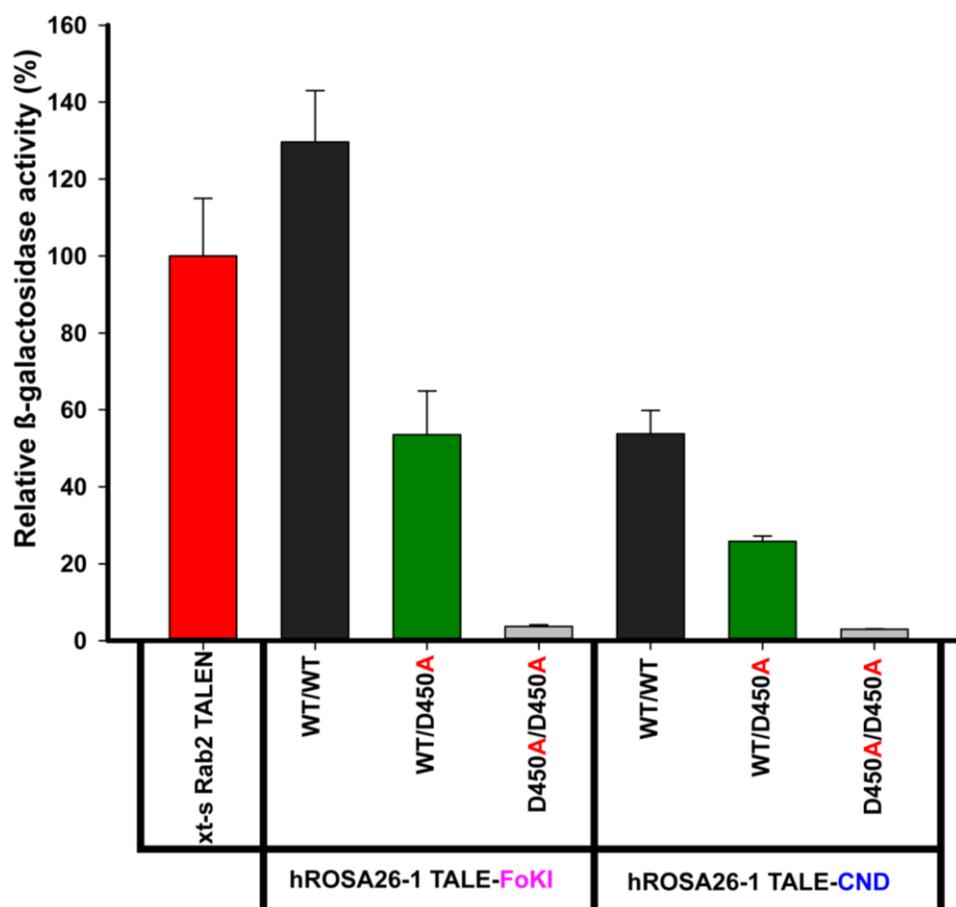
Figure 9: Assessment of TALEN nickase-mediated homology directed repair. hROSA26-1 TALEN with either the CND or FokI nuclease domain including or lacking the D450A point mutation were transiently cotransfected into HEK293 cells. The diagram shows the relative ß-galactosidase activity of each pair of homodimeric TALEN (wt/wt, black column) as compared to the respective heterodimeric (wt/D450A, green column) or homodimeric (450A/450A, grey column) nickases after 48 hours of transfection. Here Rab2-TALEN was used as positive control (red column).

3.1.3 Evaluation of the nuclease activity of TALE-CND in comparison to TALE-FokI fusion proteins

The amino acid alignment of the nuclease domain of a predicted gene of a *Clostridium* species showed 49% similarity to the FokI nuclease domain (data not shown). To access whether the nuclease activity of TALEN may be improved by the *Clostridium* nuclease domain (CND), the FokI domain was substituted with CND at the C-terminal region of TALEN specified to the *ROSA26*, *APP*, and *SPAST* genes. The working principle of each

TALE-CND pair was identical to the TALE-FokI pair by allowing the dimerization of CND from opposing target sequences, enabling the cleavage of DNA strands in the spacer region.
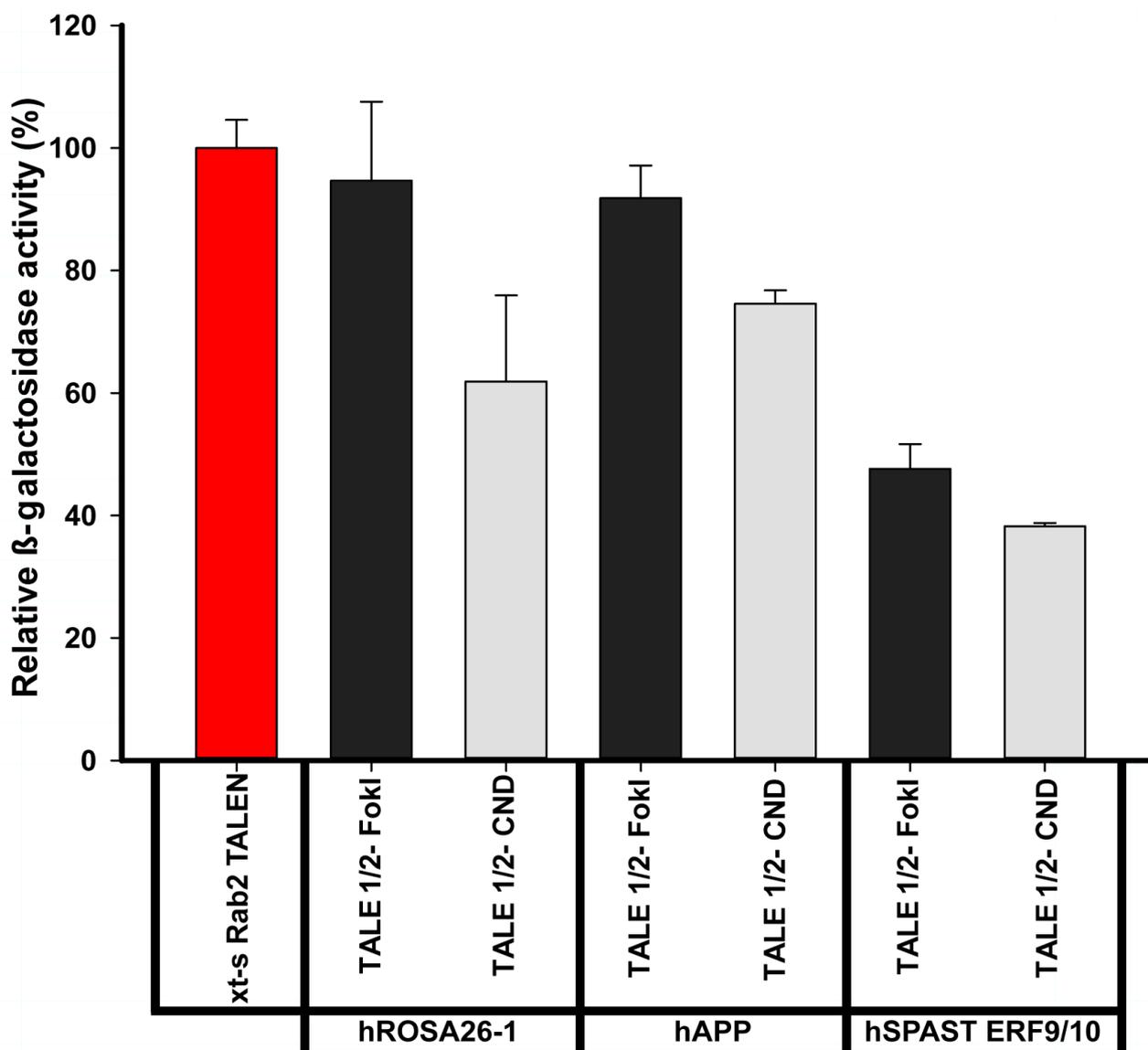
Figure 10: Comparison of nuclease activities of TALE-FokI and TALE-CND fusion proteins. The nuclease activity of three different TALEN (hROSA-1, hAPP, and hSPAST ERF9/10) harboring either the CND or FokI nuclease domain at the C-terminal region, were determined by the *in vitro* reporter ß-galactosidase assay. Here Rab2-TALEN (red column) serves as internal control. The nuclease activity of TALE-FokI and TALE-CND constructs are shown as black and grey. columns, respectively.

Upon transient transfection of the TALE-FokI and TALE-CND constructs along with the reporter into HEK293 cells, *in vitro* reporter assay revealed that all TALE-CND pairs showed >70% nuclease activity as compared to the TALE-FokI versions (Figure 10). Overall, these results suggested that the nuclease activity of the FokI domain is superior to CND.

3.1.4. Optimisation of spacer length for enhancing the nuclease activity of TALEN

To test whether the activity of TALEN is significantly affected by the length of the spacer in between the opposing TALEN target sequences as reported previously (Miller et al., 2011), human CDK1-TALEN (A, B) and mouse Cdk1-TALEN (C, D) were selected for assembling four different TALEN pair combinations with distinct spacer lengths (AB-15 bp, BC-10 bp, CD-16 bp, and AD-21 bp), respectively.
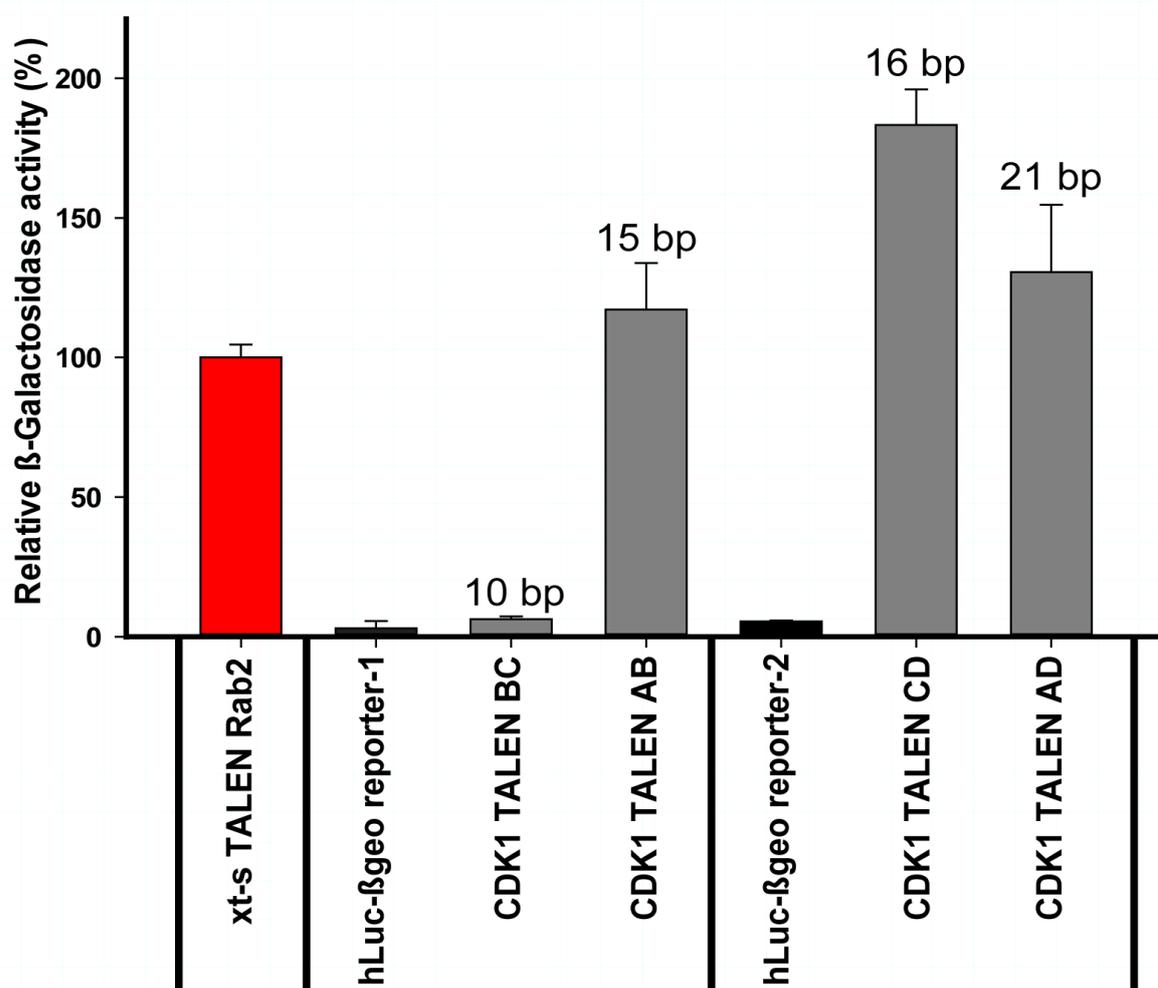
Figure 11: Optimisation of spacer length for efficient TALEN activity. The *in vitro* reporter assay shows the relative ß-galactosidase activity of four different CDK1 TALEN combinations (grey columns) with distinct spacer lengths of 10 bp, 15 bp, 16 bp, and 21 bp as compared to Rab2-TALEN, positive control (red column). A, B, C, and D denotes the individual TALEN construct used for the experiment.

Upon the co-transfection of all four combinations of TALEN pairs having distinct spacer length into HEK293 cells, the *in vitro* ß-galactosidase reporter assay revealed that pairs having spacer lengths of 15 bp, 16 bp, and 21 bp showed comparable or superior nuclease activity as compared to the Rab2-TALEN (15 bp spacer) internal control (Figure 11). In contrast, a spacer length of 10 bp dramatically diminished the nuclease activity. Overall these data demonstrated that a spacer length of 15-16 bp is optimal for TALEN activity.

3.1.5. Optimised expression of TALENs in one-cell embryos

By using the TALEN designer algorithm and the modular design protocol (Wefers et al., 2013a), TALEN pairs were constructed to target the *Fus* gene which causes 10% of familial amytrophic lateral sclerosis (fALS) cases, and to the *3110043O21Rik* gene associated with frontotemporal lobar degeneration (FTLD), respectively. The coding region of TALE were cloned into the pCAG-TALEN-poly(A) mammalian expression vector, providing the CAG promoter and a polyadenylation signal sequence (Figure 12A). The nuclease activities of these TALEN were evaluated by co-transfection of the expression and reporter vectors into HEK293 cells as described previously (Wefers et al., 2013b) and found to exhibit specific nuclease activity (Figure 8). For the pronuclear microinjection into one-cell embryos, the MluI digested pCAG-TALEN-Fus15-poly(A) vectors were first *in vitro* transcribed (IVT) by T7 polymerase, followed by polyadenylation using poly(A) polymerase as the standard two step protocol of the T7-mMessage transcription kit. Using this two-step IVT protocol, a smeared appearance of the mRNA preparation was frequently observed (Figure 12C, TALEN-poly(A)) due to inconsistent production of single species TALEN mRNA. This effect was noted for TALEN IVTs, but not for the shorter ZFN mRNAs, possibly because of the larger repetitive coding region of TALEN (3 kb) resulting in a predominant population of truncated products, which contaminate the second step of polyadenylation. To circumvent this problem for the reliable production of full-length TALEN mRNAs suitable for pronuclear microinjection, the coding region of TALE was cloned into the pT7-TALEN-95A vector (Figure 12B) which provides a T7 promoter and a region of 95 adenine residues located downstream of the TALEN coding region for the production of TALEN-95A mRNAs in a single step. Using the pT7-TALEN-95A vector for IVT, single populations of mRNA transcripts of the expected size of 2494 bp were obtained (Figure 12C, TALEN-95A). To confirm whether this 95A tail is able to support the efficient translation of coding regions upon pronuclear microinjection and to determine the optimal RNA concentration, a Venus coding control vector (pCAG-Venus-95A) was generated. Upon the pronuclear injection of Venus-95A mRNA at 90 ng/µl, green fluorescence was found in all two-cell embryos (Figure 12D). To determine the potency of TALEN-95A mRNAs for mutagenesis of the *Rik* and *Fus*

genes, concentrations of 90 ng/µl, 45 ng/µl, and 20 ng/µl TALEN mRNA were used for pronuclear microinjection.

Figure 12: TALEN mRNA production for pronuclear microinjection. (**A**) Plasmid pCAG-TALEN-poly(A) contains a CAG promoter (CAG) and a bovine poly(A) signal sequence for expression of TALEN-Fus 15 proteins in mammalian cells. TALEN mRNA is produced from MluI linearised plasmid by a two-step procedure using T7 polymerase for *in vitro* transcription and poly(A) polymerase for polyadenylation. The arrow marks the translational start site. (**B**) Plasmid pT7-TALEN-95A provides a T7 promoter (T7), TALE coding regions, and a region of 95 adenine (95A) nucleotides preceded by an AleI site. TALEN-95A mRNA can be produced from the AleI linearised pT7-TALEN-95A plasmid in a single-step

by using only T7 polymerase. (**C**) Agarose gel electrophoresis of mRNA products, transcribed with T7 polymerase from MluI linearised pCAG-TALEN-Fus15-poly(A) plasmid followed by polyadenylation with poly(A) polymerase (left gel, TALEN-poly(A)) using the two step protocol, or from AleI linearised pT7-TALEN-Fus15-95A plasmid in a single step of *in vitro* transcription by using T7 polymerase alone (right gel, TALEN-95A). (D) Pronuclear microinjection of mRNA produced from pCAG-Venus-95A into one-cell mouse zygotes. The manipulated embryos were cultured to the two-cell stage, which were analysed for Venus expression by fluorescence microscopy (Top panel: bright light, lower panel: green fluorescence).

3.2 Modification of the *ROSA26* locus in human cells

The Rosa26-1-TALEN was designed and constructed to target the human *ROSA26* locus (Irion et al., 2007) having the specific chromosomal coordinates of Chr3: 94, 37,891: 94, 37, 938. Efficient nuclease activity of ROSA26-1-TALEN in the β-galactosidase reporter assay (Figure 8) promoted me to investigate whether human cell lines could be engineered for generating cellular genetic models. For the easy detection of ROSA26-1-TALEN mediated genome alterations, an AvrII site was chosen in the TALEN-B site, the loss of which in the TALEN modified cells act as an indicator of NHEJ or HR events (Figure 13A). ROSA26-1-TALEN were transfected into the HeLa cell line. After 10 days, genomic DNA was extracted from transfected cells and a PCR product covering the TALEN target site was amplified to investigate TALEN mediated editing events. However, PCR-RFLP and sequencing of the derived PCR products did not detect TALEN mutagenesis events, perhaps due to a predominant fraction of wild-type molecules masking the lower proportion of TALEN-modified cells. Hence to selectively enrich the mutant cell population, a novel reporter system was developed by cloning the neomycin-resistance protein (Neo^R) just after the β-galactosidase sequence in the pCMV-TALEN-Rep. After the co-transfection of ROSA26-1-TALEN and pCMV-TALEN-Neo^R-Rep into the HeLa cell line, 0.8 µg/µl of G418 treatment was administered at the 2nd and 3rd day post-transfection to enrich for the TALEN-modified cells. After 10 days of G418 treatment, the drug selected cells were subjected to DNA extraction and PCR amplification to investigate TALEN mediated genome editing events. Capillary electrophoresis of the AvrII digested PCR amplified products flanking the TALEN target site revealed a minor fraction of 61, 374, 430, and 486 bp fragments in association with digested wild-type fragments (152 bp, 355 bp) (Figure 13B, C). These results demonstrate the generation of various knockout alleles containing predicted sequence deletions of 448, 135, 79, and 23 bp nucleotides. In a heterogeneous population of cells, the estimated cleavage rate of ROSA26-1-TALEN was 8.30% and the estimated frequency of NHEJ events was 4.24%, calculated by using the formula: % Gene modification: 100* (1-(1-fraction cleaved)$^{1/2}$) (Reyon et al., 2012). Moreover, subsequent

DNA sequencing of the pooled PCR product derived from transfected colonies showed mixed sequence peaks that start after the TALEN-B site, confirming the generation of knockout alleles by NHEJ events (Figure 13D). Taken together, these results suggest that ROSA26-1-TALEN was effective for generating knockout mutations in a human cell line.
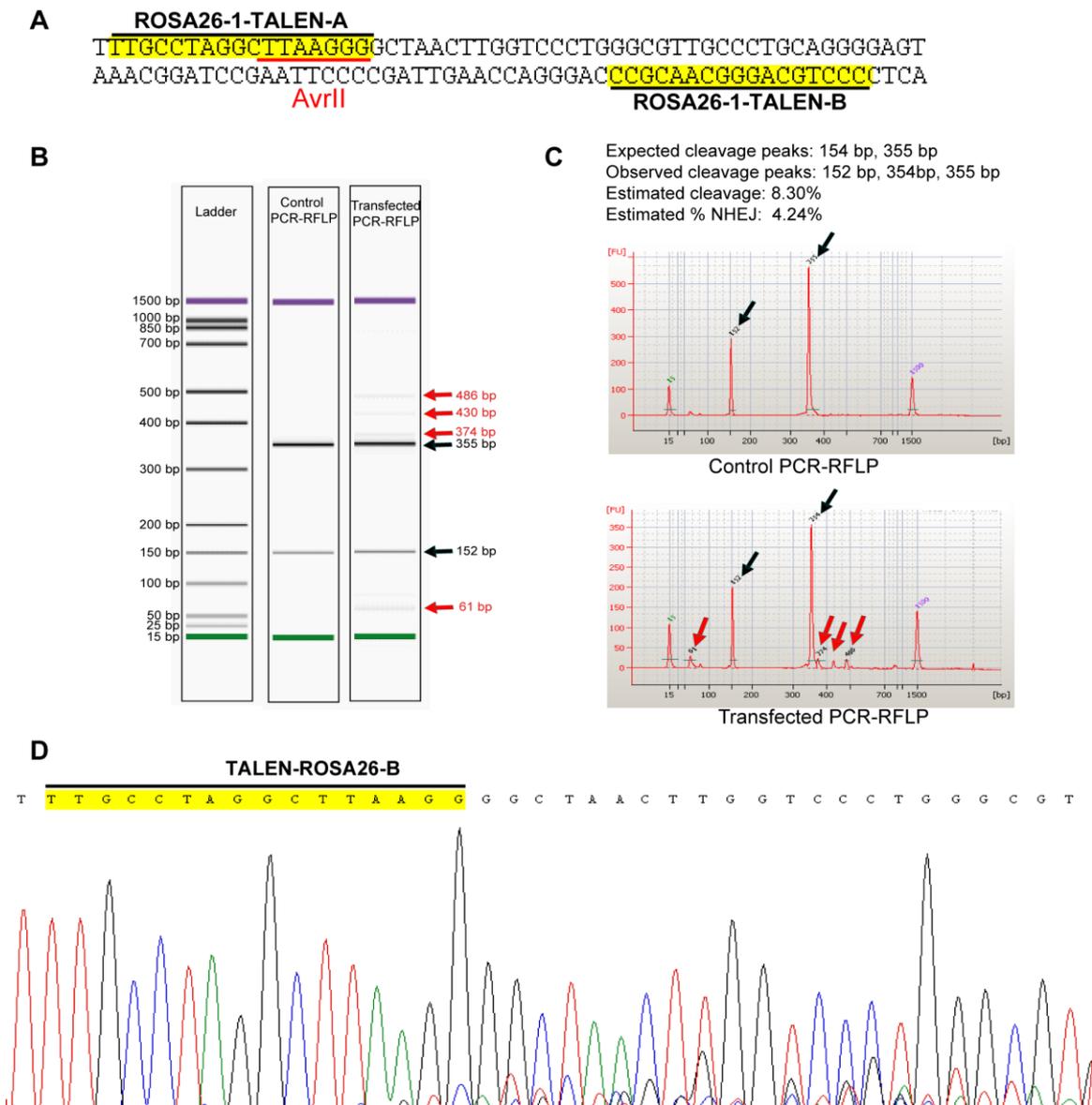
Figure 13: Modification of the human *ROSA26* locus in HeLa cells. (**A**) The binding sites of the ROSA26-1-TALEN pair (left and right) are highlighted in yellow; the AvrII site in the TALEN-B is underlined in red, as marker for detecting the TALEN mediated mutagenesis. (**B**, **C**) PCR-RFLP assay of AvrII digested PCR product of endogenous *ROSA26* locus derived from the HeLa cells transfected either with the negative control (pBlueScript II KS(+)) or together with the ROSA26-1-TALEN pair and pCMV-TALEN-Neo[R]-Rep is demonstrated in a virtual-gel image (B) and an electrophoretic trace (**C**). Black arrows indicate the AvrII digested PCR-RFLP cleavage products of the correct size, while the red arrows denote the uncleaved PCR products in both the virtual-gel and the electrophoretic trace

image. The sizes of the expected and observed fragments generated by the AvrII digestion of PCR products, the fraction of the PCR product cleaved, and estimated indel frequencies based on the quantification of cleaved and uncleaved PCR products using the equation described in methods are indicated. (**D**) Sanger sequencing of PCR products derived from the pool of transfected cells revealed the initiation of mixed peaks downstream of the TALEN-B site (highlighted in yellow) and continues to downstream suggesting the occurrence of NHEJ event in the spacer region.

3.3 Generation of mouse disease models

3.3.1 Generation of a *3110043O21Rik* knockout mouse disease model

To create frame shift mutations within the mouse *3110043O21Rik* homolog of the human *C9orf72* gene, I designed the TALEN pair (TALEN-Rik2) targeting a sequence located downstream of the start codon within the second exon of the murine *3110043O21Rik* gene (Figure 14 and Figure 15A, B). For the simple identification of TALEN mediated genome alterations, a BccI site was chosen in the spacer region of the TALEN binding sites (Figure 14A) for PCR-RFLP analysis. To investigate the dose-dependent effect of TALEN mediated mutagenesis events, two concentrations of TALEN-95A mRNA (90 ng/µl and 45 ng/µl) were injected into the pronucleus of one-cell embryos. Upon pronuclear microinjection of the 90 ng/µl and 45 ng/µl of TALEN-Rik2-95A mRNA preparation, 51 (51 of 165 = 31%) and 31 (31 of 120 = 26%) live pups were obtained from the transfer of manipulated embryos into the oviduct of the pseudo-pregnant CD1 females (Table 1).

3.3.1.1 PCR-RFLP and HRMA screening for the identification of Rik^{KO} alleles

Fifty-one pups derived from the microinjection of TALEN-Rik2 mRNAs (95A type, 90 ng/µl) were subjected to PCR-RFLP analysis of the founder's PCR products flanking the TALEN binding sites. The PCR-RFLP assay identified twenty-one mutant mice (21 of 51 = 41.2%) by exhibiting the predicted BccI resistant fragments (Figure S1). To further characterise TALEN induced sequence alterations, the founders PCR products were further examined using High Resolution Melt Analysis (HRMA). Representative HRMA results from mutant founders are shown (Figure 14C, Figure 15A, B), and the melting curve pattern of eight mutant founders distinguished from the wild-type control are shown (Figure S2). The melting profiles of PCR products derived from the founders R23, R29, and R33 showed a close association with the wild-type curve suggesting the presence of biallelic mutations. These founders were further characterised by subcloning of the PCR products amplified from tail DNA. Sequence analysis revealed the presence of either monoallelic or bi-allelic

3110043O21Rik mutant alleles (Figure 14A). Similarly, 31 pups derived from the microinjection of the TALEN-Rik2 mRNAs (95A type, 45 ng/µl) were subjected to PCR-RFLP analysis and identified twelve mutant mice (12 of 31 = 38.7%) exhibiting the characteristic BccI resistant fragments indicating the presence of mutant *3110043O21Rik* alleles. These results confirm that the pronuclear delivery of 95A type TALEN mRNAs leads to a high mutagenesis rate.

Table 1: TALEN mediated Rik^{KO} mutants

Micro injection	TALEN mRNA Conc. (ng/µl)	Transferred Embryos (n)	No of Pups (%)	Males (n)	Females (n)	No. of Mutants (%)	Founder´s NHEJ (%)
TALEN-Rik2	90	165	51 (30.9)	25	26	21 (41.2)	21 (41.2)
TALEN-Rik2	45	120	31 (25.83)	15	16	12 (38.7)	12 (38.7)

The table shows the number of mutant founder mice and mutant alleles obtained from the microinjection of Rik-TALENs into the pronuclei of one-cell mouse embryos. The concentration of TALEN mRNAs and the number of pups (males or females) obtained from the transfer of manipulated embryos into pseudo-pregnant females are given. The overall frequency of gene editing is determined by the number of mice harboring mutant alleles modified by NHEJ events in comparison to the total number of pups obtained from the transfer of manipulated embryos into pseudo-pregnant mice.

3.3.1.2 Characterisation of the Rik^{KO} founders

Eleven out of 21 mutant founders obtained from the pronuclear microinjection of TALEN-Rik2 mRNAs (95A type, 90 ng/µl) were chosen for further characterisation of modified *3110043O21Rik* alleles by subcloning and sequence analysis of PCR products. Sequence analysis of the subcloned PCR products of founders R5-R32 revealed the presence of 12 mutant alleles (Figure 14A), exhibiting deletions of 1-36 nucleotides or a two bp insertion within the TALEN target regions. The mutant alleles from four founders (R12b, R21, R24, and R33) showed 6 or 9 nucleotide deletions that preserve the same translational RIK reading frame. The 36 bp deletion present in founder R22 includes the start codon resulting in the complete ablation of the translational reading frame, however the translation of mutant mRNA may be initiated at a downstream ATG (codon 146) followed by scrambled 336 amino acids and a stop codon. Seven founders (R10, R12a, R5, R29, R18, R23, and R32) showing the disruption of the C9ORF72 reading frame by deletion of 6-9 amino acids and predicted translation of 8-11 additional amino acids (Figure 14B). This result showed that TALEN-Rik2 mRNAs (90 ng/µl and 45 ng/µl) strikingly enhanced *Rik* endogenous

genetic modifications in 41.2% (21/51) and 38.7% (12/31) of the pups obtained from pronuclear microinjections.

A

			Genotype
	TALEN-Rik2A	**TALEN-Rik2B**	
3110043O21Rik	GGATGTCGACTATCTGCCCCCCACCATCTCCTGCTGTTGCCAAGACAGAGA		
	BccI		
Founder			
R10	GGATGTCGACTATCTGCCCCCCACC-TCTCCTGCTGTTGCCAAGACAGAGA		Δ1bp
R12a	GGATGTCGACTATCTGCCCCCCACC-TCTCCTGCTGTTGCCAAGACAGAGA		Δ1bp
R12b	GGATGTCGACTATCTGCCCCCCAC------CTGCTGTTGCCAAGACAGAGA		Δ6bp
R5	GGATGTCGACTATCTGCCCCCCACCA-CTCCTGCTGTTGCCAAGACAGAGA		Δ1bp
R21	GGATGTCGACTATCTGCCCCCCAC------CTGCTGTTGCCAAGACAGAGA		Δ6bp
R24	GGATGTCGACTATCTGCCCCCCAC------CTGCTGTTGCCAAGACAGAGA		Δ6bp
R29	GGATGTCGACTATCTGCCCCC-A------CCTGCTGTTGCCAAGACAGAGA		Δ8/+1bp
R33	GGATGTCGACTATCTGCCCCCC---------TGCTGTTGCCAAGACAGAGA		Δ9bp
R18	GGATGTCGACTATCTGCCCCCCA----------CTGTTGCCAAGACAGAGA		Δ10bp
R23	GGATGTCGACTATCTGCC----------------------AAGACAGAGA		Δ23bp
R22	-------------//------------------TGTTGCCAAGACAGAGA		Δ36bp
R32	GGATGTCGACTATCTGCCCCCCACCATTTCTCCTGCTGTTGCCAAGACAGA		+2bp

B

		Predicted protein
3110043O21RIK	MSTICPPPSPAVAKTEIALSG/456 aa/LMTF*	**481aa**
Founder		
R10	MSTICPPPLLLLPRQRLL*	8 + 10 aa
R12a	MSTICPPPLLLLPRQRLL*	8 + 10 aa
R12b	MSTICPPP--AVAKTEIALSG/456 aa/LMTF*	Δ S9, P10 / 479 aa
R5	MSTICPPPLLLLPRQRLL*	8 + 10 aa
R21	MSTICPPP--AVAKTEIALSG/456 aa/LMTF*	Δ S9, P10 / 479 aa
R24	MSTICPPP--AVAKTEIALSG/456 aa/LMTF*	Δ S9, P10 / 479 aa
R29	MSTICPHLLLPRQRLL*	6 + 10 aa
R33	MSTICPP---AVAKTEIALSG/456 aa/LMTF*	Δ P8, S9, P10 / 478 aa
R18	MSTICPPLLPRQRLL*	7 + 8 aa
R23	MSTICQDRDCFKW*	5 + 8 aa
R22	--------------------/332 aa/LMTF*	Δ M1 - W145 /336 aa
R32	MSTICPPPFLLLLPRQRLL*	8 + 11 aa

C

		TALEN-Rik2A	TALEN-Rik2B
R23	GGATGTCGACTATCTGCC	----------------------	AAGACAGAGA
R23-15	GGATGTCGACTATCTGCC	----------------------	AAGACAGAGA

Figure 14: Generation of TALEN-RIK knockout alleles. (**A**) Sequence alignment of exon 2 of the mouse *3110043O21Rik* (analogous position of human *C9orf72*) gene in

comparison to the mutant alleles amplified by PCR from the tail DNA of founders produced by TALEN-Rik2 embryo injections. The translational start site of the *3110043O21Rik* gene is indicated by an arrow and the TALEN binding sites are marked. Nucleotide deletions or insertions are shown as red dashes or red letters, respectively. The genotype categorises mutant alleles as a product of NHEJ-associated deletion (Δ) or insertion (+); alleles exhibiting reading frame shifts are shown in red. Founder R12 contained two mutant alleles (R12a, R12b) showing the deletion of 1 or 6 bp, respectively. (**B**) Predicted amino acid sequence alignment of the 3110043O21RIK protein of the founders generated by TALEN-Rik2 mediated mutagenesis events. The founder's with distinct amino acids as compared to wild-type are indicated with red. All of the founders showed initial 5 to 8 amino acids sequence similarity to the wild-type, then either had deletion of 2-3 amino acids to remain in the reading frame of RIK protein (R12b, R21, R24, and R33) or generating new amino acids result in the out of translational reading frame of RIK protein (R10, R12a, R5, R29, R18, R23, and R32). Founder R22 lost the translational start site (Δ ATG) which resulted in complete ablation of translational reading frame or into translational initiation at the downstream ATG codon 146 and the production of a truncated protein. (**C**) Melting curve analysis of triplicate PCR products amplified from the tail DNA of founder R23 (red curves, overlaid) to their offspring R23-15 (blue curves, overlaid) compared to the wild-type littermate R23-18 (grey curves, overlaid). Sanger sequencing of the cloned PCR products from the offspring's revealed germ line transmission of the mutant R23 allele.

Furthermore, these results also demonstrated the striking enhancement of genomic editing by using an increased dose of TALEN mRNA. Since, 63% (7/11) of the characterised mutations lead to a truncated translational reading frame and *3110043O21Rik* knockouts mutants were produced at an effective rate of 41%, an average of only three pups is sufficient to obtain one knockout allele. In conclusion, TALEN 95A mRNAs and genotyping by HRM analysis enables the efficient production and identification of knockout mutants.

3.3.1.3 Germline transmission of mutant TALEN-Rik2 alleles

To confirm whether the TALEN induced mutations are transmitted to the next generation, founder R23 (WT/Δ 23 bp) was mated with wild-type and its progeny were genotyped by PCR-RFLP and HRMA. Nine of 19 pups derived from the R23 founder showed melting curves distinguished from wild-type control. Further sequencing of subcloned PCR products from the pup R23-15 confirmed the inheritance of the truncated *3110043O21Rik* alleles (Figure 14C). In conclusion, the TALEN mediated mutation was stably transmitted through the germline in a Mendelian fashion.

3.3.1.4 Sensitivity of HRMA for the detection of mutant alleles

Due to the postmitotic expression of TALEN, after the division of one-cell embryo, it is possible that multiple mutant alleles are independently generated in the same individual,

resulting in mosaicism. Therefore founders obtained from nuclease microinjections frequently exhibit a mosaic mutation pattern in somatic and germ cells (Wefers et al., 2013a). To access whether mosaic mutants can be recognised by HRM analysis, a limiting dilution experiment was performed to evaluate the sensitivity of HRMA for identification of a minor fraction of mutant alleles coexisting in the dominant population of wild-type alleles. For this purpose, Benedikt Wefers prepared test samples containing 1-50% of cloned, mutant *C9orf72* PCR products (R5 allele, 1-bp deletion; R12, 6-bp deletion) (Figure 15A, B) and 99-50% of wild-type PCR product. The presence of mutant alleles could be reliably detected by HRMA in samples containing 5% (1-bp deletion) or 2.5% (6-bp deletion) of mutant DNA (Figure 15C, D). These results demonstrated that even mosaic founders harboring a minor fraction of mutant alleles can be easily identified by melting analysis and validate HRMA is a very simple and sensitive tool to identify mutants derived from pronuclear microinjection of TALENs.

Figure 15: Identification of *Rik* mutants by HRMA and setup the sensitivity limit of HRMA. Melting curve analysis of the mutant founder R5 (**A**) (WT/ 1 bp Δ) and R22 (**B**) (WT/ 36 bp Δ), generated by TALEN-Rik2 are shown in red curves in comparison to the wild-type controls (grey curves). The target sequence of the TALEN-Rik2 in exon 2 of *Rik* is shown and the start codon is underlined. Deleted nucleotides in mutant alleles are shown as red dashes and genotypes are specified in parentheses. In order to study the sensitivity of HRMA, a

gradual decline of the population of mutant allele R5 (1bp Δ; **C**) and R12 (6 bp
Δ; **D**) was prepared by increasing the wild-type population. The limit to detect
the R5 allele was found at 5% of mutant product (green curves), and at 2.5%
for the R12 allele (turquoise curves).

3.3.2 Generation of Fus^{R513G} and Fus^{P517L} codon replacement mutants

To recapitulate the patient derived codon replacements R513G and P525L in the
mouse *Fus* gene, the analogous positions R513 and P517 were targeted using single-
stranded oligonucleotides (ODNs) as template for TALEN-induced HR. A TALEN pair was
designed and constructed to target the C-terminal exon 15 of *Fus* at the chromosomal
coordinates Chr7:127,981,782:127,981,830 (Figure 16B). The oligonucleotides ODN^{R513G}
and ODN^{P517L} contained 70 bp homology sequences (upstream and downstream) covering
exon 15, and included nucleotide replacements redefining codons 513 and 517 into glycine
(R513G) or leucine (P517L), respectively.

To avoid further processing of recombined alleles by TALEN activity, each
oligonucleotide included one silent mutation located within the TALEN-B recognition site
(Figure 16C). In addition, these replacements create a BccI (R513G model) or a BsmaI
(P517L model) restriction site and erase a HaeIII site, enabling the identification of the
targeted alleles by the simple digestion of PCR products.
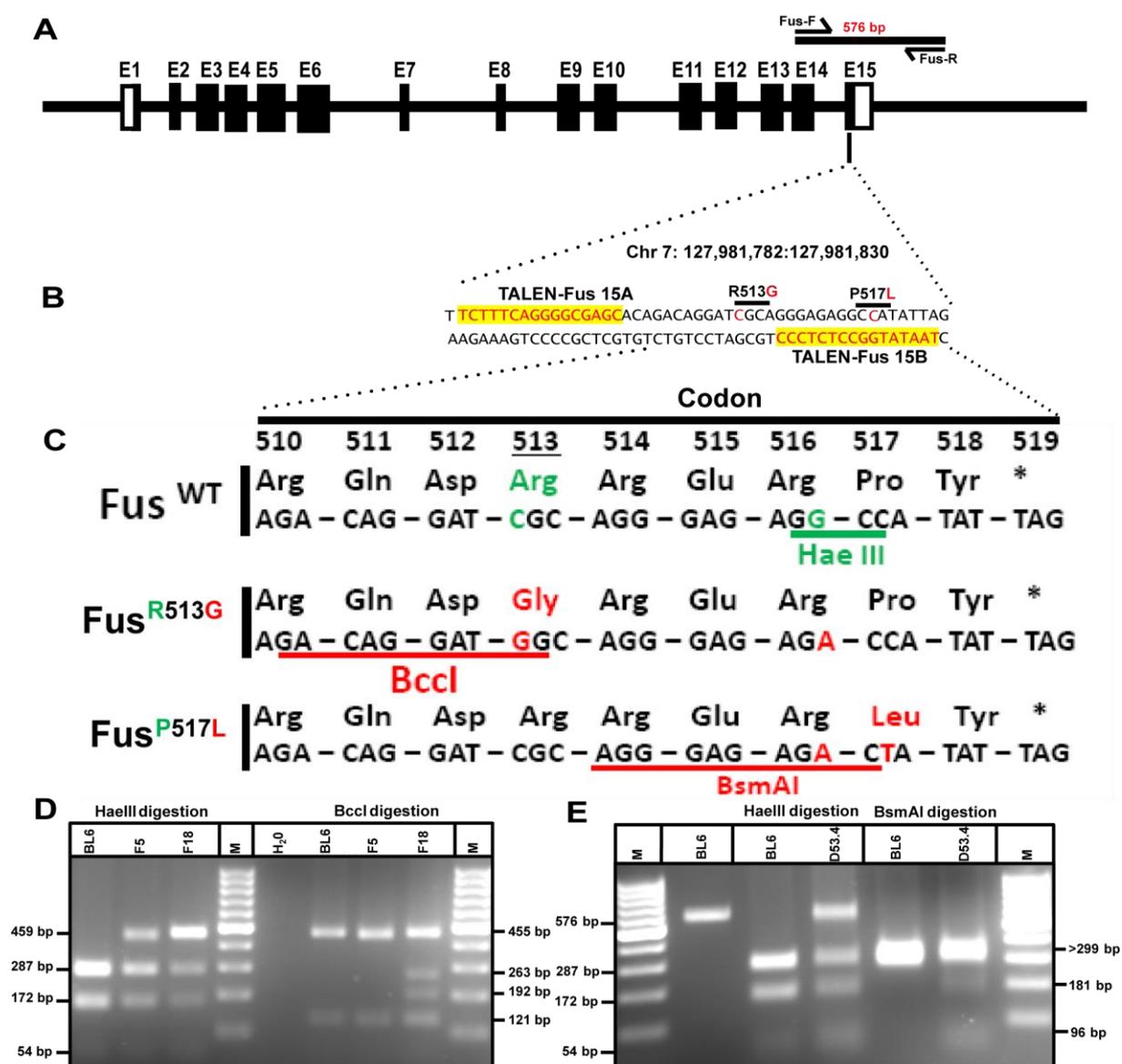
Figure 16: Overview of TALEN-Fus 15 mediated genome editing. (**A**) Schematic drawing of the *Fus* locus. Filled squares represent exons (E) and the open box indicates the exon including the untranslated regions (UTR). Fus-F and Fus-R are genotyping primers for identification of TALEN mediated mutagenesis events. (**B**) Highlight of the TALEN binding sites (in yellow) within exon 15 of *Fus* including the specific chromosomal coordinates. (**C**) Codon comparison of synthetic oligonucleotides (ODN[R513G], ODN[P517L]) and the wild-type sequence. Nucleotides, amino acids, and restriction sites that deviate from wild-type (green) are marked in red. * indicates the stop codon. (**D**) HaeIII and BccI digested PCR products of founders F5 and F18 derived from ODN[R513G] injection. The undigested HaeIII (459 bp) and digested BccI (263 bp, 192 bp) fragments indicate TALEN mediated mutagenesis events. (**E**) PCR-RFLP assay of the HaeIII and BsmAI digested PCR products of founder F4 derived from ODN[P517L] injection. The undigested HaeIII (>459 bp) and digested BsmAI (181 bp, 96 bp) fragments indicated TALEN mediated mutagenesis event. BL6: DNA from a C57BL/6N mouse.

36

3.3.2.1 PCR-RFLP and HRMA screening for identification of Fus^{R513G} and Fus^{P517L} allele

The single-stranded ODN^{R513G} or ODN^{P517L} targeting molecules together with the TALEN-Fus 15 mRNA (95A type, 20 ng/µl) were microinjected into the pronuclei of one-cell F$_1$ (C57BL/6N$^{\male}$×FVB$^{\female}$) mouse embryos. ODN^{R513G} injections yielded 83 pups (37%) from 227 transferred embryos, and ODN^{P517L} injection yielded 50 pups (38%) from 133 transferred embryos (Table 2). The fraction of live births was considerable higher in TALEN-Fus 15 microinjections as compared to the TALEN-Rik2 microinjection. All pups were screened for TALEN mediated mutagenesis events by PCR-RFLP and HRMA by PCR amplification of the TALEN target region using tail DNA. The samples of eight mice (9.6%) (ODN^{R513G} injection) and two mice (ODN^{P517L} injection) showed characteristic mutant fragments upon PCR-RFLP, and also showed distinguished melting curve profiles as compared to wild-type controls in the HRM analysis (Figure S3). As a representative, PCR-RFLP assay of founders F5, F18 (ODN^{R513G} injection), and F4 (ODN^{P517L} injection) showed the resistance of the 459 bp fragment to HaeIII digestion as compared to the wild-type control, indicating the occurrence of mutagenesis events (Figure 16D, E, left gel panel). Furthermore, the BccI digested PCR-product of founder F18 (ODN^{R513G} injection) showed the predicted 263 and 192 bp fragments as compared to wild-type, indicating the occurrence of HR (Figure 16D, right gel panel). Similarly, BsmAI digested PCR-product of founder F4 (ODN^{P517L} injection) showed the predicted 181 and 96 bp fragments as compared to wild-type, indicating the occurrence of HR (Figure 16E, right gel panel).

3.3.2.2 Characterisation of Fus^{R513G} and Fus^{P517L} mutant founders

The eight mutant founders obtained from ODN^{R513G} injections and two mutant founders from ODN^{P517L} injections were further characterised by subcloning and sequencing of PCR products flanking the TALEN binding sites. The sequence analysis of five clones each from eight mutant founders derived from the ODN^{R513G} injection revealed 14 mutant *Fus* alleles. In particular, four founders contained the desired R513G codon replacement together with (F69a, F70a) or without (F29, F37a) the silent replacement in the TALEN-Fus 15B target site. Three founders (F75a, F75b, F75c, F18, and F79) showed recombined Fus^{R513G} alleles along with unintended single or double nucleotide alterations (Figure 17A) as anticipated consequence of ODN synthesis errors. Indeed, a further characterisation of the 140 nt of ODN^{R513G} was performed by PCR amplification, subcloning, and sequencing of the clones, revealing a substantial fraction (1/3) of variant molecules in the pool of ODN^{R513G} (data not shown) molecules. Furthermore, four founders (F37b, F70b, F75d, and F5)

harboured additional modified *Fus* alleles that underwent nucleotide deletions from 1 to 57 bp without any HR event. Founder F69 exhibited nucleotide replacements within codon 512 (F69b) along with the desired recombined R513G codon replacement. Likewise, sequencing of five PCR subclones, each of the two mutated founders generated from ODN^{P517L} microinjection revealed the presence of the Fus^{P517L} recombined allele together with the silent replacement (F4, F36a) located two nucleotide upstream of the intended mutation in the TALEN-Fus 15B target region. Founder F36 was mosaic for one recombined allele with a 14 bp deletion (F36b), and another knockout allele having 12 bp deletion (F36c) due to NHEJ repair (Figure 17B).

3.3.2.3 Germline transmission of the Fus^{R513G} and Fus^{P517L} codon replacement alleles

For the establishment of *Fus* mutant mouse lines, six Fus^{R513G} founders (F5, F18, F29, F37, F70, and F75) derived from ODN^{R513G} injections, and one Fus^{P517L} founder (F36) generated from ODN^{P517L} were mated to wild type C57BL/6N mice. The resulting offsprings were genotyped by PCR and HRMA. Eight (53%) of 15 pups derived from founder F29 (Fus^{R513G}) and eight (67%) of 12 pups derived from the founder F36 (Fus^{P517L}) showed melting curves clearly differing from the wild-type control by HRMA. The subcloning and sequence analysis of PCR products confirmed the germline transmission of the parental Fus^{R513G} (Pup F29-24, Figure 17C) and Fus^{P517L} alleles (Pup F36-12, Figure 17D). Similarly the subcloning and sequencing of PCR products from the offspring of founder F18 revealed the germline transmission of the parental Fus^{511} allele at a rate of 56% (13/23) (Pup 18-11, Figure S4). All six mutant Fus^{R513G} alleles and one mutated Fus^{P517L} allele were faithfully inherited at a rate of 10-67% to next generation, arguing for a normal Mendelian inheritance of TALEN induced alleles (Table S2). These results demonstrate that TALEN and ODNs generated 6.8% recombination at *Fus* loci derived from the microinjection (One recombined founder per 15 pups, Table 2), and that mutations identified in the tail DNA of founders were faithfully inherited through their germline. In conclusion, mutagenesis by TALEN 95A mRNAs and ssODN, and genotyping by HRM analysis enables the efficient generation, and identification of targeted mouse mutants.
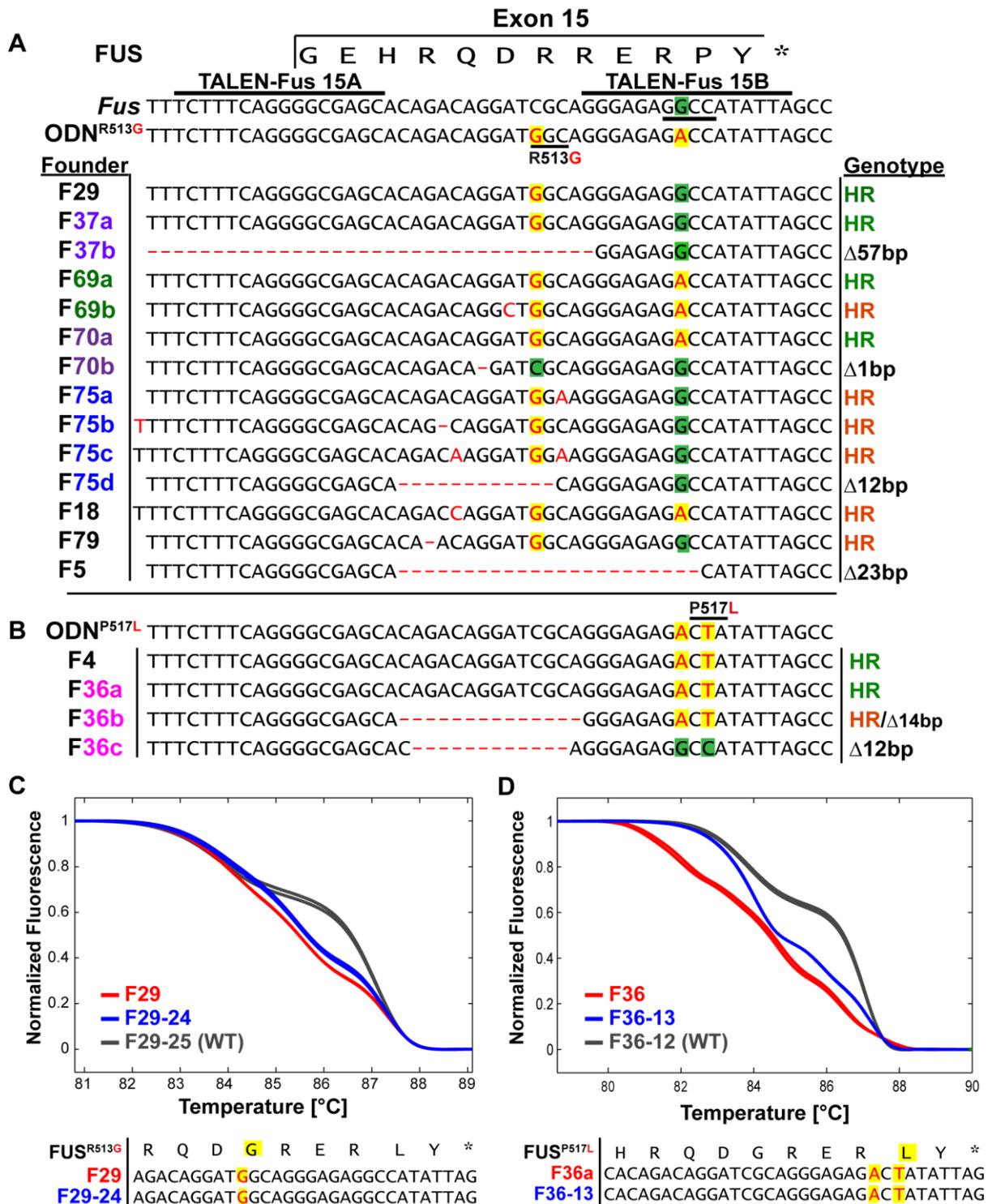
Figure 17: Generation of Fus[R513G] and Fus[P517L] mutants using TALEN-Fus 15 and ODNs. Sequence comparison of TALEN target regions within the *Fus* exon 15, of ODN[R513G], ODN[P517L], and cloned PCR products amplified with primers Fus-F and Fus-R using tail DNA from mutant founders derived from ODN[R513G] (**A**) or ODN[P517L] (**B**) microinjections, identified by both PCR-RFLP and HRMA. The exon 15 coded *Fus* sequence, the TALEN binding sites and codons 513 and 517 are shown. Nucleotides deviating from wild-type (green background) are shown in red on a yellow background. Nucleotide deletions or insertions are shown as

red dashes or in red letters. The mutants genotyped are classified as a product of either homologous recombination (HR) or NHEJ-associated deletion (Δ) or insertion (+). Melting analysis of duplicate PCR products from tail DNA of founder F29 (ODN[R513G]) (**C**) (red curves), its offspring F29-24 (blue curves) or of founder F36 (ODN[P517L]) (**D**) (red curves) and its offspring's F36-13 (blue curves) in comparison to wild-type controls (grey curves). Sequence analysis of cloned PCR products from pups F29-24 and F36-13 reconfirmed the germline transmission of the Fus[R513G] and Fus[P517L] alleles.

Table 2: TALEN mediated Fus[KI] codon replacement mutants

Microinjection	TALEN Conc. (ng/µl)	Transferred Embryos (n)	No of Pups (%)	Males (n)	Females (n)	No. of Mutants (%)	Founder´s NHEJ (%)	Founder´s HR (%)
TALEN-Fus15 + ODN[R513G]	20	227	83 (36.6)	40	43	8 (9.6)	8 (9.6)	7 (8.4)
TALEN-Fus15 + ODN[P517L]	20	133	50 (37.6)	31	19	2 (4)	2 (4)	2 (4)
TALEN-Fus15 ∑			133			10 (7.5)	10 (7.5)	9 (6.8)

Numbers of mutant founder mice and mutant alleles obtained from the microinjection of TALEN-Fus 15 together with mutagenic ODN[R513G] or ODN[P517L] into pronuclei of one-cell mouse embryos. The concentration of TALEN mRNAs and number of pups (males and females) obtained from transfer of manipulated embryos to pseudo-pregnant mice are shown. The overall frequency of gene editing is determined by number of mice harboring mutant alleles modified by HR or NHEJ events. Half of the founders derived from TALEN-Fus 15 microinjection are mosaics, containing more than one modified allele. Therefore, the combined number of mice exhibiting alleles modified by NHEJ or HR exceeds the total number of mutant founders.

3.3.2.4 Sequencing analysis of Fus[R513G] and Fus[511] loci

To further confirm the integrity of the targeted Fus[R513G] and Fus[511] loci, genomic sequences covering 3.5 kb upstream and 3.3 kb downstream region of the codon 513 were PCR amplified using the tail DNA of the heterozygous pup F29-24 (Fus[R513G]) or pup F18-11 (Fus[511]) (Figure 18A). Direct sequencing of the both PCR products of pup F29-24 harbouring the wild-type and the Fus[R513G] alleles revealed the presence of the wild-type sequence except for C to G replacement in the codon 513 that showing the mixed G/C peak (Figure 18B). Similarly, direct sequencing of both PCR products from pup F18-11 harbouring wild-type and Fus[R513G] alleles revealed the start of doubled peak at codon 511 that showing mixed C/A peak (Figure 18C) by erroneous insertion of C nucleotide, along with the G to C nucleotide replacement at codon 513 through the process of homologous recombination.

These results confirmed the genomic integrity of the Fus[R513] and Fus[511] alleles within a region of 6.6 kb, centreed on codon 513.
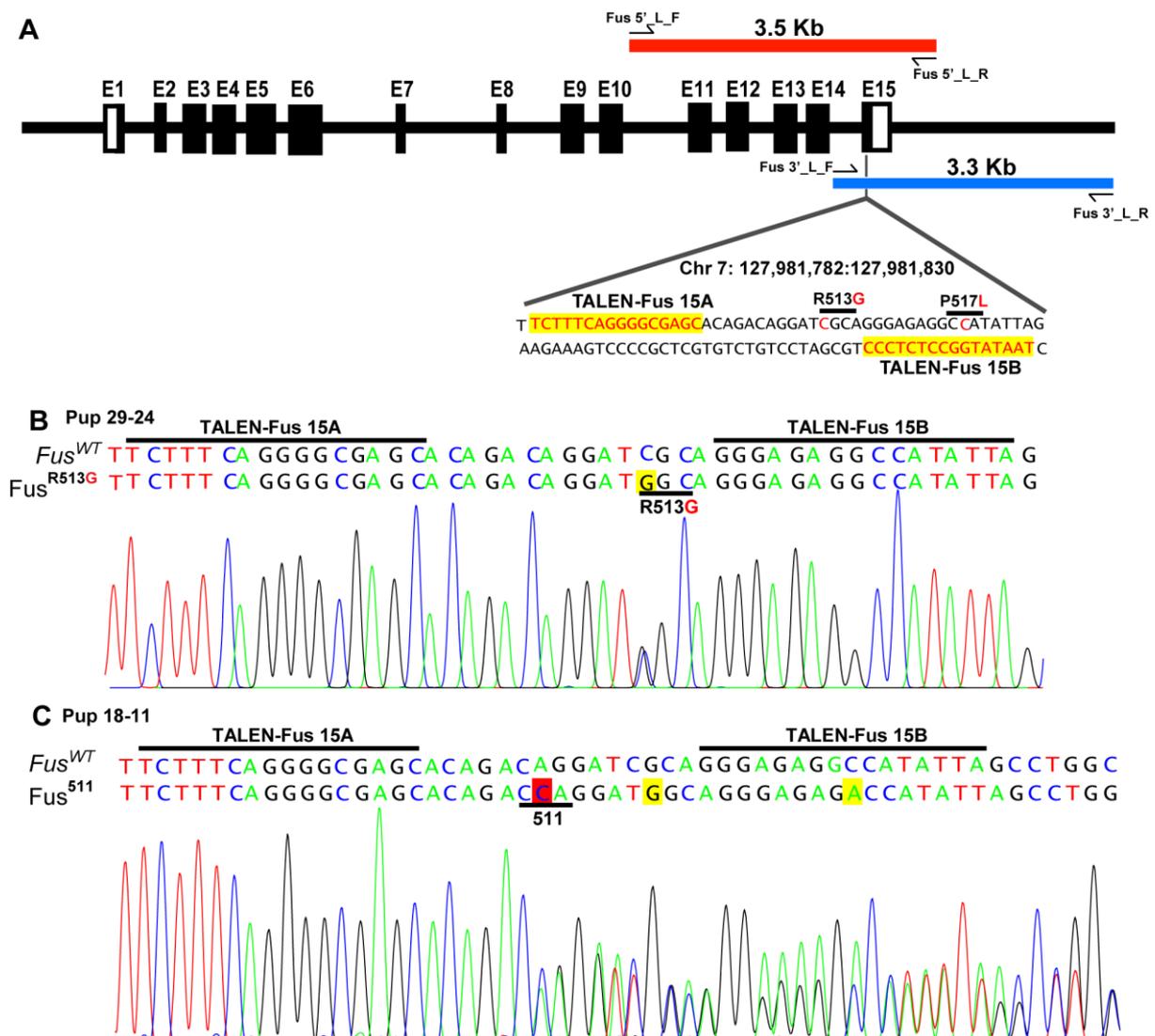
Figure 18: Sequence analysis of the Fus[R513G] and Fus[511] alleles. (A) Schematic illustration of exonic and intronic regions of the *Fus* locus with the chromosomal coordinates, where TALEN binding sites are located. PCR amplification of 3.5 kb upstream and 3.3 kb downstream from the tail DNA of offsprings (F29-24 and F18-11) having overlapping codon 513 region. **(B)** Chromatogram analysis depicts the sequencing peaks of the direct PCR products of F29-24 covering the sequence around codon 513 showing the mixed peak at the position of targeted Fus[R513G] nucleotide replacement. **(C)** Chromatogram analysis depicts the sequencing peaks of the direct PCR products of pup F18-11 showing mixed peaks starting at the codon 511 due to unintended nucleotide insertion.

3.3.2.5 Sequence analysis of the Fus[R513G] and Fus[511] transcript

To further analyse the functionality and transcription of the Fus[R513G] and Fus[511] alleles, total mRNA was isolated from the tail of the pups F29-24 and F18-11, and reverse

transcribed into cDNA. Consequently, the *Fus* transcript was amplified, flanking the exon 14 and 15, and the partial 3´ UTR region harboring the TALEN target site. Moreover, these PCR products were cloned and sequenced to confirm the functionality of the targeted alleles.
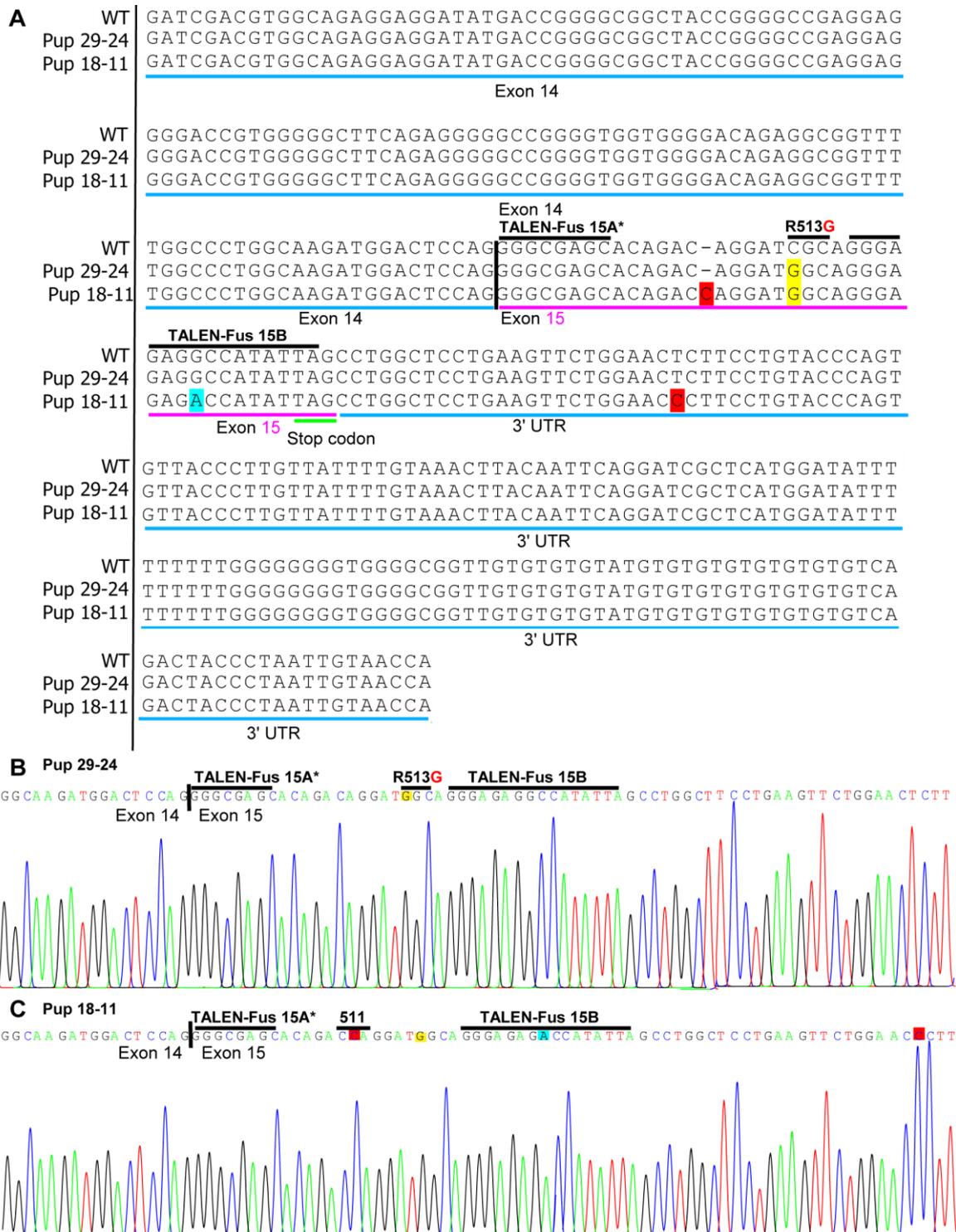
Figure 19: Sequence analysis of Fus^{R513G} and Fus^{511} cDNA. (A) Sequence comparison of the cloned PCR products representing 341 bp of the *Fus* cDNA sequence, including exons 14, 15 and

3´UTR sequences derived from the mutant pups F29-24 and F18-11 in comparison to the wild-type cDNA sequence. Chromatogram shows the sequencing peaks of the cloned PCR products derived from pup F29-24 **(B)** and Pup F18-11 **(C)** covering the codon 513 and 511 of *Fus*. The position of exon 14, exon 14-15 boundary (|), exon 15, stop codon, 3´ UTR, and TALEN binding sites are indicated. The codon replacement and unintended nucleotide insertion are highlighted on a yellow or red background, respectively. * indicates the partial TALEN-Fus 15A target site.

Upon sequencing of five cDNA clones from each founder, the sequence alignment revealed the C/G nucleotide replacements in pup 29-24, and showing frameshift (by insertion of C nucleotide) at codon 511 in pup 18-11 as compared to wild-type, which support the previous PCR sequence result (Figure 19A). The chromatogram analysis of the cloned PCR products revealed spliced cDNA sequences including the R513G codon replacement in pup 29-24 (Figure 19B) and generation of new codon (at 511 position) in pup 18-11 (Figure 19C). Overall, this transcript analysis suggests the functionality of the TALEN mediated Fus^{R513G} and Fus^{511} alleles.

3.3.2.6 Phenotypic analysis of the *Fus* mutants generated by TALEN microinjection

To investigate whether the alteration of the FUS C-terminus disturbs its nuclear localisation, mouse embryonic fibroblast cells (MEFs) were isolated from heterozygous F_2 embryos (E 13.5), harbouring the autosomal dominant Fus^{R513G}, Fus^{P517L}, or frameshift Fus^{511} allele (a kind gift from Michaela Bosch).

3.3.2.6.1 Cytoplasmic FUS mutants translocate reversibly into stress granules upon cellular stress

The FUS protein fulfills multiple functions in the RNA transcription, pre-mRNA splicing, transport, export to neuronal dendrites, and its mutation affects its subcellular localisation. The brain and spinal cord of ALS patients showed consistently stained with markers of increased oxidative stress (Barber et al., 2006). To investigate whether oxidative stress influences the functionality of the FUS protein, mutant MEFs harboring the heterozygous Fus^{R513G} or homozygous Fus^{511} allele were exposed to 0.5 mM sodium arsenite for 1 hour, which enhances the intracellular ROS (Lii et al., 2011) and is known to induce stress granules (Thomas et al., 2009). Immunofluorescence analysis using the anti-TIA-1 (T-cell-restricted intracellular antigen-1) stress granule marker revealed that >60% of cells having Fus^{511} and Fus^{R513G} alleles produced stress granules upon exposure to arsenite

(Figure 20) as compared to untreated cells. However, in wild-type cells, there was no formation of stress granule upon exposure to sodium arsenite treatment.
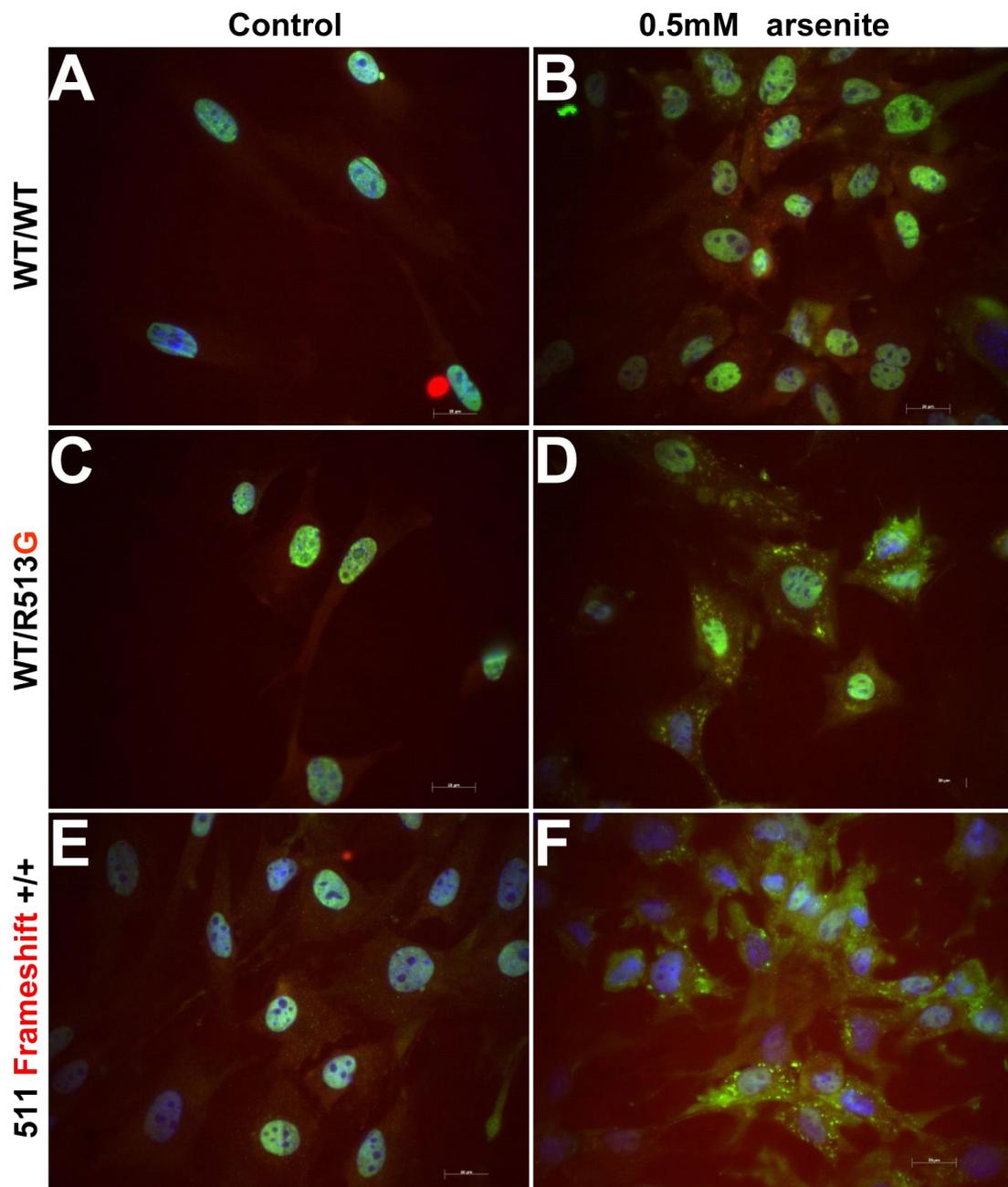
Figure 20: Mutant FUS co-localises with stress granule markers in the cytoplasm. Immunofluorescence stainings of mouse embryonic fibroblast cells derived from the 13.5 days old embryos harbouring the heterozygous codon replacement (Fus^{R513G}) or the homozygous frameshift (Fus^{511}) allele. Each culture was treated with 0.5 mM arsenite for 1 hour, and stained with anti-FUS (green), anti-TIA-1 (red) antibodies, and nuclear dye DAPI (blue). The Fus^{R513G} (**D**) as well as the Fus^{511} frame shift mutant (**F**) indicates co-localisation of FUS with the TIA-1 stress granule marker in the cytoplasm, while in wild-type remained in

nucleus and did not affect the sub-cellular distribution of the stress granule marker. The genotypes of the cell lines are shown at the left. Magnification, 630x

This result was consistent with the observation under the same conditions in HEK293, CV-1 and rat cortical neuron cell types (Bosco et al., 2010; Dormann et al., 2010; Vance et al., 2013) and demonstrated that the acute formation of stress granule was not compromised in the fALS linked FUS mutant cells. Overall, these results suggest fALS linked mutants (Fus^{511}>Fus^{R513G}) but not wild-type FUS, were dynamically and reversibly incorporated into stress granules in response to oxidative stress that impairs cellular translation initiation.

3.3.3 Off-target analysis of TALEN-Fus 15 and TALEN-Rik2

TALENs may recognise unintended genomic sites, which are very similar to the intended target sequence and may cause genomic alterations at such off-target sites. To access the frequency of such off-target effects in mutant founders derived from TALEN microinjections, four *Fus* and two *Rik* founders were analysed at five potential TALEN off-target sites (Table S3) were selected according to Doyle et al., (2012).

HRMA was performed by PCR amplification of tail DNA of mutant founders covering these off-target sites as compared to wild-type controls. The melting curves of the five off-target sites of TALEN-Rik2 (Figure 21A) and three off-target sites of TALEN-Fus 15 (Figure 21B) mutants were identical to the wild-type control, whereas the melting profile of TALEN-Fus off-site one and three from mutants were clearly distinguished from the control (marked by * and #). The further investigation of these off-target sites by sub-cloning and sequencing of PCR products revealed single-nucleotide polymorphisms existing in genome of the inbred mouse strains (Figure S5) that were used for in-house embryo production. Thus, these results argue against the presence of off-target mutations in the genome of mutant founders obtained from embryo microinjections of TALENs.
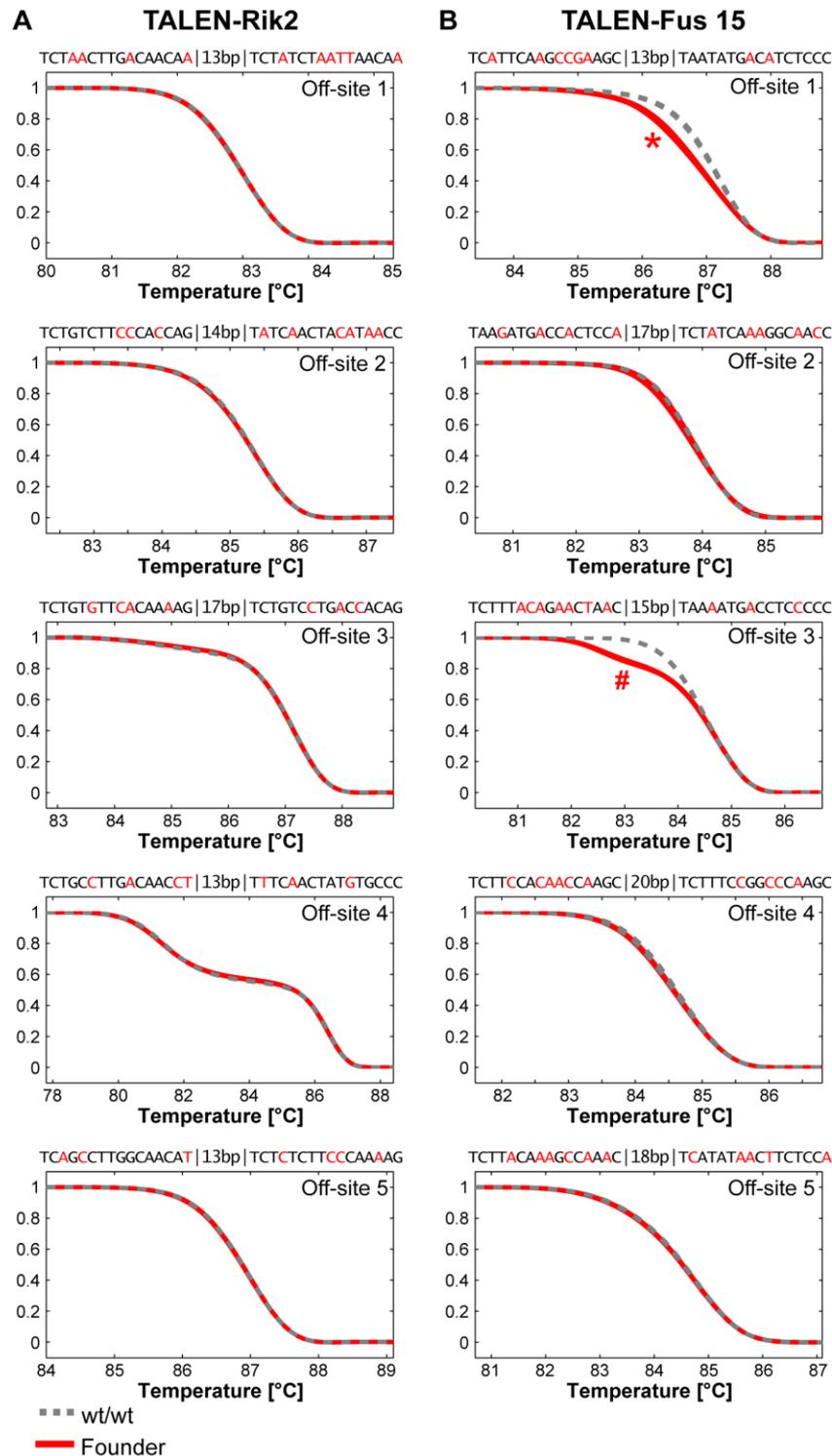
Figure 21: Genome-wide off-target analysis of TALEN-Rik2 and TALEN-Fus 15. Melting curve analysis of putative off-target sites of TALEN-Rik2 **(A)** and TALEN-Fus 15 **(B)** of wild-type mice and mutant founders (R5, R32 and F5, F29, F4, F36). The potential TALEN off-target sequence, spacer length, and mismatches (red letters) for the *3110043O21Rik* and *Fus* target sites are indicated. HRMA revealed no difference in between the founders (red curves) and wild-type controls (dotted grey curves), except for the *Fus* off-site 1 (*) and 3 (#), which were identified as polymorphisms present in variant genetic backgrounds.

3.4 CRISPR/Cas9: RNA guided genomic editing

3.4.1 Nuclease activity of CRISPR/Cas9 in comparison to TALENs and ZFNs

To test whether the CRISPR platform (Cas9 and sgRNA) could be used for mammalian genome editing, Oskar Ortiz constructed four plasmids encoding sgRNAs specific to sequences within intron 6, 8, and exon 14 of *Fus* (hereinafter called as sgRNA$^{Fus\#6}$, sgRNA$^{Fus\#8}$, and sgRNA$^{Fus\#14}$), and exon 1 of *Rab38* (sgRNA$^{Rab\#1}$).

A

Fus14 TALEN	+	-	-
Fus14 reporter	+	-	-
mCas9	-	+	+
sgRNA$^{Fus\#14}$ + Fus gRNA#14 reporter	-	+	-
sgRNA$^{Rab\#1}$ + Rab gRNA#1 reporter	-	-	+

B

Rab38 Cht-ZFN	+	-	-	-	-
Rab38 Cht-ZFN reporter	+	-	-	-	-
mCas9	-	+	+	+	+
sgRNA$^{Fus\#14}$ + Fus gRNA#14 reporter	-	+	-	-	-
sgRNA$^{Rab\#1}$ + Rab gRNA#1 reporter	-	-	+	-	-
sgRNA$^{Fus\#6}$ + Fus gRNA#6 reporter	-	-	-	+	-
sgRNA$^{Fus\#8}$ + Fus gRNA#8 reporter	-	-	-	-	+
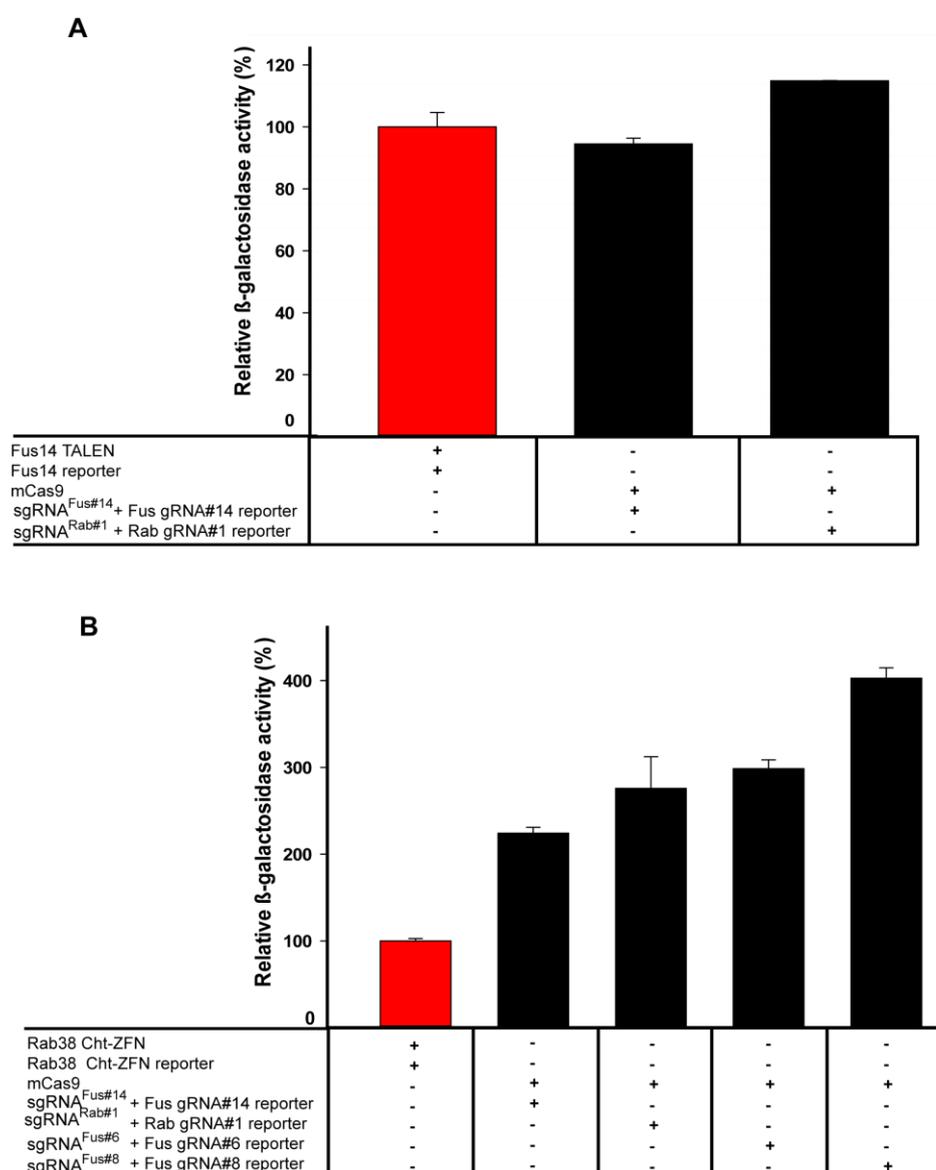
Figure 22: Efficiency of the CRISPR/Cas9 system in comparison to TALENS and ZFNs. (**A**) The reporter assay in HEK293 cells shows the relative ß-galactosidase activity of the sgRNA$^{Fus\#14}$ and sgRNA$^{Rab\#1}$ constructs (black bars) as compared to TALEN-Fus 14, which was used as internal control (red bar). (**B**) Similarly, the

nuclease activity of the sgRNA[Fus#14], sgRNA[Rab#1], sgRNA[Fus#6], and sgRNA[Fus#8] constructs (black bars) were compared to the Rab38 Cht-ZFN, which was used as internal control (red bar).

Each sgRNA plasmid was co-transfected with a Cas9 expression vector into HEK293 cells. Two days later, the nuclease activity of these sgRNA constructs was evaluated by measuring the relative ß-galactosidase activity in comparison to the internal control (Fus14 TALEN or Rab38 Cht-ZFN), as described above. The sgRNA[Fus#14] and sgRNA[Rab#1] constructs exhibited nuclease activity comparable to TALEN-Fus 14 (Figure 22A); whereas sgRNA[Fus#14], sgRNA[Rab#1], sgRNA[Fus#6], and sgRNA[Fus#8] showed a more than two-fold higher nuclease activity as compared to Rab38 Cht-ZFN (Figure 22B). These results showed that the two component CRISPR/Cas9 system (sgRNA+Cas9) represents an efficient genome modification system for mammalian cells, comparable to TALENs and ZFNs technologies. Furthermore, these results motivated me to apply this novel tool directly into the one-cell embryos for the expedite creation of new mouse models.

3.4.2 One step generation of single-gene mutant mice by pronuclear microinjection

To examine whether CRISPR/Cas9 could be used for generating mutant mice, capped Cas9-95A and sgRNA transcripts were produced by a single step of *in vitro* transcription and injected together into the pronuclei of one-cell mouse embryos, followed by genotyping of the derived offspring.

3.4.2.1 Generation of *Rab38* knockin mutants

In order to evaluate the frequency of homologous recombination events mediated by the CRISPR/Cas9 system in one-cell mouse embryos, sgRNA was constructed to target exon 1 of *Rab38* gene (sgRNA[Rab#1]) (Figure 23B). RAB38 is a member of the *Rab* small G protein family that regulates intracellular vesicle trafficking and melanosome biosynthesis (Osanai et al., 2005). A 140 nt single-stranded oligodeoxynucleotide (ODN[Rab#1]) including two point mutations and 10 silent mutations was used as targeting template molecule for double-strand break (DSB) induced homologous recombination. Upon pronuclear microinjection of capped Cas9-95A mRNA (67 ng/µl), sgRNA[Rab#1] (20 ng/µl) and single-stranded ODN[Rab#1] (30 ng/µl) into the pronucleus of mouse zygotes (Figure 23A), 94 live pups (31.9%) were recovered from 295 transferred embryos (Table 3). Notably, the birth rate of CRISPR/Cas9 injected embryos was comparable to the microinjection of TALEN mRNAs.
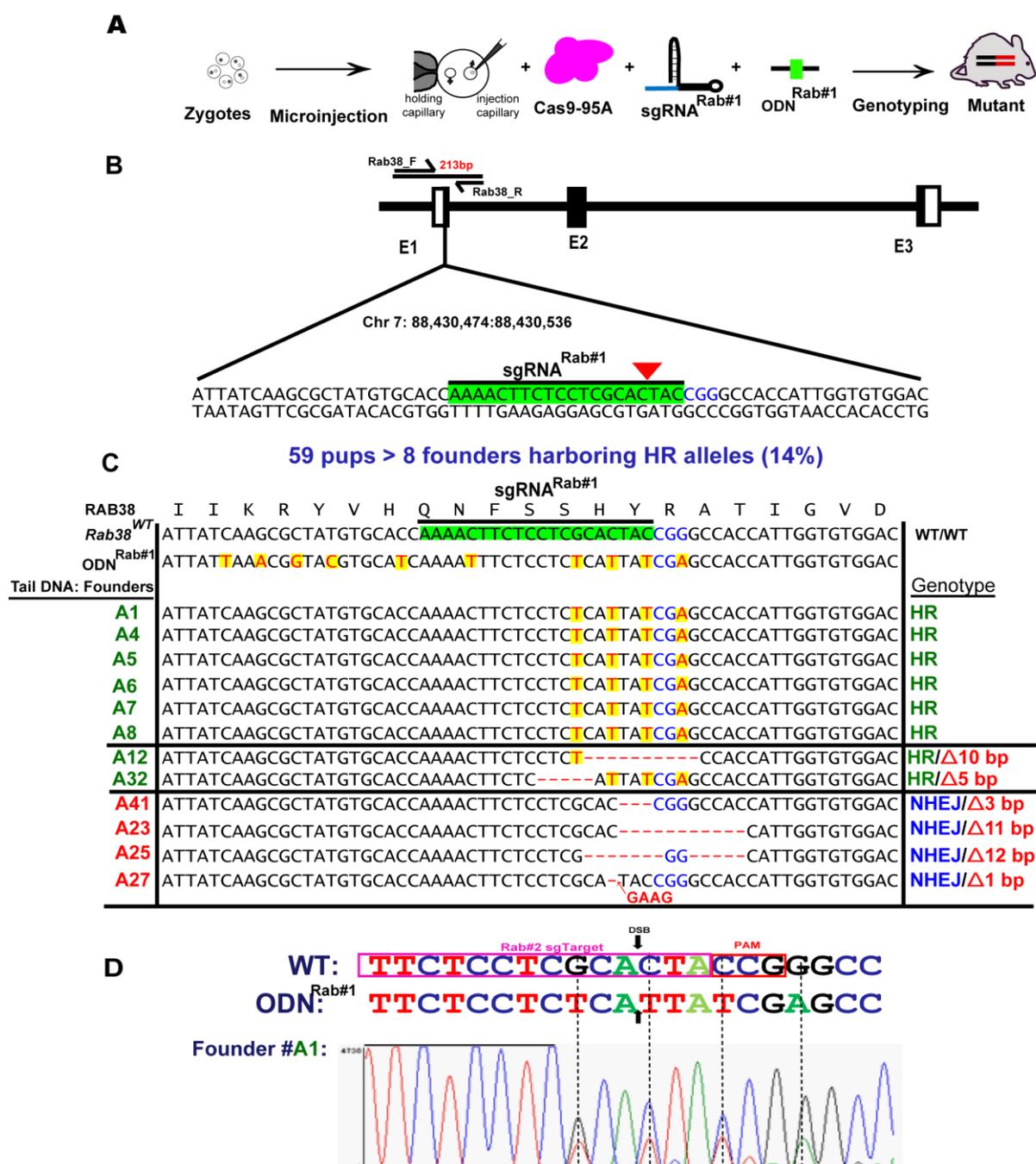
Figure 23: Generation of *Rab38* targeted knockin mice by Cas9-95A, sgRNA[Rab#1], and ODN[Rab#1]. (A) Schematic workflow of generating targeted mutant mice by CRISPR-Cas9 genome editing. Cas9 mRNAs, sgRNA[Rab#1], and a 140 bp single-stranded oligonucleotide (ODN[Rab#1]) were microinjected into the pronuclei of one-cell embryos. Seven weeks after microinjection, the pups are genotyped to detect Cas9 mediated mutagenic events. **(B)** Schematic illustration of the *Rab38* gene structure with the chromosomal coordinates attributed to the target sequence of sgRNA[Rab#1] (marked with light green background). Rab38_F and Rab38_R were used as genotyping primers to amplify a 213 bp segment covering the predicted target site; the PAM sequence is showed in cyan blue. The red arrow indicates the predicted site of double-strand break. **(C)** The comparison of sequences of Rab38[wt], ODN[Rab#1], and the PCR products from the

mutated founders derived from Cas9/sgRNA[Rab#1]microinjections, amplified with the Rab38_F and Rab38_R primer pair including the predicted DSB sites and desired nucleotide replacement sites. The position of the sgRNA and PAM sequence are indicated by a green background and cyan blue letter, respectively. Founders A1, A4, A5, A6, A7, A8, A12, and A32 harboured the precise knockin alleles; whereas founders A41, A23, A25, and A27 contained knockout alleles. The nucleotides deviating from the wild-type sequence are shown in red letters on yellow background. Deleted or inserted nucleotides are marked as dashes or letters in red, respectively. The various genotypes are described as a result of HR or NHEJ events. **(D)** The chromatogram revealed mixed sequence peaks generated from the PCR product amplified from tail DNA of founder A1, derived from Cas9/ sgRNA[Rab#1] injection, showing the precise four codon replacements, as present in ODN[Rab#1] (G>T, C>T, C>T, and G>A).

The frequency of Cas9 mediated mutagenesis events was assessed by HRMA of a 213 bp PCR product flanking the sgRNA[Rab#1] target sequence, amplified from tail DNAs of pups obtained from microinjections. The melting analysis of PCR products derived from 94 pups generated by sgRNA[Rab#1] microinjection revealed 22 mice (23.4%) showing a distinguished melting curve pattern as compared to the wild-type control (data not shown). These results were further confirmed by the direct sequencing of PCR products of the mutant founders recognised by HRMA. The chromatograms of the majority of these founders PCR products showed mixed sequencing peaks due to presence of either NHEJ or HR alleles together with or without the wild-type allele. To decipher individual mutant alleles in the mutant founders, 13 mutant pups were analysed by the mutation surveyor® DNA variant analysis software, which revealed the generation of 13.6% (8/59) HR and 10.2% (6/59) knockout alleles that were clearly distinguished from the wild-type sequence (Table 3). Six (A1, A4, A5, A6, A7, and A8) of eight knockin founders showed the four codon replacements by exchange of G to T, C to T, and G to A nucleotides from the ODN[Rab#1] targeting molecule by HR. Sequence analysis of founder A12 showed a single codon replacement followed by a 10 bp nucleotide deletion that included the PAM sequence. Similarly, founder A32 showed a five bp nucleotide deletion, preceded by three codon replacements next to the PAM sequence, suggesting the occurrence of simultaneous HR and NHEJ events.

Furthermore, four founders (A27, A41, A23, and A25) harboured deletions of one, three, 11, and 12 nucleotides or the insertion of 4 nucleotides (A27–GAAG) with or without the PAM sequence by NHEJ DNA repair (Figure 23C). In addition, the representative chromatogram of the PCR product amplified from tail DNA of founder A1 showed the doublet peak of G/T, C/T, C/T, and G/A indicating the presence of both HR and wild-type allele (Figure 23D). Taken together, these results suggest that sgRNA[Rab#1]/Cas9 are highly effective for editing the endogenous *Rab38* locus by generating 13.6% HR and 10.2% NHEJ

mutagenic events. In average, two homologous recombined mutants could be generated from the 14 pups in a single day of sgRNA microinjection.

3.4.2.1.1 Off-target analysis of founders generated by Cas9/sgRNA^Rab#1

Previous studies suggested that the terminal 12 nt of the target sequence within a sgRNA (seed) and the PAM sequence (NGG) are sufficient for efficient cleavage and that substitutions at any position within these sequences abolish the target recognition (Cong et al., 2013). During the design of the sgRNA^Rab#1, any sequences that perfectly match to the seed sequence of sgRNA and PAM sequence were completed avoided. However, for designing sgRNA, at least one site of the mouse genome contained the similar match of 10 or 11 nt followed by PAM sequence were selected. To access whether the highly effective sgRNA^Rab#1/Cas9 produced any unintended mutation in the mouse genome other than the intended target site, three putative off-target sites were identified by BLAST that include one or two mismatches in the 12 nt seed sequence of sgRNA^Rab#1 and its PAM sequence, respectively (Table S5). Upon sequencing analysis of the PCR amplified products from three putative off-target sites from the tail DNA of 13 mutant pups revealed no detectable mutation at the putative sites. These data provide no evidence for unintended off-site mutagenesis activity in genomic loci containing the one to two base pair mismatches.

3.4.2.2 Generation of *Fus14* Knockout mutant

Although TALENs were effectively used to generate the specific *Fus* KI mutants, I further tested whether the CRISPR/Cas9 technology as well enables to create frameshift *Fus* mutants as a model of amyotrophic lateral sclerosis (ALS). To access this question, a sgRNA expression vector (sgRNA^Fus#14) was constructed targeting exon 14 of the *Fus* gene with the specific chromosomal coordinates Chr7:127,981,446:127,981,499 (Figure 24B). Firstly, the ß-galactosidase reporter assay revealed a high nuclease activity of the sgRNA^Fus#14 in HEK293 cells (Figure 22A), encouraging the pronuclear microinjection of sgRNA^Fus#14 (20 ng/µl) along with Cas9-95A mRNA (67 ng/ul) into one-cell mouse embryos (Figure 24A). Notably, 17 live pups (17%) were obtained from the transfer of 100 manipulated embryos into the oviduct of the pseudo-pregnant foster mothers (Table 3). This birthrate is considerably lower than obtained with TALEN-Fus 15 and sgRNA^Rab#1 microinjection. Upon genotyping of the 17 pups produced by sgRNA^Fus#14 microinjection, direct sequencing of PCR products demonstrated two founders (11.8%) showed mutagenic events at the sgRNA^Fus#14 target site. Sequence analysis of a 576 bp PCR product amplified from the tail DNA of founder B4 revealed a 12 nucleotide deletion including the PAM sequence and the insertion of one extra nucleotide. However, it was not possible to amplify

the same fragment using the same primers from tail DNA of founder B3, which motivates me to investigate further by amplification of a 3.5 kb of genome centreed the exon 14 of *Fus* gene.
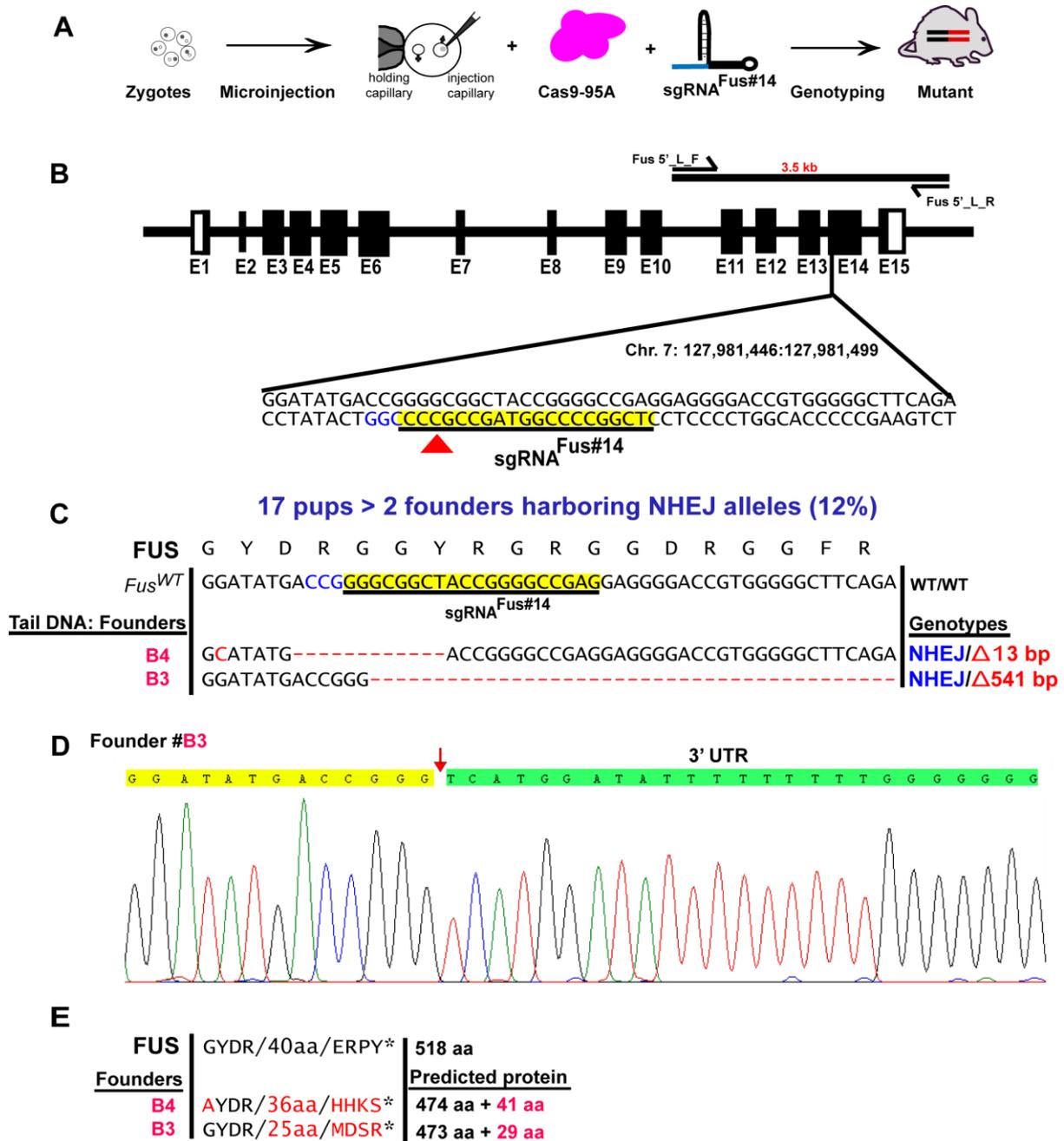
Figure 24: Creation of targeted *Fus* mutants by Cas9-95A and sgRNA^Fus#14. (A) Workflow of CRISPR/Cas9 mediated genome editing events in one-cell embryos. **(B)** Schematic illustration of the *Fus* gene architecture specified the chromosomal coordinates showing the sgRNA^Fus#14 target sequence (antisense strand; embedded in yellow background) and the TALEN binding sites. Fus5'_L_F and Fus5'_L_R indicate the genotyping primers for amplifying the 3.5 kb PCR product. **(C)** Sanger sequencing of PCR products derived from *Fus* mutant founders generated by sgRNA^Fus#14/Cas9 specified to exon 14 as

compared to the wild-type control. The PAM site is shown in cyan blue. The arrow shows the predicted cleavage site of Cas9 nuclease. Deleted or inserted nucleotides as a result of NHEJ event are showed as red dashes or in red letters, respectively. The size of deletions (Δ), insertion (+) and genotypes are shown at right of each allele. **(D)** Chromatogram analysis of PCR products from tail DNA of the B3 founder derived from sgRNA[Fus#14] microinjection revealed the seamless connection of the part of exon 14 sequence (marked with yellow background) to the 3´ UTR region (marked with bright green background) by deletion of the intervening 541 bp. **(E)** Amino acid sequence alignment of the mutant *Fus* founders are compared to the wild-type control. There were creation of additional 41 and 29 amino acids in the C-terminus of FUS in the founders B4 and B3 in comparison to wild-type.

Indeed, sequence analysis of the 3.5 kb PCR product of founder B3 showed the deletion of 541 bp nucleotides, which initiates two nucleotides downstream of the PAM sequence, and extends up to the middle of the 3´ UTR, thereby erasing exon 15. The chromatogram of the PCR product derived from tail DNA of founder B3 showed a clear breakpoint junction between partial exon 14 sequence (marked with yellow background) and the truncated 3´ UTR region (marked with bright green background) by deletion of the intervening 541 nucleotides (Figure 24D). Moreover, the amino acid sequence alignment of the B4 and B3 mutant founders generated by sgRNA[Fus#14] microinjection revealed the generation of a new reading frame of 41 and 29 C-terminal amino acids, leading to the complete disruption of the natural PY-NLS region of *Fus* (Figure 24E). These results demonstrate that sgRNA[Fus#14]/Cas9 is an efficient genome editing tool by creating 12% of frame shifted alleles at the endogenous *Fus* locus that abolishes the PY-NLS region.

Table 3: CRISPR/Cas9 mediated single site genome editing

Microinjection		Transferred embryos (n)	No of Pups (%)	Males (n)	Females (n)	No of mutants (%)	Founder´s NHEJ (%)	Founder´s HR (%)
sgRNA +/- ODN	Type of Cas9							
sgRNA[Rab#1] + ODN[Rab#1]	Cas9-95A	295	94 (31.9)	57	37	22 (23.4)	6 (10.2)*	8 (13.6)*
sgRNA[Fus#14]	Cas9-95A	100	17 (17)	9	8	2 (11.8)	2 (11.8)	-

Cas9-95A and sgRNAs targeting *Rab38* or *Fus* together with or without ODN were microinjected into one-cell mouse embryos. The number of pups (male or female) obtained from the transfer of manipulated embryos to pseudo-pregnant mice are shown. The overall frequency of genome editing is determined by the number of mice harboring the mutant alleles modified by either HR or NHEJ events. * indicates the % of mutants calculated from the sequencing results of 59 founders. The exact gene editing events of the founders are depicted in figure 23 and 24.

3.4.3 Creation of duplex genome edited mice by using two sgRNAs

Unlike TALEN, Cas9 nuclease does not directly bind to a genomic target sequence. To examine the feasibility of generating targeted deletions in the mouse genome by the administration of Cas9, two sgRNA plasmids were constructed that target intron 6 (sgRNA$^{Fus#6}$) and intron 8 (sgRNA$^{Fus#8}$) of *Fus* that located 2,632 bp apart from each other (Figure 25B). In fact, the *in vitro* ß-galactosidase assay of these sgRNAs demonstrated a twofold higher nuclease activity as compared to the ZFNs control (Figure 22B). Upon pronuclear microinjection of Cas9-166A mRNA (67 ng/µl) together with sgRNA$^{Fus#6}$ (20 ng/µl) and sgRNA$^{Fus#8}$ (20 ng/µl) transcripts into one-cell mouse embryos (Figure 25A), seven live pups (31.8%) were obtained from 22 microinjected embryos (Table 4). Indeed, PCR amplification from tail DNA of pups revealed amplification of 2.9 kb fragment in all pups except the pup C4 (14.3%) that showing a PCR amplified fragment smaller than 250 bp (Figure 25C). Moremore, sequence analysis of cloned PCR amplicon from the founder C4 confirmed a segmental deletion of the intervening 2,648 (C4.3) or 2,649 (C4.1) nucleotides, that erasing the exons 7 and 8 of *Fus*. Indeed, that region is located in between the sgRNA$^{Fus#6}$ and sgRNA$^{Fus#8}$ target sites (Figure 25D). Furthermore, chromatogram analysis of cloned PCR product revealed heterogeneous fusion sequences of partial introns 6 and 8 of *Fus* (Figure 25E, F). From gel picture and DNA sequencing data, it was confirmed the occurrence of biallelic mutations in the founder C4. Additionally, amino acid sequence alignment of mutant alleles of founder C4 revealed the truncation of the FUS reading frame by loss of 270 C-terminal amino acids, and the insertion of two additional amino acids that leads to disruption of the PY-NLS region of *Fus* (Figure 25G). Taken together, these results showed that the Cas9/sgRNA technology is amenable to generate double-mutant mice in a single step of microinjection. That indicates the wider applicability of CRISPR/Cas platform in the field of genetic engineering to create large genomic deletions and replacements in the milieu of therapeutic interventions
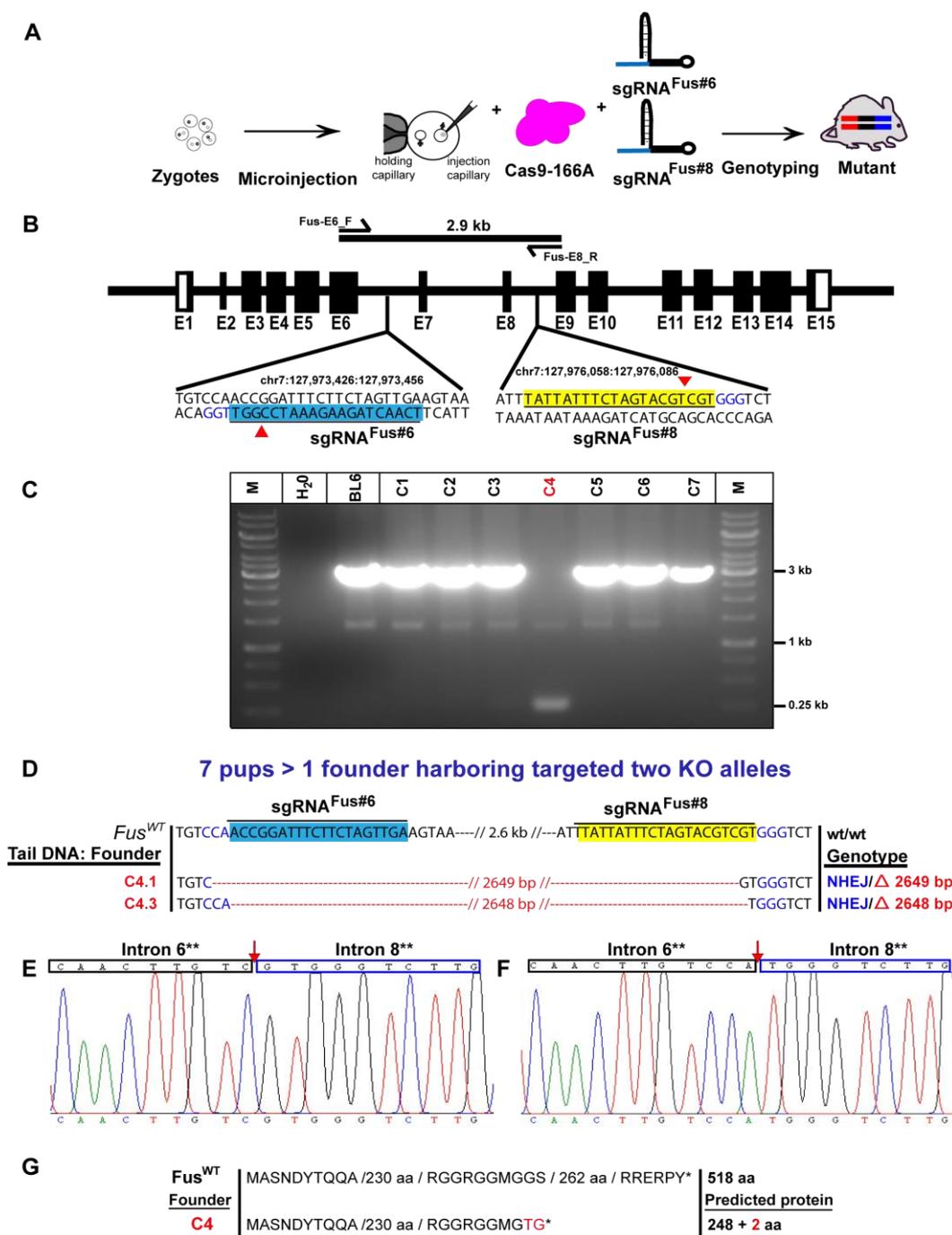
Figure 25: Duplex genomic engineering in mice with the CRISPR/Cas9 genome editing tool. (A) Schematic workflow of the single step generation of targeted alleles by CRISPR/Cas9 reagents to target two locations at the same chromosome. **(B)** The detailed architecture of *Fus* depicts the target sequences of sgRNA[Fus#6] (in blue background) and sgRNA[Fus#8] (in yellow background) including their chromosomal coordinates. The PAM sequence is shown in cyan blue letters. Fus_E6_F and Fus_E8_R were used as genotyping PCR primers to investigate the exact mutagenesis event created by sgRNA/Cas9. **(C)** Agarose gel electrophoresis of PCR products from founders derived from the microinjection of sgRNA[Fus#6] and sgRNA[Fus#8] using the Fus_E6_F and Fus_E8_R primers. All founders showed a 2.9 kb PCR product similar to wild-type except founder C4, which showed a >250 bp fragment. BL6: DNA from a C57BL/6 mouse. (**D**)

Sequence comparison of the cloned PCR product amplified from tail DNA of founder C4 in comparison to the wild-type control. Nucleotide deletions resulting from NHEJ events are shown as red dashes. The genotype of each allele is shown at the right. (**E, F**) The chromatogram peaks of mutant alleles of founder C4 revealed the seamless connection of the part of the sgRNA[Fus#6] and sgRNA[Fus#8] target sequence by the deletion of the intervening 2,648 or 2,649 nucleotides, which lead to the erasure of exons 7 and 8. (**G**) Amino acid sequence alignment of mutant alleles of founder C4 revealed the truncation of the FUS reading frame by loss of 270 C-terminal amino acids and the insertion of two additional amino acids. ** indicates the partial intron sequences

Table 4: CRISPR/Cas9 mediated gene editing at two genomic sites

Microinjection		Transferred embryos (n)	No of Pups (%)	Males (n)	Females (n)	No of mutants (%)	Founder´s NHEJ (%)
sgRNA	Type of Cas9						
sgRNA[Fus#6] + sgRNA[Fus#8]	Cas9-166A	22	7 (31.8)	3	4	1 (14.3)	2 (28.6)

Shown are mutant founder mice and mutant alleles obtained from the microinjection of sgRNA[Fus#6] and sgRNA[Fus#8] together with Cas9-166A mRNA into the pronuclei of one-cell mouse embryos. The number of pups (male or female) obtained from the transfer of manipulated embryos into pseudo pregnant females are shown. The overall frequency of gene editing is determined by the number of mice harbouring mutant alleles modified by NHEJ events. The percentage of the mutants and NHEJ alleles are calculated from the number of live births

.

4 Discussion

The discovery of programmable DNA binding proteins (PDPs) provides a remarkable progress in the field of gene targeting. PDPs can be selectively bound to user defined target sequences at any desired location of the genome. Different functional domains can be attached to the PDPs for achieving cleavage or nicking of DNA, activation or repression of transcription, and for modifying or removing of epigenetic marks. Within the last two decades, four novel technologies such as: mega nucleases, zinc finger nucleases (ZFNs), transcription activator-like effector nucleases (TALENs), and the CRISPR/Cas9 system have been developed that can be used for engineering of specific DNA target sequences by manipulating either PDPs or RNA to achieve site-specific genome engineering.

4.1 Efficient construction of sequence specific TALENs for genome modification

My experiments show the efficient generation of TALENs specific to human and mouse genome sequences by Golden gate cloning. This work also demonstrates the functional validation of TALENs with a varying degree of nuclease activity in the ß-galactosidase reporter assay (Figure 8). In fact, nine out of fourteen (64%) constructed TALEN pairs exhibited a comparable or superior nuclease activity as compared to the reference control. In agreement with the previous study of Cermak et al., (2011), my results demonstrate that the Golden gate cloning is an efficient assembly method for constructing TALEN arrays compared to PCR based assembly (Zhang et al., 2011), which often leads to error-prone recombination of the repetitive TALE modules or by commercial TALEN synthesis (Morbitzer et al., 2010), which is more expensive. The reasons for the variable nuclease activity among the TALEN pairs have not been clearly understood. Possible explanations may include inhibitory effects of chromatin structure, epigenetic modification, or inefficient expression and/or folding of particular TALENs.

4.1.1 Nickases show reduced cleavage efficiency

In this study, I have found that TALE nickases induce homologous recombination events by cleavage of one DNA strand. Indeed, TALE nickases have demonstrated nuclease-like activity, albeit at a lower efficiency to nucleases, and completely absence of the nuclease-like activity in homodimeric nickase pairs (Figure 9). This result thus lends further credence to an earlier report (Ramirez et al., 2012) that each TALEN specifically cuts only one DNA strand to which it is designed, whereas other TALE nickases support the FokI

stabilization that promote homologous recombination by reducing unwanted error-prone NHEJ. The possible explanations of nickase-promoting HDR by converting nicks into a DSB may occur either due to collapse of the replication fork, or weak residual homodimerisation of active nickase monomers that may lead to cleavage at the intended target site.

Other approaches can be used to increase the specificity and efficiency of TALEN. Recently, TALE-MutHI, another type of programmable nickases has been reported, in which monomeric MutHI, a DNA mismatch repair endonuclease, causes site specific nicking at GATC sites in un- or hemi-methylated DNA (Gabsalilow et al., 2013). Likewise nickases, the FokI domain also incorporates different mutations such as EL/KK (EL:KK denotes Q486E,I499L and E490K,I538K mutations) or ELD/KKK or ELD/KKR (ELD: Q486E,I499L,N496D, KKK: E490K,I538K,H537K, or KKR: E490K,I538K,H537R mutations) with sharky (S418P and K441E mutations) to generate obligate heterodimeric ZFNs architectures, thus enhancing the nuclease activity as well as reducing off-site activity (Doyon et al., 2008). These ELD/KKR mutations have been successfully implemented in a heterodimeric TALENs scaffold, resulting in high or comparable mutation rates and reduced toxicity in zebrafish (Cade et al., 2012). However, introduction of these ELD/KKR mutations within the present +176/+44 TALEN heterodimeric scaffold used in my studies has substantially decreased the nuclease activity than its homodimeric counterpart (data not shown). The diminishing activity of heterodimeric ELD/KKR TALENs is not clearly understood, but may be attributed to different TALEN architectures.

4.1.2 Programmable TALE-CND fusion proteins show nuclease activity

The present study addressed whether the *Clostridium*-derived nuclease domain (CND) can substitute the FokI catalytic domain, to improve the nuclease activity of TALEN. The main finding of this study is that the FokI catalytic domain can be effectively replaced with the CND domain to generate active TALE-CND fusion proteins. However, the TALE-CND fusion proteins exhibit only 70% of nuclease activity as compared to TALE-FokI proteins in the ß-galactosidase reporter assay (Figure 10). Nonetheless, the active catalytic residues of the CND are still unknown, which are indispensable for maintaining nuclease activity, and needs to be addressed in future.

4.1.3 Spacer lengths play a vital role in TALEN efficiency

My results showed that spacer lengths in between the opposite target sequences affect the activity of TALENs. Indeed, TALENs having spacer lengths of 15 bp, 16 bp, and 21 bp increased nuclease activity as compared to the standard. In contrast, nuclease activity of

TALENs was diminished, having the spacer lengths of 10 bp (Figure 11). This finding is consistent with the findings of previous reports (Christian et al., 2010; Miller et al., 2011). In contrast, spacer lengths of 16 to 40 bp in-between TALEN pairs reported the restoration of nuclease activity (Li et al., 2011), in which +231 C-terminal residues were included in TALEN. This discrepancy could result from the different +44 C-terminal TALEN residues in my study. This finding together with findings from other studies (Miller et al., 2011; Christian et al., 2010) suggests that spacer lengths of 14-16 bp in-between TALEN pairs are optimal for enhancing the nuclease induced mutagenesis. In contrast, spacer lengths of just 10 or 12 bp interfere with the nuclease activity.

4.1.4 Optimisation of TALEN mRNA for pronuclear microinjection

This study shows the establishment of a routine procedure by optimising TALEN mRNA production for *in vivo* mutagenesis. Evidence that enhanced TALEN mRNA production leads to improved nuclease expression could be demonstrated in two instances.

First, cloning of a 95 polyadenylation (95A) tail into the C-terminal region of the TALEN coding vector, producing robust full-length TALEN mRNAs by omitting the second polyadenylation step of the *in vitro* transcription kit (Figure 12C). This result clearly suggests faulty polyadenylation of long coding regions of TALEN due to contamination of truncated transcribed products in the two-step *in vitro* transcription protocol. This finding supports previous results (Mendez and Richter, 2001), where they have shown oocyte mRNA having short poly(A) tail (~20-40 nucleotide long) are dormant, whereas elongated tail (~200 nucleotides) enabling effective translations. Furthermore, this result strongly support the findings of Yamagata et al., (2005) in which the increasing length of the mRNA poly(A) tail dramatically enhanced oocyte protein expression upon cytoplasmic injection.

Second, pronuclear microinjection of 95A encoded Venus mRNAs at the concentration of 90 ng/µl leads to robust Venus expression in all two-stage embryos in fluorescent microscopy (Figure 12D). In contrast, cytoplasmic microinjection of TALEN mRNAs have yielded to high rate of NHEJ mediated knockout alleles (>40%), tolerating larger volumes (Qiu et al., 2013; Sung et al., 2013). Nonetheless, this cytoplasmic route has unable to co-delivery of targeting molecules into the nucleus for precise genome targeting. Indeed, this study shows robust Venus expression upon pronuclear microinjection of Venus 95A mRNA, suggesting that the pronuclear route is another alternative to cytoplasmic injection for delivering TALEN mRNAs together with targeting molecules.

To my knowledge, this is the first report of using TALEN-95A constructs for enhancing *in vivo* TALEN mutagenesis. In conclusion, this study addresses various parameters in terms of the activity, delivery, and concentration of TALEN mRNAs for pronuclear microinjection to achieve high rates of mutagenesis. This study also recommends the TALEN-95A strategy should be implemented for targeting endogenous loci in cell lines or organisms of interest to achieve higher mutagenesis rates.

4.2 Generation of cellular genetic models

The question addressed by the present study was whether TALENs can be used to generate cellular genetic models. To this end, I generated cellular genetic models by permanent transfection of TALENs into the HeLa cell line. Evidence for the generation of cellular models was demonstrated in two ways. First, AvrII digestion of PCR products shows different shorter fragments derived from mutagenised alleles in a lower density, as compared to the predicted fragments of the wild-type PCR product represented in a higher density. Second, sequencing of PCR products derived from pooled transfected colonies reveals overlapping sequence peaks in association with the wild-type sequence (Figure 13). These results suggest the generation of knockout alleles having a spectrum of indel mutations by NHEJ events. The predicted sequence deletions harbouring a mixture of knockout alleles are calculated at a rate of 4.24%. This finding is consistent with the previous report (Miller et al., 2011), showing 3% genome modification at 37°C, and by subjecting TALEN transfected cells to 30°C resulting into 9% genome modification. However, other investigators demonstrate high throughput TALEN mutagenesis (22.2%) in endogenous human genes (Reyon et al., 2012). The higher mutagenesis frequency in that report might be explained due to U2OS cell line or FLASH method of TALEN construction. In addition, TALENs mediate site-specific genome modification in human embryonic stem cells and induced pluripotent stem cell (Hockemeyer et al., 2011). Moreover, TALENs were successfully applied to generate various cellular disease models such as: PCS (MVA) syndrome (premature chromatid separation with mosaic variegated aneuploidy) (Ochiai et al., 2013), chronic hepatitis B virus infection (Bloom et al., 2013), mitochondrial diseases (Bacman et al., 2013), and duchenne muscular dystrophy (Ousterout et al., 2013).

4.3 Generation of mouse disease models

4.3.1 Efficient generation and germline transmission of Rik[KO] alleles

This study shows the generation of a *C9orf72* mouse disease model as a representative of frontotemporal lobar degeneration. Generation of the *C9orf72* mouse

disease model has been demonstrated by induction of frame shift mutations that lead to the premature termination of the C9ORF72 protein due to the truncation of the translational reading frame. Indeed, pronuclear microinjections of two different doses of TALEN-Rik2-95A mRNAs (45 ng/µl, 90 ng/µl) have induced targeted deletions at the *C9orf72* locus at the rate of 39% and 41% (Table 1). Furthermore, 63% (seven out of 11) of the characterised mutations lead to a truncated translational reading frame (Figure 14). Interestingly, these rates of gene editing are eight fold higher as compared to previous findings (Wefers et al., 2013a), clearly suggesting that TALEN-95A mRNAs at the higher dose in pronuclear injection lead to a substantial enhancement of *in vivo* mutagenesis. However, increasing concentrations of TALEN mRNAs from 45 to 90 ng/µl has little impact on TALEN mutagenesis These findings thus lend further credence to the previous results (Qiu et al., 2013; Sung et al., 2013), where high rate of NHEJ mediated knockout alleles (>40%) have been reported. Nonetheless, the present study uses pronuclear microinjection for TALEN delivery rather than cytoplasmic delivery used by the previous investigators for achieving higher mutagenesis rate. Since the modified knockout loci are first identified in the tail DNA of founders; it is essential to check whether the same mutant alleles transmit to the germ cell population to establish breeding colonies. In fact, backcrossing of the mutant founder to wild-type C57BL/6 mice have allowed transmission of the mutant allele to its progeny at a rate of 47%, thereby confirming the contribution of mutant cells to the germline in a Mendelian fashion.

In conclusion, the establishment of Rik^{KO} mutants by the TALEN-95 mRNA may contribute to decipher the underlying mechanism of frontotemporal lobar degeneration, and help for the future development of therapeutic intervention.

4.3.2 Efficient generation of codon replacement Fus^{KI} alleles by TALEN and oligonucleotides

This study shows the generation of *Fus* disease mouse models having precise codon replacements mediated by TALENs and targeting oligonucleotides. Evidence that recapitulates patient derived codon replacements in the generated *Fus* mouse models has been demonstrated by sequencing and HRM analysis of PCR products of founders (Figure 17). Indeed, pronuclear injection of a lower dose of TALEN-95A mRNA (20 ng/µl) together with specific mutagenic ODN for each model (Fus^{R513G} and Fus^{P517L}) have achieved target replacement at a rate of 6.8% (Table 2). Interestingly, the rate of homologous recombination in this study is four-fold higher than the previous report (Wefers et al., 2013a), reconfirming that the TALEN-95A mRNAs accomplish to enhance mutagenesis rate. As a matter of fact,

this study not only demonstrates the generation of several mutant founders having precise HDR-mediated codon replacements, but also showing the mutagenic alleles having unintended nucleotide insertions, deletions or replacements. Upon further investigation by sub-cloning and sequencing, these alterations were found as a result of error-prone synthesis of oligonucleotides that rule out the speculation of unexpected nucleotide recruitment by the homologous recombination machinery. Hence, quality and length of ODNs should be monitored meticulously before pronuclear injection to avoid introduction of unwanted mutations.

Although targeted homologous recombination events were achieved by using 70 nt homology sequence flankings the intended mutation, a previous report showed that a minimum of 50 nt of homology is sufficient to obtain a high recombination rate in mammalian cell lines (Chen et al., 2011). Therefore, it will be of future interest to determine the *in vivo* recombination rate of ODNs in relation to the molecules' length.

Furthermore, each of seven mated founders transmitted the mutant alleles to 10-67% of their offspring (Table S2), thereby confirming the contribution of mutant cells to the germline. In addition, homozygous mutants were also generated by breeding of the heterozygous mutants for further analysis. In contrast, Hicks et al., (2000) reported that the knockout of *Fus* results into chromosomal instability and perinatal lethality in homozygous mutants. The discrepancy in life expectancy of these mutants could be the reason of difference in type and location of mutation in the *Fus* gene. In the study of Hicks and colleagues, targeted deletion occurred from exon 12 to 15, whereas in my study the nucleotide replacements and frameshift mutations were induced in exon 15 of the *Fus* gene.

In addition, a minor proportion of founders show the presence of more than two alleles suggesting mosaicism. However, this result is not surprising, as nuclease mediated gene targeting (ZFNs, TALENs) might occur after the first or second cycle of genome replication, thereby leading to multiple different targeting events. For this reason, all the F_1 founders should undergo sequencing for the identification of correctly targeted alleles.

4.3.2.1 Cellular stress recruits mutant FUS into cytoplasmic stress granules

This study demonstrates that the generated *Fus* mutants exhibit disease phenotypes. Evidence that *Fus* mutants show disease phenotypes can be shown by two means. First, the *Fus* mutants Fus[R513G], Fus[P517L], and Fus[511] show cytoplasmic accumulation of FUS protein but not in wild-type (data not shown). Interestingly, frameshift mutants (Fus[511]) have showed

comparatively higher cytoplasmic mislocalisation than the missense mutants (R513G, P517L) (data not shown), which have only single amino acid substitutions in the NLS. This study indicates a disturbance in the nuclear transport mechanism of FUS, which results into cytoplasmic mislocalisation. The cytoplasmic mislocalisation of these *Fus* mutants is consistent with previous reports (Bosco et al., 2010; Dormann et al., 2010) in HeLa cells, and rat neuronal cells, or HEK293 cells by expressing HA or GFP tagged FUS constructs. Thus, this study along with the previous reports provides evidence that the C-terminal domain responsible for the nuclear/cytoplasmic distribution of the FUS protein, and fALS linked mutations disrupt this equilibrium towards the cytoplasm.

Second, this study shows that upon exposure of cellular stress such as sodium arsenite, mutant FUS recruited into cytoplasmic stress granules. Especially, the frameshift mutant (Fus[511]) exhibits higher degree of stress granule formation than the codon replacement mutant Fus[R513G] (Figure 20), which is consistence with previous cytoplasmic mislocalisation experiments. Nonetheless, sodium arsenite treatment in FUS-WT has unaltered partitioning of FUS protein without showing any cytoplasmic mislocalisation or stress granule formation. Together with previous reports (Bosco et al., 2010; Dormann et al., 2010), this study demonstrates that only cytoplasmic mislocalised FUS protein is recruited into stress granule, and also the degree of cytoplasmic mislocalisation is directly correlated with the extend of stress granule formation. Thus, the recruitment of stress granules from cytoplasmic mislocalised protein might be an important cellular mechanism leading to the FUS pathology.

In conclusion, the generation of *Fus* mutants by TALEN-95 mRNAs and ssODN, and its first disease phenotypes may help to understand the mechanism of amyotrophic lateral sclerosis, and may contribute to future therapeutic intervention.

4.3.3 Founder mutants do not exhibit off-target mutations

This study shows that the mutants generated by TALEN are not showing off-target activity. Indeed, HRMA and sequencing of tail PCR products of mutant founders show no evidence for off-site activity at five predictable known binding sites of TALENs, except at the *Fus* off-site 1 and 3 (Figure 21). In fact, by further investigation, it was found that the presence of single-nucleotide polymorphism (SNP) at the off-sites are due to strain polymorphism present in inbred mouse harbouring mixed genetic background (Figure S5) that exclude the speculation over the off-site processing of TALEN. Furthermore, this study cannot rule out the possibility that nonspecific effects might have caused embryonic toxicity. In particular, the unknown off-site activity of nucleases can be addressed by whole-genome

sequencing. Pragmatically, C57BL/6 embryos can be used for gene targeting experiments rather than the mixed genetic mouse strain (DBA/2 x C57BL/6 x FVB/N). On the contrary, the number of live births of C57BL/6 embryos is about half as compared to FVB strain, such that two day of microinjection required to recover sufficient pups. In addition, TALEN should be designed very carefully to select SNP-free unique target sites for gene targeting experiments.

4.4 HRMA is a universal tool for high throughput genotyping

Genotyping of founders augments a work overload to screen for mutants as well as for establishing mutant breeding colonies. In this study, HRMA was demonstrated as an easy genotyping tool for the faster identification of desired mutants. Notably, HRMA easily identified the mutant alleles of *C9orf72* and *Fus* founders, and their offsprings to detect nucleotide deletions and insertions (Figure 14, 17), and futher identified mosaic founders (Figure 15). In general, HRMA has two major advantages over traditional genotyping approaches. First, HRMA does not require any restriction enzyme that helps in simplifying the TALEN design paradigm, which always relies upon the elimination or creation of restriction sites for screening out the mutants. Therefore, by using HRMA, any suitable TALEN target site can be selected for gene targeting, and silent mutations in targeting molecules are no more needed, which may alter the expression of the targeted gene. Second, HRMA bypasses the traditional PCR-RFLP assay, which depends on expensive restriction enzyme as well as ethidium bromide based agarose gel electrophoresis.

In conclusion, HRMA easily identifies TALEN mediated founders and their offsprings by their characteristics melting curves, representing a universal and sensitive tool for high-throughput genotyping.

4.5 CRISPR/Cas: ushering era of gene targeting

The CRISPR/Cas system provides adaptive immunity from invading nucleic acids by guiding the Cas9 protein for chopping out foreign DNA. Recently, the CRISPR/Cas system has been further simplified by using Cas9 protein along with a single chimeric RNA, enabling effective DNA cleavage (Jinek et al., 2012).

4.5.1 Functional validation of sgRNAs and Cas9

This study shows the recapitulation of bacterial CRISPR/Cas system in mammalian cells. Indeed, five constructed sgRNAs show comparable or superior nuclease activity as compared to TALENs or ZFNs in the β-galactosidase reporter assay (Figure 22). This finding

is in parallel with the previous results (Cong et al., 2013; Mali et al., 2013), where sgRNA along with Cas9 effectively induce precise cleavage at endogenous genomic loci of human and mouse cells, or induced pluripotent stem cells.

Therefore, these results reconfirm that a minimal two-component system is sufficient for efficient CRISPR/Cas-mediated genome modification in mammalian cells, and should applicable to other cell types and species.

4.5.2 One-step generation of single targeted mutant mice by CRISPR/Cas genome editing

The question addressed by the present study was whether the CRISPR/Cas system can be used to generate targeted mouse mutants. Evidence for the generation of mouse mutants by CRISPR/Cas can be demonstrated by two means. First, pronuclear microinjection of sgRNA specific to the first exon of *Rab38* together with a mutagenic ODN have produced precise knockin allele at the rate of 13.6% (Eight mutants out of 59 mice) (Figure 23, Table 3). This rate of homologous recombination is two-fold higher than the TALEN-mediated HR event (Panda et al., 2013). Second, pronuclear microinjection of sgRNA specific to exon 14 of *Fus* resulted in 12% (Two mutants out of 17 mice) of knockout allele (Figure 24). These findings are confirmed by the work of Wang et al., (2013) and Shen et al., (2013).

However, the *Fus* exon 14 has proven difficult to target by TALEN (Table S4) due to unknown reason. Perhaps, due to the presence of multiple CpG methylation sites in the TALEN target site (Table S1), which undergoes epigenetic modification, and causes inaccessibility for the recognition by TALEN proteins. The failure of the Fus-14 TALEN can be explained by previous reports (Deng et al., 2012b; Valton et al., 2012) showing that 5-methylcytosine residues are not recognised by the RVD 'HD', rather it strongly adherents to 'NG' TALE RVD due to structural resemblance of thymine and 5-methylcytosine region, enabling the van der Waal's interaction with the Cα atom of glycine (Deng et al., 2012a). Nonetheless, recent findings demonstrate that the Cas9 mediated cleavage is unaffected by DNA methylation (Hsu et al., 2013), which adds a further advantage for CRISPR/Cas gene targeting.

In conclusion, these findings demonstrate that CRISPR/Cas9 can site-specifically cleave DNA in mouse embryos with in a less time due to its easy designing and construction, and paves the way for its use in the generation of gene-disrupted animals.

4.5.3 CRISPR/Cas-mutant founders don not exhibit off-target mutations

Although CRISPR/Cas provides a simple tool for efficient genome editing the specificity of the sgRNA guided Cas9 nuclease is a major concern for its wide application. Hence, this study addressed whether mutant founders generated by CRISPR/Cas exhibit off-site mutations. This study shows that mutant founders generated by sgRNA/Cas9 have not exhibited off-site activity. Indeed, three putative bona fide off-target sites of thirteen founders (generated by sgRNA[Rab#1] injection) were analysed by HRMA, followed by sequence analysis of the PCR products, and found no undesired genomic alterations (data not shown). Nevertheless, whole genome sequence profiling of these mutants may provide a deeper insight into the range of potential off-site activity of the CRISPR/Cas9 system. In this study, the putative off-sites of the sgRNA[Rab#1] harbour one or two mismatch nucleotides that are located 8 to 12 bp upstream of the PAM sequence (Table S5). In consistence with previous findings, this study demonstrates that Cas9 tolerates single base mismatches at the distal PAM region (Cong et al., 2013; Jiang et al., 2013; Jinek et al., 2012). It has also been reported that the specificity of Cas9-mediated DNA cleavage is sequence and locus-dependent, governed by the quantity, position, and location of the mismatches (Hsu et al., 2013). In a manner of analogue double FokI for inducing cleavage of opposing target sequence in ZFNs or TALENs, double nicking strategy of Cas9 protein is effectively applied to ameliorate off-site activity with improved specificity, and also facilitate high efficient homology directed repair (Ran et al., 2013).

4.5.4 One-step generation of a double targeted mutant by CRISPR/Cas

This study shows that the CRISPR/Cas technology can be used for the efficient deletion of long genomic regions, facilitating the generation of mice carrying mutations in two different sites in a single-step of microinjection. Here, this study has chosen *Fus* gene as target because the frameshift *Fus* mutant exhibited a disease phenotype as shown in figure 20. Indeed, the co-injection of Cas9 with sgRNA[Fus#6] and sgRNA[Fus#8] into one-cell embryos has produced mutant that carried mutations at two target sites (Table 4). Interestingly, this mouse harbours biallelic mutations along with the targeted deletion of the intervening 2.6 kb segment that includes exon 7 and 8, having a truncated protein domain, which contains the predicted 250 aa instead of 519 aa (Figure 25). Consistent with the previous report (Wang et al., 2013), multiplex genome edited mice can be generated within a short time frame of seven weeks, thereby avoiding the time-consuming intercross of single mutants, which ultimately saving resources. Moreover, pronuclear microinjection of CRISPR/Cas with gene

targeting vectors has enabled the generation of sophisticated mouse models harboring conditional and reporter alleles (Yang et al., 2013).

This result together with the previous published reports demonstrates that more than one sgRNA can be easily deployed to drive the Cas9 protein at multiple locations to achieve multiplex genome editing.

4.6 CRISPR/Cas9 versus TALENs

Despite the successful application of TALENs for generating cellular and mouse models, a newly characterised CRISPR/Cas system may make TALENs obsolete. Firstly, CRISPR/Cas requires only one new guide RNA to program the nuclease, whereas TALENs requires two engineered proteins for the cleavage of one target site. In this perspective, a typical TALEN requires 1632 bp of repeat coding regions to be assembled for each target sequence. In contrast, CRISPR/Cas requires only 20 nucleotide complementary sequence of a 100 nucleotide guide RNA, representing a more promising platform for expedite mutagenesis at lower costs within a short time frame.

Despite the suceessful application of CRISPR/Cas system, the potential drawback of this system is about its off-site activity. Within 20 bp target sequence of guide RNA, the eight bp further from the NGG PAM motif are very tolerant of single-base mismatches, which concern about specificity of targeting. In contrary, TALENs recognise 32 bp of their target sequences, would bind fewer off-target sequences.

The second milestone of the CRISPR/Cas technology is the remarkable application for multiplex genome editing; it provides a greater avenue for genome engineering rather than ZFNs or TALENs, which are always cumbersome, time-consuming, laborious, and proven difficult for simultaneously targeting multiple sites due to their cellular toxicity.

4.7 Conclusions and outlook

My work establishes a routine procedure for empowering the genome editing toolbox by expediting the production of mouse disease models to unravel underlying disease mechanisms. By use of two site-specific nucleases such as TALENs and CRISPR/Cas, I could generate six different mouse disease models. Moreover, for the first time, this study reveals that TALEN-95A mRNAs substantially enhance the production of mouse mutants and serve as a straightforward solution of yielding robust full-length TALEN mRNAs for *in vivo* mutagenesis experiments. Additionally, by using TALEN-95A mRNAs with or without oligonucleotides, I accomplished the generation of *C9orf72* knockout and two *Fus* knockin mouse disease models as a representative of frontotemporal lobar degeneration and familial amyotrophic lateral sclerosis. Although the present study provides new interesting insight into the neurodegeneration research area by producing these disease models by TALENs, further detailed studies such as biochemical, cellular, pathological, and behavioral analysis are required to decipher the mechanisms of disease, and possible invention of effective therapy, which is the long sought goal of ALS and FTLD research.

In spite of the fact that TALENs and CRISPR/Cas9 substantially enhance the frequencies of NHEJ and HR, a clear preference inclines toward the CRISPR/Cas9 because of its simple design, easier applicability, high efficiency, and remarkable ability of multiplex genome editing. Indeed, by adopting the CRISPR/Cas9 tool in one-cell embryos, I could generate simplex or duplex genome edited mice. Alternatively, CRISPR/Cas9 can be applied for the transcriptional activator, repressor, modulation of epigenetic mark, and genome architecture. However, an increasing recognised constraint of Cas9-mediated gene editing applications concerns their specificity of targeting. Ultimately, the most straightforward option for genome editing applications is to employ nickase enzymes rather than nucleases.

In light of the substantial progress of the targetable nucleases, I think now is the appropriate time for transitioning the exciting field beyond the proof-of-concept stage to the age of application. In fact, both nuclease technologies provide a wide avenue for targeted genome modification in species, in which ES cells or nuclear transfer technologies are not fully established, and to produce livestock models for economic interest. Most interestingly, $Cas9_{nuclease-null}$ fusions should be used for targeted genome regulation in a manner akin to use of small-molecule drugs for correcting epigenetic misregulation of gene expression, controlling inflammation, autoimmunity, or repressing transcription of viral genes. In essence, these targetable nucleases should widely applicable in rat as well as large animals' especially in pig, a potential donor for xenotransplantation in humans. Moreover, these nuclease platforms should be broadly used in epigenetics and cancer studies to address unknown players or novel pathways to find out the best therapy. The upcoming exciting application of these targetable nucleases are in patient-derived induced pluripotent stem cell lines for the correction of specific disease mutations and by establishing nuclease-mediated gene therapy as a tool for personalised medicine.

5 Materials

5.1 Instruments

Instruments	Company with type and cat. no.
Autoclave	Aigner, type 667-1ST
Balances	Sartorius, LC6201S, LC220-S
Centrifuge	Eppendorf 5424, cat. no. 5424 000.010
Centrifuge, refrigerated	Eppendorf 5424R, cat. no. 5404 000.014
Thermoshaker	Eppendorf Thermomixer comfort, cat. no. 5355 000.011
PCR thermocycler with gradient temperature functionality	Eppendorf, Mastercycler pro, cat. no. 6321 000.515
UV spectrophotometer	Nanodrop 1000
Transilluminator, long wave, UV 366 nm	
UV protected goggles	Carl Roth
Gel imaging system	Herolab
Electroporator for electro-competent bacteria	Bio-Rad Gene Pulser Xcell, cat. no. 165 2660
Electroporation cuvette (2 mm)	Bio-Rad, cat. no. 1652086
Luminometer	Berthold Centro LB 960 Centro
Cell counting chamber	Neubauer improved, Marienfeld, cat. no. 0640010
Horizontal shaker	Promax 2020
Stereomicroscope	Leica, Labovert FS
Warming plate	Minitube International, cat. no. HT200W

Transfer pipettes (HB 1.80 1.20, L=160 mm, 125-134 µm, BW=45°, BL= 10 mm)	Biomedical instruments
Holding pipettes (BM 100T-15, broad, ID=20-25 µm, straight)	Biomedical instruments
Pronucleus injection capillaries (BM100F-10, end firepolished, PI-1.6, Barnow)	Biomedical instruments
Pipette loading tips	Eppendorf Microloader tip
Microinjector device for pronucleus injections	Eppendorf Femtojet, cat. no. 5247 000.013
Microinjector device for holding embryos	Eppendorf CellTram vario, cat. no. 5176 000.033
Micromanipulators (left and right handed)	Leica or Narishige
Inverted stereomicroscope	Leica DMI3000B
Surgical instruments: fine forceps, serrefine clamp, fine iris scissors, needle holder, suture needles, suture silk, wound clips and applicator	Fine Science Tools
HRMA device (LightScanner)	BioFire Diagnostics, cat. no. LSCN-ASY-0011
Cryostat	Mikrom, HM 560
DNA/RNA electrophoresis chip analyser	Agilent, 2100 Bioanalyser
Electric homogenizer	IKA, Ultra-Turrax T25 basic
Fridges (4 °C)	Liebherr
Freezer (−20 °C)	*Liebherr*
Freezer (−80 °C)	Heraeus HFU 686 Basic
Gel documentation system	Herolab, E.A.S.Y.
Glass pipettes	Hirschmann
Glassware	Scotsman, AF 30

Ice machine	Scotsman
Imaging analyser	Fuji, FLA-3000
Incubators (for bacteria)	New Brunswick Scientific, innova 4230
Incubators (for cell culture)	Heraeus
laminar flow	Nunc Microflow 2
pH-meter	InoLab, pH Level 1
Power supplies for electrophoresis	Thermo, EC250-90, EC3000-90; Pharmacia Biotech, EPS200; Consort, E443
Thermomixer	Eppendorf, comfort
UV-DNA/RNA-crosslinker	Scotlab, Crosslinker SL-8042; Stratagene, UV-Stratalinker 1800
UV-lamp	Benda, N-36
Water bath	Leica, HI1210; Memmert, WB7
Water conditioning system	Millipore, Milli-Q biocel

5.2 Chemicals

Chemicals	**Company with cat. no.**
Ampuwa	Fresenius
Agarose (for gel electrophoresis)	Biozyme, cat. no. 870055
Ampicillin	Sigma
dNTPs solution mix (100 mM (each)	Thermo Scientific, cat. no. R1121
Albumin fraction V	Roth
Bacto agar	Difco, cat. no. 214010
Bacto peptone	BD Biosciences, cat. no. 211820
Bis-tris	Sigma
Blocking reagent	Roche, Perkin Elmer
Boric acid	Merck
Bovine serum albumin (BSA, 20 mg/mL)	NEB, Sigma
Dithiotreitol (DTT)	Roche
DMEM	Gibco
DMSO	Sigma

DTT	Roche, cat. No. 10 708 984 001
Ethidium bromide solution	Fluka, cat. no. 46067
SOC medium	New England Biolabs, cat. no. B9020S
Carbenicillin disodium salt, sterile filtered (50 mg/ml)	Applichem, cat. no. A 1491,0010
Yeast extract	Difco, cat. no. 210934
Sodium Chloride (NaCl)	Merck, cat. no. 1064005000
X-Gal (5-bromo-4-chloro-3-indolyl-beta-D-galacto pyranoside	Fermentas/Thermo Scientific, cat. no. R0941
DMEM, without glutamine	Gibco, cat. no. 21969-035
PBS	Invitrogen, cat. no. 14190-094
FCS	PAA, cat. no. A15-151 or equivalent
L-Glutamine 200 mM	Gibco, cat. no. 25030032
Trypsin-EDTA 0.25 %	Gibco, cat. no. 25200056
Ethanol p.a.	Merck, cat. no. 1.00983
EDTA disodium salt dihydrate	Sigma, cat. no. E4884
3 M sodium acetate, pH 5.2	Sigma, cat. no. S7899
Luciferase assay reagent	Promega, cat. no. E1483
Trizma base BioXtra	Sigma, cat. no. T6791
Trizma hydrochloride BioXtra	Sigma, cat. no. T6666
Water, for embryo transfer	Sigma, cat. no. W1503
Sterile filter unit millex GV, 0.22 µm	Millipore, cat. no. SLGV033RS
MF Membrane Filter 0.025 µm VSWP	Millipore, cat. no. VSWP02500
Ultrafree centrifugal filters PTFE membrane	Millipore, cat. no. UFC30LG25

M2 medium (suitable for mouse embryo culture)	Sigma, cat. no. M7167
M16 medium (suitable for mouse embryo culture)	Sigma, cat. no. M7292
Mineral oil (suitable for mouse embryo culture)	Sigma, cat. no. M8410
Rompun (Xylazine hydrochloride, 2% solution)	Bayer Healthcare
Ketanest 50 (Ketamine hydrochloride 50 mg/ml)	Parke-Davis
Tris, 1 M, pH: 8.0	Invitrogen, cat. no. 15568-025
sodium dodecylsulfate (SDS)	Invitrogen, cat. no. 24730020
Proteinase K	Sigma, cat. no. P6556
EDTA, 0.5 M, pH 8.0	Invitrogen, cat. no. AM9260G
Isopropanol	Merck, cat. no. 1096342500
LC Green Plus+ Dye	Bioké, cat. no. BCHM-ASY-0005
Mineral oil (for molecular biology)	Sigma, cat no. M5904
TE buffer pH 8.0	Invitrogen, cat. no. AM9858
Trizol	Invitrogen
Tryptone	BD Biosciences
NorthernMax-Gly Gel Prep/Running buffer	Ambion, cat. no. AM8678
RNaseZAP®	Life Technologies, cat. no. AM9780
Tween 20	Sigma, cat. no. P9416
G418 disulfate salt	Sigma, cat. no. G8168
Paraformaldehyde	Sigma, cat. no. P6148
Sodium arsenite	Sigma, cat. no. 35000

5.3 Consumables and others

Consumables	Company with cat. no.
GeneRuler 1 kb DNA ladder	Thermo Scientific, cat. no. SM0311
GeneRuler 100 bp DNA ladder	Thermo Scientific, cat. no. SM0241
6x DNA loading dye	Thermo Scientific, cat. no. R0611
Millenium RNA size marker	Ambion, cat. no. AM7150
Glyoxal loading dye	Ambion, cat. no. AM8551
pH test strips (pH 4.5-10)	
Centrifuge tubes (15 mL, 50 mL)	Corning
Coverslips (24 x 50 mm, 24 x 60 mm)	Menzel Gläser
Films for autoradiography	Kodak: Biomax MS, Biomax MR
Filter paper	Whatman 3MM
Filter tips 10 µL, 20 µL, 200 µL, 1 mL	Art, Starlab
Gloves	Kimberley-Clark, Safeskin PFE Safeskin, Nitrile
Hybond N Plus (nylon membrane)	Amersham
Pasteur pipettes	Brand
PCR reaction tubes (0.2 mL), lids	Biozyme
plastic pipettes (1 mL, 5 mL, 10 mL, 25 mL)	Greiner
Oligonucleotides	Metabion
Orange G	Sigma, cat. no. O3756
0.2-ml tubes	Eppendorf, cat. no. 0030 124.332
1.5-ml tubes	Eppendorf, cat. no. 0030 123.328
15-ml conical polypropylene tubes	Greiner Bio-One, cat. no. 188271
50-ml conical polypropylene tubes	Greiner Bio-One, cat. no. 227261
PCR cap-strips 0.2 ml	Biozyme, cat no. 711070

PCR 96 well plate	Biozyme, cat no. 710884
Petri dishes (96 mm × 15 mm)	BD Biosciences, cat. no. 351007
96-well white measurement plate	Thermo Scientific, cat. no. 236105
15 cm culture plate	Nunc, cat. no. 168381
12-well culture plate	Starlab, cat. no. CC7682-7512
6-well tissue culture plates	Nunc, cat. no. 140685
60 mm cell culture dish	BD Falcon, cat. no. 353004
Depression (concavity) slides	Electron Microscopy Sciences, cat. no. 71878-01
FrameStar 96 well black frame white plate	4titude, cat. no. 4ti-0961
Adhesive foil seal for 96 well plates	Kisker Biotech, cat. no. G040-TS

5.4 Commonly used stock solutions

Solutions		Ingredients
loading buffer for agarose gels	15%	Ficoll 400
	1-2%	Bromophenol Blue (at-300 bp)
	1-2%	Xylene Cyanol FF (at-4 kb)
PBS (1x)	171 mM	NaCl
pH 7.4	3.4 mM	KCl
	10 mM	Na_2HPO_4
	1.8 mM	KH_2PO_4
TAE (10 X)	0.4 M	Tris base
	0.1 M	Acetate
	0.01 M	EDTA
TBE (10X)	0.89 M	Tris base
	0.89 M	Boric acid
	0.02 M	EDTA
Tris-HCl	1 mM	Tris base

TE (Tris-EDTA)	10 mM	Tris-HCL pH 7.4
	1 mM	EDTA
HEK293 cell culture medium	500 ml	DMEM
	50 ml	FCS
	5 ml	L-Glutamine
Luciferase substrate	25 mM	Gly-Gly
stored aliquots at -80 ^{0}C	15 mM	$MgSO_4$
	4 mM	EGTA
	2 mM	ATP
	1 mM	DTT
	100 µM	Coenzyme A
	75 µM	Luciferin
	15 mM	K_2HPO_4/KH_2PO_4
Lysis buffer (DNA)	50 mM	Tris-HCl pH 8.0
	100 mM	EDTA
	1%	SDS
	8 µl/ml	Proteinase K
	100 mM	NaCl
$T_{10}E_1$	10 mM	Tris
sterile filter	0.1 mM	EDTA pH: 7.4
stored at –80 ^{0}C		Water (Embryo grade)

5.5 Kits

Kit	Company with cat. no.
QIAquick PCR purification kit	Qiagen, cat. no. 28104
QIAquick gel extraction kit	Qiagen, cat. no. 28704
MinElute gel extraction kit	Qiagen, cat. no. 28604
QIAprep Spin Miniprep Kit	Qiagen, cat no. 27104
QIAGEN Plasmid Maxi Kit	Qiagen, cat no. 12162
β-Gal reporter gene assay	Roche, cat. no. 11758241001
mMESSAGE mMACHINE T7 Ultra kit	Ambion, cat. no. AM1345
MEGAshortscript™ T7 Kit	Ambion, cat. no. AM1354
MegaClear kit	Ambion, cat. no. AM1908
Wizard genomic DNA purification kit	Promega, cat. no. A1125
StrataClone Blunt PCR cloning kit	Agilent Technologies, cat. no. 240207-5
Protoscript M-MuLV Taq-RT PCR kit	New England Biolabs, cat. no. E6400S
DNA 1000 Kit	Agilent, cat. no. 5067-1504
Gibson Assembly® Master Mix	New England Biolabs, cat. No. E2611L
In-Fusion® HD EcoDry™ Cloning Kit	Clontech, cat. No. 638912

5.6 Molecular biology reagents

5.6.1 *E. coli* strains

Strain	Company
DH5α competent cells	Invitrogen
E. coli XL Blue cells	Stratagene

5.6.2 Solutions

Solution	Ingredients	
Ampicillin selection agar		LB agar with 100 µg/mL Ampicillin
Ampicillin selection medium		LB medium with 50 µg/mL Ampicillin
Carbenicillin selection agar		LB agar with 100 µg/mL Carbenicillin
Carbenicillin selection medium		LB medium with 50 µg/mL Ampicillin
LB agar	98.5 %	LB-Medium
	1.5 %	Bacto agar
LB medium (Luria-Bertani)	10 g	Bacto peptone
	5 g	yeast extract
	5 g	NaCl
	ad 1 L	H_2O

5.6.3 Enzymes

Enzyme	Company with cat. no.
AleI	NEB, cat. no. R0634S
Alkaline phosphatase, calf intestinal (CIP)	NEB, cat. no. M0290
BamHI-HF	NEB, cat. no. R3136
BccI	NEB, cat. no. R0704S
BsmaI	NEB, cat. no. R0529S
BbsI	NEB, cat. no. R0539S
BsmBI (Esp3I)	ThermoScientific, cat. no. FD0454

BstBI	NEB, cat. no. R0519
DNase I (RNase-free)	Roche, cat. no. 04716728001
EcoRV-HF	NEB, cat. no. R3195
HaeIII	NEB, cat. no. R0108S
hCG (Human chorionic gonadotrophin)	Sigma, cat. no. CG5
Herculase II hot start polymerase	Agilent, cat. no. 600310
Hyaluronidase type IV-S from bovine testes, embryo tested	Sigma, cat. no. H4272
KpnI-HF	NEB, cat. no. R3142
NcoI-HF	NEB, cat. no. R3193
NruI	NEB, cat. no.R0192
PCR-Mastermix 5x	5 PRIME
Phire hot start II DNA polymerase	Fermentas/Thermo Scientific, cat. no. F-122S
PMSG (Pregnant mare serum gonadotropin)	Sigma, cat. no. G4877
Proteinase K	Roche, cat. no. 03115887001
RNase A	Serva, cat. no. 34388.01
T4 DNA ligase (400 U/µl)	New England Biolabs (NEB), cat. no. M0202
XbaI	NEB, cat. no. R0145

5.6.4 Oligonucleotides

5.6.4.1 Oligonucleotides for genotyping

Name	Sequence (5' to 3')	Conditions			Product
ROSA26_F	AGCACTGGTTTCTCAAGCAAAAGCTAA	94 ^{0}C	1 min		
		56.2 ^{0}C	1 min	30X	509 bp
ROSA26_R	CGCAATACCTTTATGGGAGTTCTCTGC	72 ^{0}C	1.5 min		
Rik_F	TTAGCTGAAATGGTTTGGAGAC	94 ^{0}C	1 min		
		59.5 ^{0}C	1 min	30X	418 bp
Rik_R	CATCACTGAGAAGCACTTGG	72 ^{0}C	1.5 min		
Fus-F	CTATGGAGATGATCGACGTG	94 ^{0}C	1 min		
		59 ^{0}C	30 sec	30X	576 bp
Fus-R	TGGTTACAATTAGGGTAGTCTG	72 ^{0}C	1.3 min		
Rab38_F	GGCCTCCAGGATGCAGACACC	94 ^{0}C	40 sec		
		58 ^{0}C	40 sec	30X	213 bp
Rab38_R	CCAGCAATGTCCCAGAGCTGC	72 ^{0}C	60 sec		
Fus-E6_F	GTATTCTGCTTTCTCATTCCACTG	95 ^{0}C	20 sec		
		59 ^{0}C	20 sec	30X	2.9 KB
Fus-E8_R	ACGAAACATCATGTCTGTCC	72 ^{0}C	1.5 min		
Fus_HRM_F	CGTTCGGATAATGTGAGACCTG	98 ^{0}C	5 sec		
		60 ^{0}C	5 sec	40X	140 bp
Fus_HRM_R	CAAAGGTAGCCGCCAACAAG	72 ^{0}C	5 sec		

Rik_HRM_F	CGTTCGGATAATGTGAGACCTG	98 ^{0}C	5 sec		
		62 ^{0}C	5 sec	40X	140 bp
Rik_HRM_R	CAAAGGTAGCCGCCAACAAG	72 ^{0}C	5 sec		

5.6.4.2 Oligonucleotides for PCR amplification

Name	Sequence (5' to 3')	Conditions			Product
Fus 5'_L_F	GTCATCAAGCACCTTTACCTG	95 ^{0}C	20 sec		
		64 ^{0}C	20 sec	30X	3.5 KB
Fus 5'_L-R	TGGTTACAATTAGGGTAGTCTG	72 ^{0}C	2 min		
Fus 3'_L_F	ACAAGGGTAACACTGGGTAC	95 ^{0}C	20 sec		
		64 ^{0}C	20 sec	30X	3.3 KB
Fus 3'_L_F	ACTCTTGTCTAGCAGTGATTCTC	72 ^{0}C	2 min		
Rik OS1_F	TGACTGACAGGCTTCACAGAGAGC	98 ^{0}C	5 sec		
		66 ^{0}C	5 sec	40X	140 bp
Rik OS1_R	CTACTGGGGACTGATGACTACCTG	72 ^{0}C	5 sec		
Rik OS2_F	CACAGGGACTTTGTGTGCACTCTT	98 ^{0}C	5 sec		
		66 ^{0}C	5 sec	40X	177 bp
Rik OS2_R	AAACCAGAGCATGGCTTTGAAAAA	72 ^{0}C	5 sec		
Rik OS3_F	GAAGATAAACAGGAGCCGCATGAA	98 ^{0}C	5 sec		
		66 ^{0}C	5 sec	40X	192 bp
Rik OS3_R	TGACTCACTAAGGGCCATTCCTTC	72 ^{0}C	5 sec		
Rik OS4_F	TACAGGCTTCACTCTGTGGGGTTT	98 ^{0}C	5 sec		
		66 ^{0}C	5 sec	40X	186 bp
Rik OS4_R	CCAGATCTGACTCAGGTAATGTGA	72 ^{0}C	5 sec		

Rik OS5_F	AGTGGCCCCACACAGAAGAGTAAG	98 ^{0}C	5 sec		
		66 ^{0}C	5 sec	40X	188 bp
Rik OS5_R	AGGAATGTGTGGGCAAATCTTGTT	72 ^{0}C	5 sec		
Fus OS1_F	CCAACCACCCATGGCTTCTTATTA	98 ^{0}C	5 sec		
		66 ^{0}C	5 sec	40X	164 bp
FusOS1_R	GCACTGGGGTAGCATACACATC	72 ^{0}C	5 sec		
Fus OS2_F	GCTTTCCTTGTTTTAGCACTCTGC	98 ^{0}C	5 sec		
		66 ^{0}C	5 sec	40X	176 bp
FusOS2_R	CTGCAGCCACTCCCTAAACTTCTT	72 ^{0}C	5 sec		
Fus OS3_F	CTCCCTTCCCTCTGTCTGTCTCTG	98 ^{0}C	5 sec		
		66 ^{0}C	5 sec	40X	141 bp
Fus OS3_R	TTTCTGGGTTACCTGGGGTCAGTA	72 ^{0}C	5 sec		
Fus OS4_F	CCCAAGCAGCTGGACTAAGGATCT	98 ^{0}C	5 sec		
		66 ^{0}C	5 sec	40X	164 bp
Fus OS4_R	ACACCTGGTGGTAGTTCATTGCTT	72 ^{0}C	5 sec		
Fus OS5_F	GTGAGTTCAAGTCCAGCCCAGTCT	98 ^{0}C	5 sec		
		66 ^{0}C	5 sec	40X	149 bp
Fus OS5_R	GCTTTGTGGCAGGCACTTTTATTC	72 ^{0}C	5 sec		
Fus 513 _F	TGGGTAGGGTAGTTCAGTAAC	95 ^{0}C	20 sec		
		55.5^{0}C	20 sec	30X	140 bp
Fus 513 _R	ACAAGGGTAACACTGGGTAC	72 ^{0}C	30 sec		

5.7 Immunohistochemistry

5.7.1 Solutions

Solution	Ingredients	
Blocking solution	1x	PBS
	10%	FCS
	0.5%	Tween 20
PBS-T	1x	PBS
	0.25%	Triton-X 100

5.7.2 Antibodies

Antibody	Dilution	Company
anti-FUS/TLS (4H11), mouse monoclonal	1 : 500	Santa Cruz Biotechnology
TIA1 antibody (sc-1751), goat polyclonal	1:300	Santa Cruz Biotechnology
Donkey-anti-goat	1:500	Life Technologies

5.8 Mouse strains

5.8.1 Wild type mouse strains

Mouse Strain	Description
C57Bl/6J	Black coat colour, wild type mouse line
DBA/2	Black coat colour, wild type mouse line
FVB/N	Albino coat colour, wild type mouse line
CD1	Albino coat colour, wild type mouse line
BDF1	Black coat colour, Hybrid mouse line crossing between C57BL/6 and DBA/2

5.8.2 Generated mouse strains

Mouse Strain	Description
Rik^{KO}	Targeted knockout by TALEN mediated NHEJ
Fus^{R513G}	Targeted knockin by TALEN mediated HR
Fus^{P517L}	Targeted knockin byTALEN mediated HR
Fus$^{double\ KO}$	Targeted knockout by CRISPR/Cas9 mediated NHEJ

6 Methods

6.1 Cloning and work with plasmid DNA

6.1.1 Production of competent bacteria

Electro competent *E.coli* bacteria were routinely used for cloning of a plasmid DNA. For cloning of normal plasmids, conventional DH5α strain was used, whereas for cloning of complicated plasmids (i.e. containing hairpins or inverted terminal repeats), the recombination deficient strains strains SURE® and Stabl2™ were used. Electro competent bacteria were prepared as follows: a single colony was picked up from the overnight incubated LB agar plate at 37 °C having without antibiotic selection. The single colony was inoculated in 5 ml of LB medium, and allow to grow overnight at 37 °C. From that 5 ml culture medium, 2.5 ml of a preparatory culture were transferred to 250 ml LB medium, and incubated on an orbital shaker at 37 °C. The density of the bacterial population was constantly monitored with a photometer at 600 nm until it attained 0.5. The absorption should not exceed 0.65. Afterwards, the bacterial suspension was split into four 50 ml tubes and followed by cooling on ice for 10 minutes. Then, the tubes were centrifuged at 4,000 rpm for 15 minutes at 4 °C. Subsequently, the supernatants were discarded, and the pellets were carefully resolved in 25 ml of ice-cold 10% glycerol and pooled in two 50 ml tubes. Then, the tubes were centrifuged at 4,000 rpm for 15 minutes at 4 °C; that step was repeated twice. Finally, the bacteria were resuspended in 800 µl of 10 % glycerol that dispensed into the 50 µl aliquots and immediately stored at −80 °C. The transformation efficiency was checked for each batch by transformation with 10 pg pUC18 control plasmid.

6.1.2 Transformation of competent bacteria

For transformation, one aliquot of electro competent *E. coli* was thawed on ice, and 1 µl of ligation batch or 10 pg of pure plasmid were added. The suspension was thoroughly mixed and transferred into an electroporation cuvette. Electroporation was performed with a Biorad electroporation system according the manufacture's instruction, and then the cell suspension was transferred immediately into 1 ml of SOC medium. Consequently, the mixture was incubated at 37 °C for 30–60 min for reviving the full population of the transformed bacteria. Afterwards, the bacteria were plated on LB agar plates containing either 100 µg ampicillin or 50 µg kanamycin antibiotics and incubated overnight at 37 °C.

6.1.3 Isolation of plasmid DNA

Plasmid DNA was isolated from the transformed bacteria using the following kits: the Qiagen Miniprep kit was used firstly for screening of the corrected transformed clones, and the Qiagen MaxiPrep kit or Qiagen HiSpeed Plasmid maxi kit for higher yield plasmid preparation. At first step, the plasmid DNA was extracted from the transformed overnight culture by Qiagen MiniPrep Kit for screening out the correctly transformed clones. Afterwards, Qiagen Plasmid Maxi Kit was used for higher yield of plasmid DNA. For MiniPrep production, a single colony was inoculated in 2–3 ml of LB medium with desired antibiotic overnight at 37 °C. Similarly, for the MaxiPrep production, 100 μl of MiniPrep culture were dispensed in 250 ml of LB medium with appropriate antibiotics and incubated overnight at 37 °C. For future purposes, 500 μl of bacterial culture was mixed with 500 μl of glycerol and stored in −80 °C. The isolation of plasmid DNA is based upon the modified alkaline lysis procedure, followed by binding of plasmid DNA to Qiagen resin under appropriate low-salt and pH condition. RNA, proteins, dyes, and low molecular weight impurities are removed by a medium-salt wash. Afterwards, plasmid DNA is eluted in a high-salt buffer, and then concentrated and desalted by isopropanol precipitation. After isolation of DNA, the concentration was measured by the spectro-photometer. The optical density (OD) was measured at a wavelength of 260 nm, and quality of the DNA was determined by the OD_{260}/OD_{280} ratio, which should not exceed a value of 1.8 (OD_{260}= 1.0 corresponds to 50 μg/mL double stranded and 33 μg/ml single-stranded DNA). Subsequently the DNA was stored in -20 °C for future purposes.

6.1.4 Restriction digest of plasmid DNA

For the complete digestion of the plasmid DNA, 10 units (U) of restriction enzyme were used per μg of DNA. The reaction conditions and the type of buffer were chosen according to manufacturer's instructions. The restriction digest was incubated for 1–2 hrs at an appropriate temperature according to the manufacturer's instruction. For generating blunt end, the digested DNA was incubated with klenow fragment of DNA polymerase I. Therefore, 5 U klenow fragment and 25 nM dNTPS were added and incubated at RT for 20 min. Afterwards, the samples was subjected to 75 °C for 20 min to inactivate the Klenow fragment. Similarly, in order to prevent the re-ligation of digested open ends of plasmids, 10 units alkaline phosphatase (CIP) were added and incubated at 37 °C for 45 min to remove the terminal phosphates of the vector fragment.

6.1.5 Gel electrophoresis and isolation of the DNA fragment

Prior to gel electrophoresis, different proportion of agarose gel was prepared in advance. DNA samples were supplemented with DNA loading buffer, and inoculated on agarose gels containing the ethidium bromide, an intercalating dye for visualization of the DNA fragments. For example, 0.9% agarose gel was used for separation of larger DNA fragments, whereas 2–4% gel was prepared for separating smaller digested fragments. The agarose gel was run in the presence of 1X TAE buffer at a voltage of 100 V for 30–60 min, which depends on the size of the fragments. After separation of the bands, the DNA was visualized using long wave UV light (366 nm). The desired band was recovered by cutting the band very carefully using a scalpel. Subsequently, the DNA was extracted from the gel silica using the Qiagen Gel Extraction Kit or Qiagen MiniElute Gel Extraction kit following the manufacturer's instructions. Afterwards, the concentration of isolated DNA was measured by spectrophotometer and stored at in -20 °C for future purposes.

6.1.6 Ligation of DNA fragments

For the ligation of the linearised vector and the insert, a molar ratio of 1:3 (vector DNA: insert) was used. Whereas for the ligation of the very short inserts (<500 bp), a molar ratio of 1:6 was used. Ligation master mixture was prepared by the addition of T4 DNA ligase buffer, T4 DNA ligase (600 U), and together with the vector and insert in a total volume of 15 µl. Consequently, the reaction was incubated for one hr at room temperature for sticky end ligation or overnight incubation at 16 °C for blunt end ligation. Afterwards, the ligation mixture undergoes dialysis to remove salts. Then, the one µl of the reaction batch was used for transformation, rest mixture was stored at -20 °C for the backup purposes. For the ligation of PCR fragments into a standard vector (here pSC-B-amp/kan), the Blunt PCR Cloning Kit StrataClone was used (see session 6.4.3.6).

6.2 Construction and functional validation of site specific nucleases

6.2.1 Construction of TALENs

6.2.1.1 TALENs target site selection

The "TALEN*designer*" (www.talen-design.de) web tool was used for selecting of TALEN target sequences, as described previously (Wefers et al., 2013a). Selected target sites consist two recognition sequences of 15 bp preceded by a T, separated by a spacer of

14–15 bp. To minimize off-target recognition, potential off-target sites were analysed using the "Paired Target Finder" (https://tale-nt.cac.cornell.edu) (settings: spacer length 13–20 bp, cutoff 3.0) (Doyle et al., 2012).

6.2.1.2 Construction and expression of TALENs

For the expression of TALENs in mammalian cells, pCAG-TAL-linker-X-A/G/C/T-poly A expression vector was used (Figure S6) that contains a CAG hybrid promoter region and a transcriptional unit comprising a sequence coding for the N-terminal 110 amino acids of TAL nuclease, C-terminal 44 amino acids that located upstream and downstream of a pair of BsmBI restriction sites. To derive TAL element DNA binding domains, I used the TAL effector motif (repeat) #11 of the *Xanthomonas* Hax3 protein (LTPEQVVAIASNIGGKQALETVQRLLPVLCQAHG) to recognise A, the TAL effector motif #5 (LTPQQVVAIASHDGGKQALETVQRLLPVLCQAHG) derived from the Hax3 protein to recognise C, and the TAL effector motif #4 (LTPQQVVAIASNGGGKQALETVQRLLPVLCQAHG) from the *Xanthomonas* Hax4 protein to recognise T. To recognise a target G nucleotide, the TAL effector motif #4 from the Hax4 protein was used with replacement of the amino acids 12 into N and 13 into N (LTPQQVVAIASNNGGKQALETVQRLLPVLCQAHG). These elements were obtained from gene synthesis (Genscript, Piscataway, NJ, USA), and further amplified by PCR using primers that include BsaI sites outside of the coding region. For a 15 bp TALEN target sequence, seven elements each are pooled in a pair of reactions together with BsaI and T4 DNA ligase to create unique overhangs. Full-length ligation products were recovered by gel extraction and inserted by seamless cloning (Gibson assembly) into pCAG-TALEN opened with BsmBI. The integrity of all TALEN expression vectors was confirmed by DNA sequencing.

6.2.1.2.1 Construction and expression of TALEN-95 A vector

pT7-TALEN-95A was derived from pCAG-TAL-Linker-poly (A) vector by replacement of the poly(A) signal sequence with a segment of 95 adenine residues derived from a mouse Oct4 cDNA clone.

6.2.1.3 Single-stranded oligodesoxynucleotide design.

The oligodeoxynucleotides ODN^{R513G} (5'-TGGGTAGGGTAGTTCAGTAACACGTAATCTAACATAACTTTTTCTTTCAGGGGCGAGCA CGACAGGAT**G**GCAGGGAGAG<u>A</u>CCATATTAGCCTGGCTCCTGAAGTTCTGGAACTCTTC

CTGTACCCAGTGTTACCCTTGT-3'),   ODN[P517L]   (5'-
TCAGTAACACGTAATCTAACATAACTTTTTCTTTCAGGGGCGAGCACAGACAGGATCGC
AGGGAGAG**A**C̲TATATTAGCCTGGCTCCTGAAGTTCTGGAACTCTTCCTGTACCCAGTGT
TACCCTTGTTATTTTGTAAACT-3'),   and   ODN[Rab#1]   (5'-
CACCTCACAAGGAGCACCTGTACAAGCTGCTGGTGATCGGCGACCTGG**TA**GTGGGCA
AGACCAGCATTAT̲TAA̲ACG̲GTAC̲GTGCA̲TCAAAA̲TTTCTCCTC̲TCA̲TTA̲TCGA̲GCCACCA
TTGGTGTGACTTCGCGCTGAAGGTGC-3') were synthesized and HPLC purified by
Metabion (Martinsried, Germany), each having a length of 140 nt, including the targeted
mutation (shown in boldface type) and a silent replacement (underlined), covering 70 bp
upstream and downstream of the targeted codon.

6.2.2 Construction of CRISPR/Cas

6.2.2.1 sgRNA target site selection

The "http://www.genome-engineering.org/" web tool was used for selecting of sgRNA
target sequences, which also predicts the putative off-target loci for determining specificity,
as described previously (Hsu et al., 2013). Selected target sites consist 23 nucleotides
containing the NGG, a PAM sequence to maximize the Cas9 specificity to modify only one
site of genome. In order to reduce the off-site activity, the target site of sgRNA was selected
as uniquely located in whole genome, and in which at least two mismatches lie within the
PAM-proximal region in the genomic off-target loci, and avoided if this site has fewer than
three mismatches in the unintended sites.

6.2.2.2 Construction and expression of sgRNA

The expression vector pbs-T7-sgRNA was digested with BbsI and treated with
alkaline phosphatase, and the linearised vector is gel purified (Figure S7). A pair of oligos for
each target site is annealed, phosphorylated, and ligated into the linearised vector. The
integrity of all sgRNA expression vectors were confirmed by DNA sequencing.

6.2.2.3 Construction and expression of Cas9

The codon optimised version of the *S. pyogenes* Cas9 was cloned in-between the
nuclear localisation sequence (NLS) region of pCAG-poly(A) vector to ensure nuclear
compartmentalisation in mammalian cells. 95 or 166 adenine residues derived from a mouse
Oct4 cDNA clone were cloned into the pCAG-Cas9-poly(A) expression vector by
replacement of the poly(A) sequence. The integrity of all pCAG-Cas9-95/166(A) expression
vectors were confirmed by DNA sequencing.

6.2.3 Construction of reporter plasmids

Nuclease reporter plasmids were created by the insertion of a pair of annealed sense and anti-sense oligonucleotides (Metabion, Martinsried, Germany) of TALEN or sgRNA target sequences, into the generic reporter plasmid pCMV-TALEN/CRISPR-Rep by BstBI and NruI restriction digestion (Figure S8). Consequently, the constructed reporter plasmids were sent for sequencing to confirm the integrity.

6.2.4 Assessment of the nuclease activity

6.2.4.1 Culture of the HEK293 cells

Due to easy in handling, cultivation, and higher transfection efficiency, HEK293 cells are commonly used for the nuclease activity assay. At first, the frozen HEK293 cells were thawed slowly in a water bath at 37 °C. The thawed HEK293 cells were cultured in 5 ml of DMEM medium containing 10% FCS (vol/vol) and L-glutamine, and centrifuged at 1200 rpm for 5 min to obtain the pellet. Then, the cell pellet was resuspended in 12 ml DMEM medium in 10 cm dishes and cultured at 37 °C. The confluent cells were split one day before transfection. To obtain the $1x10^6$ cells, cells were washed twice before trypsinisation step. Afterwards, the trypsin was inactivated by supplemented with fresh medium containing the FCS. Then, the isolated cells were seeded into 10 cm dishes containing DMEM medium, and cultured again at 37 °C in a 5% CO_2 atmosphere to synchronise all cells to same stage of cell division.

6.2.4.2 Functional validation of TALENs or CRISPR/Cas

A total of $1x10^6$ cells were transfected by co-electroporation with 5 µg of each TALEN expression plasmid, or 6 µg of Cas9 expression plasmid and 2 µg of sgRNA expression plasmid, together with the 5 µg of TALEN reporter and 5 µg of the luciferase expression plasmid pCMV-TALEN/CRISPR-Rep. Here the plasmid pCMV-TALEN/CRISPR-Rep with or without sgRNA plasmid serve as an internal control. After transfection, cells were splitted into three wells, which treat as a technical replicates. Forty-eight hours after transfection, cells were lysed to extract the whole protein samples. β-galactosidase activity was assessed using the β-galactosidase reporter gene assay following the manufacturer's instructions, and Centro LB 960 luminometer was used to detect the fluorescent signals. In parallel, luciferase substrate was added to the protein samples, and chemiluminescent signals were measured in the luminometer. Here luciferase activity was measured as transfection control. The triplicate β-galactosidase values of each transfected DNA mixture were normalised in relation to the levels of luciferase activity of the same samples, and the mean value and

SEM of the β-galactosidase activities were determined. The values obtained from co-transfection of TALEN expression and reporter plasmids were compared with the transfection of reporter plasmid without TALEN plasmids to determine the relative nuclease efficiency.

6.3 *In vitro* transcription of TALENs or CRISPR/Cas

Briefly, TALEN or Cas9 mRNAs were prepared in a single step by *in vitro* transcription from the pT7-TALEN-95A or pT7-Cas9-95/166A plasmid DNA, linearised with XbaI and AleI, using mMessage mMachine T7 ultra kit, by omitting the second polyadenylation step (Figure 12). However, sgRNA was prepared by the amplification of the target sequence from the pT7-sgRNA plasmid, followed by IVT using MEGAshortscript™ T7 Kit. The transcribed RNA is purified by MEGAclear kit. Afterwards, the quality of the synthesized mRNAs was controlled by denaturing agarose gel electrophoresis, using NorthernMax-Gly system and the RNA Millenium size marker. Each mRNAs are mixed with targeting molecules (15 ng/ml) in injection buffer and stored at −80 °C as single-use aliquots.

6.4 Identification of mutant founders

6.4.1 Pronuclear microinjection of nuclease mRNA and oligos

For microinjections, one-cell embryos were recovered by mating of the (DBA2x C57BL/6) F_1 males with superovulated FVB/N females. Superovulation was done by injection of pMSG (7.5 U) and HCG (7.5 U). In order to obtain the *in vivo* mutagenesis, one-cell embryos were injected with either only mRNA of TALEN or CRISPR (Cas9 and sgRNA) with or without the targeting oligonucleotides (ODNR[513G], ODN[P517L], and ODN[Rab#1]) into the larger pronucleus, but not into cytoplasm.

In test experiments, It was showed that microinjection of Venus mRNA (90 ng/ml) using pronuclear capillaries led to green fluorescence in all two-stage embryos (Figure 12D), whereas the cytoplasmic delivery of the same volume is less effective and labels only ~10% of embryos.

6.4.2 Embryo transfers

For the transfer of microinjected embryos into the oviducts of pseudo-pregnant females, CD1 females (8–10 weeks old) are mated in single pairs overnight to vasectomized CD1 males. Typically, 150 fertilized embryos are obtained from 15 superovulated FVB females. Survived embryos (~100) were immediately transferred without delay in groups of

20 into oviducts of five plug-positive CD1 foster mothers by anesthetized with 0.25 ml of Rompun/Ketanest, and make a 5-mm skin incision parallel to the dorsal midline above the position of the left or right. All mice indicated normal development, and appeared healthy. Mice were handled according to institutional guidelines approved by the animal welfare, and use committee of the government of Upper Bavaria and housed in standard cages in a specific pathogen-free facility on a 12-h light/dark cycle with *ad libitum* access to food and water.

6.4.3 Genotyping of the founders

6.4.3.1 Tail DNA isolation

Using the Wizard genomic DNA purification kit, genomic DNA was isolated from tail tips of founder mice and their progeny, according to manufacturer's instructions.

6.4.3.2 Polymerase Chain Reaction (PCR)

Targeted genomic region was amplified with locus specific primers. A set up a 50- µl PCR reaction containing the following components

Amounts	Components
1 µl	Genomic DNA (100–200 ng)
10 µl	5× Herculase II buffer
1 µl	dNTP mix (10 mM each)
1 µl	Forward PCR primer (10 µM)
1 µl	Reverse PCR primer (10 µM)
1 µl	Herculase II hot start polymerase
35 µl	DNase-free H_2O

The specific conditions (*i.e.* primer sequences, initiation/annealing/elongation temperatures, cycle duration, and number of repetitions) were adjusted individually for each PCR reaction and can be found in the materials section 5.6.4.

6.4.3.3 RFLP analysis of PCR products

According to the specific experiment, set up the control digestions of resultant founder with wild-type samples. The 25 µl of PCR products were used for restriction digestion with specific enzymes for 1 hr at the temperature recommended by the manufacturer.

Amounts	Components
20 µl	Purified PCR product
2 µl	10× restriction buffer
10 U	Restriction enzyme
Adjusted to 25 µl	DNase-free H_2O

The incubation temperature is dependent on the type of restriction enzyme used. Afterwards, the samples were mixed with DNA loading dye and subjected to gel electrophoresis to check the nuclease mediated editing events.

6.4.3.4 Direct sequencing

Another 25 µl of PCR products were column purified by the QIAquick PCR purification kit and the purified PCR products were subjected to direct sequencing either by forward or reverse primers.

6.4.3.5 HRMA

For identification of nuclease mediated founders, 140 bp of target regions of the genomic loci were amplified. For this, add in duplicate 40 ng of genomic DNA from founder mice along with the wild-type control mice in a 96-well black/white measurement plate. The targeted genomic regions were amplified by using locus-specific HRMA primers in a 10 µl reaction with following components:

Amounts	Components
40 ng	Genomic DNA
2 µl	5× Phire reaction buffer
0.2 µl	dNTP mix (10 mM each)
1 µl	10x LC Green Plus$^+$ dye
0.25 µl	Forward PCR primer (10 µM)
0.25 µl	Reverse PCR primer (10 µM)
0.2 µl	Herculase II hot start polymerase
Adjusted to 10 µl	DNase-free H_2O

The specific conditions (*i.e.* primer sequences, initiation/annealing/elongation temperatures, cycle duration, and number of repetitions) were adjusted individually for each PCR reaction and can be found in the materials section 5.6.4.

6.4.3.6 Subcloning of mutant alleles

PCR products of founders harboring mutant alleles were subcloned by using StrataClone blunt PCR cloning kit according to the manufacturer's instructions. Here the PCR products generated by Herculase II polymerase are blunt-ended. The ligation mixture was prepared by the following components:

Amounts	Components
3 µl	StrataClone blunt cloning buffer
1 µl	PCR product
1 µl	StrataClone blunt vector mix

Incubate the mixture at RT for 5 min and then pipette 1 µl of the ligation mixture to a freshly thawed 50 µl aliquot of StrataClone SoloPack competent cells, followed by 20 min incubation on ice. Afterwards, chemical transformation was done in a water bath at 42 °C for 45 sec, followed by 2 min incubation on ice. Then, added 250 µl prewarmed SOC medium and incubate the cells at 37 °C for 1 hr with agitation. Mix 25 µl of cells with 40 µl of 2% (wt/vol) X-gal and plate the mixture on prewarmed LB-carbenicillin plates. Subsequently, incubate the plates overnight at 37 °C, preceded by isolation of the plasmid DNA by using the mini-prep kit according to the manufacturer's instructions. At last, sequence of the inserted alleles were checked by using the T3 or T7 sequencing primer; compare the sequence with a wild-type sequence to identify the type and location of mutation.

6.5 Analysis of RNA

6.5.1 Isolation of RNA

For RNA work, all materials were treated with RNaseZap® and only RNase-free solutions, tubes and pipette tips were used to prevent contamination. After the cutting, the tail of mouse was immediately frozen on dry ice. Then, the sample was stored at -80 °C or immediately processed. Afterwards, the tail was homogenized in Trizol, and total RNA was isolated following manufacturer's instructions. Then, RNA concentration was measured with a spectrophotometer, where an OD_{260} of one corresponds to 40 µg RNA per ml. Pure RNA has an OD_{260}/OD_{280} ratio of ~2.0.

6.5.2 Reverse transcription polymerase chain reaction (RT-PCR)

Total RNA was reverse transcribed into cDNA using the Protoscript M-MuLV Taq-RT PCR kit in presence of oligo $dT_{23}VN$, according to the manufacturer's protocol. The following reaction batch was used:

Amounts	Components
1-10 µl (1 ng–1 µg)	RNA
2 µl	Primer dT$_{23}$VN/Gene specific primer
4 µl	dNTP mix
Add up to 16 µl	Nuclease free water

Then, warm the mixture for 5 min at 70 °C, followed by spinning and promptly chill on ice. Afterwards, following components were added to 16 µl RNA/primer/dNTP solution and mix well by pipetting up and down:

Amounts	Components
16 µl	RNA/primer/dNTP mixture
2 µl	10X RT Buffer
0.5 µl	Murine RNase Inhibitor
1 µl	M-MuLV Reverse Transcriptase
Add up to 20 µl	Nuclease free water

The cDNA reaction was incubated at 42 °C for 60 min; reverse transcriptase was inactivated at 85 °C for 5 min. The cDNA was either processed immediately or frozen at -20 °C. An amount of 1 µl of cDNA template was used for further RT-PCR analysis.

6.6 Immunocytochemistry analysis of MEFs

For inducing stress, confluent cells were first treated with 0.5 mM sodium arsenite for 1 hr, followed by three times washing the cells with PBS. For immunocytochemistry of MEFs, stressed cells were fixed with 4% paraformaldehyde (PFA) for 20 min in PBS, and subsequently blocked for 20–30 min in blocking solution, and were washed with PBS for three times. Meanwhile, primary antibodies such as mouse anti-TIA and anti-FUS/TLS were diluted in blocking solution in the ratio of 1:300, 1:500, respectively. Afterwards, the fixed cells were incubated with the primary antibodies for overnight at 4 °C. After the overnight incubation, the cells were washed with PBS for 3 times, consequently incubated with secondary antibody (diluted in blocking solution in the ratio of 1:500) for 1 hr, then washed with PBS. To visualize nuclei and the stress granules, stressed cells were treated DAPI (2 µg/ml) at room temperature for 5 min followed by washing with PBS. Cover slips were mounted onto glass slides and undergoing microscopic analysis.

7 References

Ash, P.E.A., Bieniek, K.F., Gendron, T.F., Caulfield, T., Lin, W.-L., Dejesus-Hernandez, M., van Blitterswijk, M.M., Jansen-West, K., Paul, J.W., 3rd, Rademakers, R., et al. (2013). Unconventional translation of C9ORF72 GGGGCC expansion generates insoluble polypeptides specific to c9FTD/ALS. Neuron *77*, 639–646.

Ayala, Y.M., Zago, P., D'Ambrogio, A., Xu, Y.-F., Petrucelli, L., Buratti, E., and Baralle, F.E. (2008). Structural determinants of the cellular localization and shuttling of TDP-43. J. Cell Sci. *121*, 3778–3785.

Bacman, S.R., Williams, S.L., Pinto, M., Peralta, S., and Moraes, C.T. (2013). Specific elimination of mutant mitochondrial genomes in patient-derived cells by mitoTALENs. Nat. Med. *19*, 1111–1113.

Barber, S.C., Mead, R.J., and Shaw, P.J. (2006). Oxidative stress in ALS: a mechanism of neurodegeneration and a therapeutic target. Biochim. Biophys. Acta *1762*, 1051–1067.

Bassett, A.R., Tibbit, C., Ponting, C.P., and Liu, J.L. (2013). Highly efficient targeted mutagenesis of Drosophila with the CRISPR/Cas9 system. Cell Rep. *4*, 220–228.

Beurdeley, M., Bietz, F., Li, J., Thomas, S., Stoddard, T., Juillerat, A., Zhang, F., Voytas, D.F., Duchateau, P., and Silva, G.H. (2013). Compact designer TALENs for efficient genome engineering. Nat. Commun. *4*, 1762.

Bhakta, M.S., and Segal, D.J. (2010). The generation of zinc finger proteins by modular assembly. Methods Mol. Biol. Clifton NJ *649*, 3–30.

Bibikova, M., Golic, M., Golic, K.G., and Carroll, D. (2002). Targeted chromosomal cleavage and mutagenesis in Drosophila using zinc-finger nucleases. Genetics *161*, 1169–1175.

Bitinaite, J., Wah, D.A., Aggarwal, A.K., and Schildkraut, I. (1998). FokI dimerization is required for DNA cleavage. Proc. Natl. Acad. Sci. U. S. A. *95*, 10570–10575.

Bloom, K., Ely, A., Mussolino, C., Cathomen, T., and Arbuthnot, P. (2013). Inactivation of hepatitis B virus replication in cultured cells and in vivo with engineered transcription activator-like effector nucleases. Mol. Ther. J. Am. Soc. Gene Ther. *21*, 1889–1897.

Boch, J., and Bonas, U. (2010). Xanthomonas AvrBs3 family-type III effectors: discovery and function. Annu. Rev. Phytopathol. *48*, 419–436.

Boch, J., Scholze, H., Schornack, S., Landgraf, A., Hahn, S., Kay, S., Lahaye, T., Nickstadt, A., and Bonas, U. (2009). Breaking the code of DNA binding specificity of TAL-type III effectors. Science *326*, 1509–1512.

Boillée, S., Vande Velde, C., and Cleveland, D.W. (2006). ALS: a disease of motor neurons and their nonneuronal neighbors. Neuron *52*, 39–59.

Bosco, D.A., Lemay, N., Ko, H.K., Zhou, H., Burke, C., Kwiatkowski, T.J., Jr, Sapp, P., McKenna-Yasek, D., Brown, R.H., Jr, and Hayward, L.J. (2010). Mutant FUS proteins that cause amyotrophic lateral sclerosis incorporate into stress granules. Hum. Mol. Genet. *19*, 4160–4175.

Briggs, A.W., Rios, X., Chari, R., Yang, L., Zhang, F., Mali, P., and Church, G.M. (2012). Iterative capped assembly: rapid and scalable synthesis of repeat-module DNA such as TAL effectors from individual monomers. Nucleic Acids Res. *40*, e117.

Cade, L., Reyon, D., Hwang, W.Y., Tsai, S.Q., Patel, S., Khayter, C., Joung, J.K., Sander, J.D., Peterson, R.T., and Yeh, J.R.J. (2012). Highly efficient generation of heritable zebrafish gene mutations using homo- and heterodimeric TALENs. Nucleic Acids Res. *40*, 8001–8010.

Calsou, P., Delteil, C., Frit, P., Drouet, J., and Salles, B. (2003). Coordinated assembly of Ku and p460 subunits of the DNA-dependent protein kinase on DNA ends is necessary for XRCC4-ligase IV recruitment. J. Mol. Biol. *326*, 93–103.

Capecchi, M.R. (2005). Gene targeting in mice: functional analysis of the mammalian genome for the twenty-first century. Nat. Rev. Genet. *6*, 507–512.

Carbery, I.D., Ji, D., Harrington, A., Brown, V., Weinstein, E.J., Liaw, L., and Cui, X. (2010). Targeted genome modification in mice using zinc-finger nucleases. Genetics *186*, 451–459.

Cermak, T., Doyle, E.L., Christian, M., Wang, L., Zhang, Y., Schmidt, C., Baller, J.A., Somia, N.V., Bogdanove, A.J., and Voytas, D.F. (2011). Efficient design and assembly of custom TALEN and other TAL effector-based constructs for DNA targeting. Nucleic Acids Res. *39*, e82.

Chandrasegaran, S., and Smith, J. (1999). Chimeric restriction enzymes: what is next? Biol. Chem. *380*, 841–848.

Chang, N., Sun, C., Gao, L., Zhu, D., Xu, X., Zhu, X., Xiong, J.W., and Xi, J.J. (2013). Genome editing with RNA-guided Cas9 nuclease in zebrafish embryos. Cell Res. *23*, 465–472.

Chen, F., Pruett-Miller, S.M., Huang, Y., Gjoka, M., Duda, K., Taunton, J., Collingwood, T.N., Frodin, M., and Davis, G.D. (2011). High-frequency genome editing using ssDNA oligonucleotides with zinc-finger nucleases. Nat. Methods *8*, 753–755.

Choulika, A., Perrin, A., Dujon, B., and Nicolas, J.F. (1995). Induction of homologous recombination in mammalian chromosomes by using the I-SceI system of Saccharomyces cerevisiae. Mol. Cell. Biol. *15*, 1968–1973.

Christian, M., Cermak, T., Doyle, E.L., Schmidt, C., Zhang, F., Hummel, A., Bogdanove, A.J., and Voytas, D.F. (2010). Targeting DNA double-strand breaks with TAL effector nucleases. Genetics *186*, 757–761.

Cong, L., Ran, F.A., Cox, D., Lin, S., Barretto, R., Habib, N., Hsu, P.D., Wu, X., Jiang, W., Marraffini, L.A., et al. (2013). Multiplex genome engineering using CRISPR/Cas systems. Science *339*, 819–823.

Cruts, M., Gijselinck, I., Van Langenhove, T., van der Zee, J., and Van Broeckhoven, C. (2013). Current insights into the C9orf72 repeat expansion diseases of the FTLD/ALS spectrum. Trends Neurosci. *36*, 450–459.

Cui, X., Ji, D., Fisher, D.A., Wu, Y., Briner, D.M., and Weinstein, E.J. (2011). Targeted integration in rat and mouse embryos with zinc-finger nucleases. Nat. Biotechnol. *29*, 64–67.

DeJesus-Hernandez, M., Mackenzie, I.R., Boeve, B.F., Boxer, A.L., Baker, M., Rutherford, N.J., Nicholson, A.M., Finch, N.A., Flynn, H., Adamson, J., et al. (2011). Expanded GGGGCC hexanucleotide repeat in noncoding region of C9ORF72 causes chromosome 9p-linked FTD and ALS. Neuron *72*, 245–256.

Deltcheva, E., Chylinski, K., Sharma, C.M., Gonzales, K., Chao, Y., Pirzada, Z.A., Eckert, M.R., Vogel, J., and Charpentier, E. (2011). CRISPR RNA maturation by trans-encoded small RNA and host factor RNase III. Nature *471*, 602–607.

Deng, D., Yan, C., Pan, X., Mahfouz, M., Wang, J., Zhu, J.-K., Shi, Y., and Yan, N. (2012a). Structural basis for sequence-specific recognition of DNA by TAL effectors. Science *335*, 720–723.

Deng, D., Yin, P., Yan, C., Pan, X., Gong, X., Qi, S., Xie, T., Mahfouz, M., Zhu, J.-K., Yan, N., et al. (2012b). Recognition of methylated DNA by TAL effectors. Cell Res. *22*, 1502–1504.

Dickinson, D.J., Ward, J.D., Reiner, D.J., and Goldstein, B. (2013). Engineering the Caenorhabditis elegans genome using Cas9-triggered homologous recombination. Nat. Methods *10*, 1028–1034.

Donoho, G., Jasin, M., and Berg, P. (1998). Analysis of gene targeting and intrachromosomal homologous recombination stimulated by genomic double-strand breaks in mouse embryonic stem cells. Mol. Cell. Biol. *18*, 4070–4078.

Dormann, D., and Haass, C. (2013). Fused in sarcoma (FUS): an oncogene goes awry in neurodegeneration. Mol. Cell. Neurosci. *56*, 475–486.

Dormann, D., Rodde, R., Edbauer, D., Bentmann, E., Fischer, I., Hruscha, A., Than, M.E., Mackenzie, I.R.A., Capell, A., Schmid, B., et al. (2010). ALS-associated fused in sarcoma (FUS) mutations disrupt Transportin-mediated nuclear import. EMBO J. *29*, 2841–2857.

Doyle, E.L., Booher, N.J., Standage, D.S., Voytas, D.F., Brendel, V.P., Vandyk, J.K., and Bogdanove, A.J. (2012). TAL Effector-Nucleotide Targeter (TALE-NT) 2.0: tools for TAL effector design and target prediction. Nucleic Acids Res. *40*, W117–122.

Doyon, Y., McCammon, J.M., Miller, J.C., Faraji, F., Ngo, C., Katibah, G.E., Amora, R., Hocking, T.D., Zhang, L., Rebar, E.J., et al. (2008). Heritable targeted gene disruption in zebrafish using designed zinc-finger nucleases. Nat. Biotechnol. *26*, 702–708.

Eisenschmidt, K., Lanio, T., Simoncsits, A., Jeltsch, A., Pingoud, V., Wende, W., and Pingoud, A. (2005). Developing a programmed restriction endonuclease for highly specific DNA cleavage. Nucleic Acids Res. *33*, 7039–7047.

Flisikowska, T., Thorey, I.S., Offner, S., Ros, F., Lifke, V., Zeitler, B., Rottmann, O., Vincent, A., Zhang, L., Jenkins, S., et al. (2011). Efficient immunoglobulin gene disruption and targeted replacement in rabbit using zinc finger nucleases. PloS One *6*, e21045.

Fonfara, I., Curth, U., Pingoud, A., and Wende, W. (2012). Creating highly specific nucleases by fusion of active restriction endonucleases and catalytically inactive homing endonucleases. Nucleic Acids Res. *40*, 847–860.

Friedland, A.E., Tzur, Y.B., Esvelt, K.M., Colaiácovo, M.P., Church, G.M., and Calarco, J.A. (2013). Heritable genome editing in C. elegans via a CRISPR-Cas9 system. Nat. Methods *10*, 741–743.

Fujii, R., Okabe, S., Urushido, T., Inoue, K., Yoshimura, A., Tachibana, T., Nishikawa, T., Hicks, G.G., and Takumi, T. (2005). The RNA binding protein TLS is translocated to dendritic spines by mGluR5 activation and regulates spine morphology. Curr. Biol. CB *15*, 587–593.

Gabriel, R., Lombardo, A., Arens, A., Miller, J.C., Genovese, P., Kaeppel, C., Nowrouzi, A., Bartholomae, C.C., Wang, J., Friedman, G., et al. (2011). An unbiased genome-wide analysis of zinc-finger nuclease specificity. Nat. Biotechnol. *29*, 816–823.

Gabsalilow, L., Schierling, B., Friedhoff, P., Pingoud, A., and Wende, W. (2013). Site- and strand-specific nicking of DNA by fusion proteins derived from MutH and I-SceI or TALE repeats. Nucleic Acids Res. *41*, e83.

Gaj, T., Mercer, A.C., Sirk, S.J., Smith, H.L., and Barbas, C.F., 3rd (2013). A comprehensive approach to zinc-finger recombinase customization enables genomic targeting in human cells. Nucleic Acids Res. *41*, 3937–3946.

Gal, J., Zhang, J., Kwinter, D.M., Zhai, J., Jia, H., Jia, J., and Zhu, H. (2011). Nuclear localization sequence of FUS and induction of stress granules by ALS mutants. Neurobiol. Aging *32*, 2323.e27–40.

Geurts, A.M., Cost, G.J., Freyvert, Y., Zeitler, B., Miller, J.C., Choi, V.M., Jenkins, S.S., Wood, A., Cui, X., Meng, X., et al. (2009). Knockout rats via embryo microinjection of zinc-finger nucleases. Science *325*, 433.

Gijselinck, I., Van Langenhove, T., van der Zee, J., Sleegers, K., Philtjens, S., Kleinberger, G., Janssens, J., Bettens, K., Van Cauwenberghe, C., Pereson, S., et al. (2012). A C9orf72 promoter repeat expansion in a Flanders-Belgian cohort with disorders of the frontotemporal lobar degeneration-amyotrophic lateral sclerosis spectrum: a gene identification study. Lancet Neurol. *11*, 54–65.

Gitcho, M.A., Baloh, R.H., Chakraverty, S., Mayo, K., Norton, J.B., Levitch, D., Hatanpaa, K.J., White, C.L., 3rd, Bigio, E.H., Caselli, R., et al. (2008). TDP-43 A315T mutation in familial motor neuron disease. Ann. Neurol. *63*, 535–538.

Gratz, S.J., Cummings, A.M., Nguyen, J.N., Hamm, D.C., Donohue, L.K., Harrison, M.M., Wildonger, J., and O'Connor-Giles, K.M. (2013). Genome engineering of Drosophila with the CRISPR RNA-guided Cas9 nuclease. Genetics *194*, 1029–1035.

Gupta, A., Christensen, R.G., Rayla, A.L., Lakshmanan, A., Stormo, G.D., and Wolfe, S.A. (2012). An optimized two-finger archive for ZFN-mediated gene targeting. Nat. Methods *9*, 588–590.

Haft, D.H., Selengut, J., Mongodin, E.F., and Nelson, K.E. (2005). A guild of 45 CRISPR-associated (Cas) protein families and multiple CRISPR/Cas subtypes exist in prokaryotic genomes. PLoS Comput. Biol. *1*, e60.

Halford, S.E., Catto, L.E., Pernstich, C., Rusling, D.A., and Sanders, K.L. (2011). The reaction mechanism of FokI excludes the possibility of targeting zinc finger nucleases to unique DNA sites. Biochem. Soc. Trans. *39*, 584–588.

Hashimoto, Y., Ray Chaudhuri, A., Lopes, M., and Costanzo, V. (2010). Rad51 protects nascent DNA from Mre11-dependent degradation and promotes continuous DNA synthesis. Nat. Struct. Mol. Biol. *17*, 1305–1311.

Hicks, G.G., Singh, N., Nashabi, A., Mai, S., Bozek, G., Klewes, L., Arapovic, D., White, E.K., Koury, M.J., Oltz, E.M., et al. (2000). Fus deficiency in mice results in defective B-lymphocyte development and activation, high levels of chromosomal instability and perinatal death. Nat. Genet. *24*, 175–179.

Hockemeyer, D., Soldner, F., Beard, C., Gao, Q., Mitalipova, M., DeKelver, R.C., Katibah, G.E., Amora, R., Boydston, E.A., Zeitler, B., et al. (2009). Efficient targeting of expressed and silent genes in human ESCs and iPSCs using zinc-finger nucleases. Nat. Biotechnol. *27*, 851–857.

Hockemeyer, D., Wang, H., Kiani, S., Lai, C.S., Gao, Q., Cassady, J.P., Cost, G.J., Zhang, L., Santiago, Y., Miller, J.C., et al. (2011). Genetic engineering of human pluripotent cells using TALE nucleases. Nat. Biotechnol. *29*, 731–734.

Horvath, P., and Barrangou, R. (2010). CRISPR/Cas, the immune system of bacteria and archaea. Science *327*, 167–170.

Hsu, P.D., Scott, D.A., Weinstein, J.A., Ran, F.A., Konermann, S., Agarwala, V., Li, Y., Fine, E.J., Wu, X., Shalem, O., et al. (2013). DNA targeting specificity of RNA-guided Cas9 nucleases. Nat. Biotechnol. *31*, 827–832.

Huang, C., Zhou, H., Tong, J., Chen, H., Liu, Y.J., Wang, D., Wei, X., and Xia, X.G. (2011). FUS transgenic rats develop the phenotypes of amyotrophic lateral sclerosis and frontotemporal lobar degeneration. PLoS Genet. *7*, e1002011.

Hwang, W.Y., Fu, Y., Reyon, D., Maeder, M.L., Tsai, S.Q., Sander, J.D., Peterson, R.T., Yeh, J.R.J., and Joung, J.K. (2013). Efficient genome editing in zebrafish using a CRISPR-Cas system. Nat. Biotechnol. *31*, 227–229.

Irion, S., Luche, H., Gadue, P., Fehling, H.J., Kennedy, M., and Keller, G. (2007). Identification and targeting of the ROSA26 locus in human embryonic stem cells. Nat. Biotechnol. *25*, 1477–1482.

Ito, D., Seki, M., Tsunoda, Y., Uchiyama, H., and Suzuki, N. (2011). Nuclear transport impairment of amyotrophic lateral sclerosis-linked mutations in FUS/TLS. Ann. Neurol. *69*, 152–162.

Jasin, M. (1996). Genetic manipulation of genomes with rare-cutting endonucleases. Trends Genet. TIG *12*, 224–228.

Jiang, W., Bikard, D., Cox, D., Zhang, F., and Marraffini, L.A. (2013). RNA-guided editing of bacterial genomes using CRISPR-Cas systems. Nat. Biotechnol. *31*, 233–239.

Jinek, M., Chylinski, K., Fonfara, I., Hauer, M., Doudna, J.A., and Charpentier, E. (2012). A programmable dual-RNA-guided DNA endonuclease in adaptive bacterial immunity. Science *337*, 816–821.

Jinek, M., East, A., Cheng, A., Lin, S., Ma, E., and Doudna, J. (2013). RNA-programmed genome editing in human cells. eLife *2*, e00471.

Kabashi, E., Bercier, V., Lissouba, A., Liao, M., Brustein, E., Rouleau, G.A., and Drapeau, P. (2011). FUS and TARDBP but not SOD1 interact in genetic models of amyotrophic lateral sclerosis. PLoS Genet. *7*, e1002214.

Kay, S., Hahn, S., Marois, E., Hause, G., and Bonas, U. (2007). A bacterial effector acts as a plant transcription factor and induces a cell size regulator. Science *318*, 648–651.

Kim, Y.G., Cha, J., and Chandrasegaran, S. (1996). Hybrid restriction enzymes: zinc finger fusions to Fok I cleavage domain. Proc. Natl. Acad. Sci. U. S. A. *93*, 1156–1160.

Kino, Y., Washizu, C., Aquilanti, E., Okuno, M., Kurosawa, M., Yamada, M., Doi, H., and Nukina, N. (2011). Intracellular localization and splicing regulation of FUS/TLS are variably affected by amyotrophic lateral sclerosis-linked mutations. Nucleic Acids Res. *39*, 2781–2798.

Kleinstiver, B.P., Wolfs, J.M., Kolaczyk, T., Roberts, A.K., Hu, S.X., and Edgell, D.R. (2012). Monomeric site-specific nucleases for genome editing. Proc. Natl. Acad. Sci. U. S. A. *109*, 8061–8066.

Kwiatkowski, T.J., Jr, Bosco, D.A., Leclerc, A.L., Tamrazian, E., Vanderburg, C.R., Russ, C., Davis, A., Gilchrist, J., Kasarskis, E.J., Munsat, T., et al. (2009). Mutations in the FUS/TLS gene on chromosome 16 cause familial amyotrophic lateral sclerosis. Science *323*, 1205–1208.

Laaksovirta, H., Peuralinna, T., Schymick, J.C., Scholz, S.W., Lai, S.L., Myllykangas, L., Sulkava, R., Jansson, L., Hernandez, D.G., Gibbs, J.R., et al. (2010). Chromosome 9p21 in amyotrophic lateral sclerosis in Finland: a genome-wide association study. Lancet Neurol. *9*, 978–985.

Lagier-Tourenne, C., and Cleveland, D.W. (2009). Rethinking ALS: the FUS about TDP-43. Cell *136*, 1001–1004.

Law, W.J., Cann, K.L., and Hicks, G.G. (2006). TLS, EWS and TAF15: a model for transcriptional integration of gene expression. Brief. Funct. Genomic. Proteomic. *5*, 8–14.

Ledermann, B. (2000). Embryonic stem cells and gene targeting. Exp. Physiol. *85*, 603–613.

Lee, G.S., Neiditch, M.B., Salus, S.S., and Roth, D.B. (2004). RAG proteins shepherd double-strand breaks to a specific pathway, suppressing error-prone repair, but RAG nicking initiates homologous recombination. Cell *117*, 171–184.

Levine, T.P., Daniels, R.D., Gatta, A.T., Wong, L.H., and Hayes, M.J. (2013). The product of C9orf72, a gene strongly implicated in neurodegeneration, is structurally related to DENN Rab-GEFs. Bioinforma. Oxf. Engl. *29*, 499–503.

Li, T., Huang, S., Jiang, W.Z., Wright, D., Spalding, M.H., Weeks, D.P., and Yang, B. (2011). TAL nucleases (TALNs): hybrid proteins composed of TAL effectors and FokI DNA-cleavage domain. Nucleic Acids Res. *39*, 359–372.

Liew, M., Pryor, R., Palais, R., Meadows, C., Erali, M., Lyon, E., and Wittwer, C. (2004). Genotyping of single-nucleotide polymorphisms by high-resolution melting of small amplicons. Clin. Chem. *50*, 1156–1164.

Lii, C.K., Lin, A.H., Lee, S.L., Chen, H.W., and Wang, T.S. (2011). Oxidative modifications of proteins by sodium arsenite in human umbilical vein endothelial cells. Environ. Toxicol. *26*, 459–471.

Lillico, S.G., Proudfoot, C., Carlson, D.F., Stverakova, D., Neil, C., Blain, C., King, T.J., Ritchie, W.A., Tan, W., Mileham, A.J., et al. (2013). Live pigs produced from genome edited zygotes. Sci. Rep. *3*, 2847.

Ling, S.C., Polymenidou, M., and Cleveland, D.W. (2013). Converging mechanisms in ALS and FTD: disrupted RNA and protein homeostasis. Neuron *79*, 416–438.

Liu, Y., Lv, X., Tan, R., Liu, T., Chen, T., Li, M., Liu, Y., Nie, F., Wang, X., Zhou, P., et al. (2014). A Modified TALEN-Based Strategy for Rapidly and Efficiently Generating Knockout Mice for Kidney Development Studies. PloS One *9*, e84893.

Maeder, M.L., Thibodeau-Beganny, S., Osiak, A., Wright, D.A., Anthony, R.M., Eichtinger, M., Jiang, T., Foley, J.E., Winfrey, R.J., Townsend, J.A., et al. (2008). Rapid "open-source" engineering of customized zinc-finger nucleases for highly efficient gene modification. Mol. Cell *31*, 294–301.

Mak, A.N.S., Bradley, P., Cernadas, R.A., Bogdanove, A.J., and Stoddard, B.L. (2012). The crystal structure of TAL effector PthXo1 bound to its DNA target. Science *335*, 716–719.

Mali, P., Yang, L., Esvelt, K.M., Aach, J., Guell, M., DiCarlo, J.E., Norville, J.E., and Church, G.M. (2013). RNA-guided human genome engineering via Cas9. Science *339*, 823–826.

Mashimo, T., Takizawa, A., Voigt, B., Yoshimi, K., Hiai, H., Kuramoto, T., and Serikawa, T. (2010). Generation of knockout rats with X-linked severe combined immunodeficiency (X-SCID) using zinc-finger nucleases. PloS One *5*, e8870.

McCreath, K.J., Howcroft, J., Campbell, K.H., Colman, A., Schnieke, A.E., and Kind, A.J. (2000). Production of gene-targeted sheep by nuclear transfer from cultured somatic cells. Nature *405*, 1066–1069.

Mendez, R., and Richter, J.D. (2001). Translational control by CPEB: a means to the end. Nat. Rev. Mol. Cell Biol. *2*, 521–529.

Meng, X., Noyes, M.B., Zhu, L.J., Lawson, N.D., and Wolfe, S.A. (2008). Targeted gene inactivation in zebrafish using engineered zinc-finger nucleases. Nat. Biotechnol. *26*, 695–701.

Mercer, A.C., Gaj, T., Fuller, R.P., and Barbas, C.F., 3rd (2012). Chimeric TALE recombinases with programmable DNA sequence specificity. Nucleic Acids Res. *40*, 11163–11172.

Meyer, M., de Angelis, M.H., Wurst, W., and Kühn, R. (2010). Gene targeting by homologous recombination in mouse zygotes mediated by zinc-finger nucleases. Proc. Natl. Acad. Sci. U. S. A. *107*, 15022–15026.

Meyer, M., Ortiz, O., Hrabé de Angelis, M., Wurst, W., and Kühn, R. (2012). Modeling disease mutations by gene targeting in one-cell mouse embryos. Proc. Natl. Acad. Sci. U. S. A. *109*, 9354–9359.

Miller, J.C., Tan, S., Qiao, G., Barlow, K.A., Wang, J., Xia, D.F., Meng, X., Paschon, D.E., Leung, E., Hinkley, S.J., et al. (2011). A TALE nuclease architecture for efficient genome editing. Nat. Biotechnol. *29*, 143–148.

Mishina, M., and Sakimura, K. (2007). Conditional gene targeting on the pure C57BL/6 genetic background. Neurosci. Res. *58*, 105–112.

Morbitzer, R., Römer, P., Boch, J., and Lahaye, T. (2010). Regulation of selected genome loci using de novo-engineered transcription activator-like effector (TALE)-type transcription factors. Proc. Natl. Acad. Sci. U. S. A. *107*, 21617–21622.

Morbitzer, R., Elsaesser, J., Hausner, J., and Lahaye, T. (2011). Assembly of custom TALE-type DNA binding domains by modular cloning. Nucleic Acids Res. *39*, 5790–5799.

Mori, K., Weng, S.-M., Arzberger, T., May, S., Rentzsch, K., Kremmer, E., Schmid, B., Kretzschmar, H.A., Cruts, M., Van Broeckhoven, C., et al. (2013). The C9orf72 GGGGCC repeat is translated into aggregating dipeptide-repeat proteins in FTLD/ALS. Science *339*, 1335–1338.

Morton, J., Davis, M.W., Jorgensen, E.M., and Carroll, D. (2006). Induction and repair of zinc-finger nuclease-targeted double-strand breaks in Caenorhabditis elegans somatic cells. Proc. Natl. Acad. Sci. U. S. A. *103*, 16370–16375.

Moscou, M.J., and Bogdanove, A.J. (2009). A simple cipher governs DNA recognition by TAL effectors. Science *326*, 1501.

Murakami, T., Yang, S.P., Xie, L., Kawano, T., Fu, D., Mukai, A., Bohm, C., Chen, F., Robertson, J., Suzuki, H., et al. (2012). ALS mutations in FUS cause neuronal dysfunction and death in Caenorhabditis elegans by a dominant gain-of-function mechanism. Hum. Mol. Genet. *21*, 1–9.

Neumann, M., Sampathu, D.M., Kwong, L.K., Truax, A.C., Micsenyi, M.C., Chou, T.T., Bruce, J., Schuck, T., Grossman, M., Clark, C.M., et al. (2006). Ubiquitinated TDP-43 in frontotemporal lobar degeneration and amyotrophic lateral sclerosis. Science *314*, 130–133.

Ochiai, H., Miyamoto, T., Kanai, A., Hosoba, K., Sakuma, T., Kudo, Y., Asami, K., Ogawa, A., Watanabe, A., Kajii, T., et al. (2013). TALEN-mediated single-base-pair

editing identification of an intergenic mutation upstream of BUB1B as causative of PCS (MVA) syndrome. Proc. Natl. Acad. Sci. U. S. A. *111*, 1461-1466.

Van der Oost, J., Jore, M.M., Westra, E.R., Lundgren, M., and Brouns, S.J.J. (2009). CRISPR-based adaptive and heritable immunity in prokaryotes. Trends Biochem. Sci. *34*, 401–407.

Osanai, K., Takahashi, K., Nakamura, K., Takahashi, M., Ishigaki, M., Sakuma, T., Toga, H., Suzuki, T., and Voelker, D.R. (2005). Expression and Characterisation of Rab38, a new member of the Rab small G protein family. Biol. Chem. *386*, 143–153.

Ousterout, D.G., Perez-Pinera, P., Thakore, P.I., Kabadi, A.M., Brown, M.T., Qin, X., Fedrigo, O., Mouly, V., Tremblay, J.P., and Gersbach, C.A. (2013). Reading frame correction by targeted genome editing restores dystrophin expression in cells from Duchenne muscular dystrophy patients. Mol. Ther. J. Am. Soc. Gene Ther. *21*, 1718–1726.

Panda, S.K., Wefers, B., Ortiz, O., Floss, T., Schmid, B., Haass, C., Wurst, W., and Kühn, R. (2013). Highly efficient targeted mutagenesis in mice using TALENs. Genetics *195*, 703–713.

Parant, J.M., George, S.A., Pryor, R., Wittwer, C.T., and Yost, H.J. (2009). A rapid and efficient method of genotyping zebrafish mutants. Dev. Dyn. Off. Publ. Am. Assoc. Anat. *238*, 3168–3174.

Pattanayak, V., Ramirez, C.L., Joung, J.K., and Liu, D.R. (2011). Revealing off-target cleavage specificities of zinc-finger nucleases by in vitro selection. Nat. Methods *8*, 765–770.

Pavletich, N.P., and Pabo, C.O. (1991). Zinc finger-DNA recognition: crystal structure of a Zif268-DNA complex at 2.1 A. Science *252*, 809–817.

Porteus, M.H., and Carroll, D. (2005). Gene targeting using zinc finger nucleases. Nat. Biotechnol. *23*, 967–973.

Qiu, Z., Liu, M., Chen, Z., Shao, Y., Pan, H., Wei, G., Yu, C., Zhang, L., Li, X., Wang, P., et al. (2013). High-efficiency and heritable gene targeting in mouse by transcription activator-like effector nucleases. Nucleic Acids Res. *41*, e120.

Rademakers, R., Neumann, M., and Mackenzie, I.R. (2012). Advances in understanding the molecular basis of frontotemporal dementia. Nat. Rev. Neurol. *8*, 423–434.

Ramirez, C.L., Certo, M.T., Mussolino, C., Goodwin, M.J., Cradick, T.J., McCaffrey, A.P., Cathomen, T., Scharenberg, A.M., and Joung, J.K. (2012). Engineered zinc

finger nickases induce homology-directed repair with reduced mutagenic effects. Nucleic Acids Res. *40*, 5560–5568.

Ran, F.A., Hsu, P.D., Lin, C.-Y., Gootenberg, J.S., Konermann, S., Trevino, A.E., Scott, D.A., Inoue, A., Matoba, S., Zhang, Y., et al. (2013). Double nicking by RNA-guided CRISPR Cas9 for enhanced genome editing specificity. Cell *154*, 1380–1389.

Renton, A.E., Majounie, E., Waite, A., Simón-Sánchez, J., Rollinson, S., Gibbs, J.R., Schymick, J.C., Laaksovirta, H., van Swieten, J.C., Myllykangas, L., et al. (2011). A hexanucleotide repeat expansion in C9ORF72 is the cause of chromosome 9p21-linked ALS-FTD. Neuron *72*, 257–268.

Reyon, D., Tsai, S.Q., Khayter, C., Foden, J.A., Sander, J.D., and Joung, J.K. (2012). FLASH assembly of TALENs for high-throughput genome editing. Nat. Biotechnol. *30*, 460–465.

Robberecht, W., and Philips, T. (2013). The changing scene of amyotrophic lateral sclerosis. Nat. Rev. Neurosci. *14*, 248–264.

Rouet, P., Smih, F., and Jasin, M. (1994). Introduction of double-strand breaks into the genome of mouse cells by expression of a rare-cutting endonuclease. Mol. Cell. Biol. *14*, 8096–8106.

Sander, J.D., Dahlborg, E.J., Goodwin, M.J., Cade, L., Zhang, F., Cifuentes, D., Curtin, S.J., Blackburn, J.S., Thibodeau-Beganny, S., Qi, Y., et al. (2011). Selection-free zinc-finger-nuclease engineering by context-dependent assembly (CoDA). Nat. Methods *8*, 67–69.

Sanders, K.L., Catto, L.E., Bellamy, S.R.W., and Halford, S.E. (2009). Targeting individual subunits of the FokI restriction endonuclease to specific DNA strands. Nucleic Acids Res. *37*, 2105–2115.

Santiago, Y., Chan, E., Liu, P.Q., Orlando, S., Zhang, L., Urnov, F.D., Holmes, M.C., Guschin, D., Waite, A., Miller, J.C., et al. (2008). Targeted gene knockout in mammalian cells by using engineered zinc-finger nucleases. Proc. Natl. Acad. Sci. U. S. A. *105*, 5809–5814.

Sargent, R.G., Brenneman, M.A., and Wilson, J.H. (1997). Repair of site-specific double-strand breaks in a mammalian chromosome by homologous and illegitimate recombination. Mol. Cell. Biol. *17*, 267–277.

Sasayama, H., Shimamura, M., Tokuda, T., Azuma, Y., Yoshida, T., Mizuno, T., Nakagawa, M., Fujikake, N., Nagai, Y., and Yamaguchi, M. (2012). Knockdown of

the Drosophila fused in sarcoma (FUS) homologue causes deficient locomotive behavior and shortening of motoneuron terminal branches. PloS One *7*, e39483.

Sauna, Z.E., and Kimchi-Sarfaty, C. (2011). Understanding the contribution of synonymous mutations to human disease. Nat. Rev. Genet. *12*, 683–691.

Schierling, B., Dannemann, N., Gabsalilow, L., Wende, W., Cathomen, T., and Pingoud, A. (2012). A novel zinc-finger nuclease platform with a sequence-specific cleavage module. Nucleic Acids Res. *40*, 2623–2638.

Shen, B., Zhang, J., Wu, H., Wang, J., Ma, K., Li, Z., Zhang, X., Zhang, P., and Huang, X. (2013). Generation of gene-modified mice via Cas9/RNA-mediated gene targeting. Cell Res. *23*, 720–723.

Smith, B.N., Newhouse, S., Shatunov, A., Vance, C., Topp, S., Johnson, L., Miller, J., Lee, Y., Troakes, C., Scott, K.M., et al. (2013). The C9ORF72 expansion mutation is a common cause of ALS+/-FTD in Europe and has a single founder. Eur. J. Hum. Genet. EJHG *21*, 102–108.

Smith, J., Bibikova, M., Whitby, F.G., Reddy, A.R., Chandrasegaran, S., and Carroll, D. (2000). Requirements for double-strand cleavage by chimeric restriction enzymes with zinc finger DNA-recognition domains. Nucleic Acids Res. *28*, 3361–3369.

Stepto, A., Gallo, J.-M., Shaw, C.E., and Hirth, F. (2014). Modelling C9ORF72 hexanucleotide repeat expansion in amyotrophic lateral sclerosis and frontotemporal dementia. Acta Neuropathol. (Berl.) *127*, 377–389.

Sung, Y.H., Baek, I.J., Kim, D.H., Jeon, J., Lee, J., Lee, K., Jeong, D., Kim, J.S., and Lee, H.W. (2013). Knockout mice created by TALEN-mediated gene targeting. Nat. Biotechnol. *31*, 23–24.

Syriani, E., Morales, M., and Gamez, J. (2011). FUS/TLS gene mutations are the second most frequent cause of familial ALS in the Spanish population. Amyotroph. Lateral Scler. Off. Publ. World Fed. Neurol. Res. Group Mot. Neuron Dis. *12*, 118–123.

Thomas, M.G., Martinez Tosar, L.J., Desbats, M.A., Leishman, C.C., and Boccaccio, G.L. (2009). Mammalian Staufen 1 is recruited to stress granules and impairs their assembly. J. Cell Sci. *122*, 563–573.

Valton, J., Dupuy, A., Daboussi, F., Thomas, S., Maréchal, A., Macmaster, R., Melliand, K., Juillerat, A., and Duchateau, P. (2012). Overcoming transcription activator-like effector (TALE) DNA binding domain sensitivity to cytosine methylation. J. Biol. Chem. *287*, 38427–38432.

Vanamee, E.S., Santagata, S., and Aggarwal, A.K. (2001). FokI requires two specific DNA sites for cleavage. J. Mol. Biol. *309*, 69–78.

Vance, C., Al-Chalabi, A., Ruddy, D., Smith, B.N., Hu, X., Sreedharan, J., Siddique, T., Schelhaas, H.J., Kusters, B., Troost, D., et al. (2006). Familial amyotrophic lateral sclerosis with frontotemporal dementia is linked to a locus on chromosome 9p13.2-21.3. Brain J. Neurol. *129*, 868–876.

Vance, C., Scotter, E.L., Nishimura, A.L., Troakes, C., Mitchell, J.C., Kathe, C., Urwin, H., Manser, C., Miller, C.C., Hortobágyi, T., et al. (2013). ALS mutant FUS disrupts nuclear localization and sequesters wild-type FUS within cytoplasmic stress granules. Hum. Mol. Genet. *22*, 2676–2688.

Wang, H., Yang, H., Shivalila, C.S., Dawlaty, M.M., Cheng, A.W., Zhang, F., and Jaenisch, R. (2013). One-step generation of mice carrying mutations in multiple genes by CRISPR/Cas-mediated genome engineering. Cell *153*, 910–918.

Wang, J., Friedman, G., Doyon, Y., Wang, N.S., Li, C.J., Miller, J.C., Hua, K.L., Yan, J.J., Babiarz, J.E., Gregory, P.D., et al. (2012). Targeted gene addition to a predetermined site in the human genome using a ZFN-based nicking enzyme. Genome Res. *22*, 1316–1326.

Waugh, D.S., and Sauer, R.T. (1993). Single amino acid substitutions uncouple the DNA binding and strand scission activities of Fok I endonuclease. Proc. Natl. Acad. Sci. U. S. A. *90*, 9596–9600.

Wefers, B., Meyer, M., Ortiz, O., Hrabé de Angelis, M., Hansen, J., Wurst, W., and Kühn, R. (2013a). Direct production of mouse disease models by embryo microinjection of TALENs and oligodeoxynucleotides. Proc. Natl. Acad. Sci. U. S. A. *110*, 3782–3787.

Wefers, B., Panda, S.K., Ortiz, O., Brandl, C., Hensler, S., Hansen, J., Wurst, W., and Kühn, R. (2013b). Generation of targeted mouse mutants by embryo microinjection of TALEN mRNA. Nat. Protoc. *8*, 2355–2379.

Wiedenheft, B., Sternberg, S.H., and Doudna, J.A. (2012). RNA-guided genetic silencing systems in bacteria and archaea. Nature *482*, 331–338.

Wu, Y., Gao, T., Wang, X., Hu, Y., Hu, X., Hu, Z., Pang, J., Li, Z., Xue, J., Feng, M., et al. (2014). TALE nickase mediates high efficient targeted transgene integration at the human multi-copy ribosomal DNA locus. Biochem. Biophys. Res. Commun. Published online February 28, 2014. http://dx.doi.org/10.1016/j.bbrc.2014.02.099

Yamagata, K., Yamazaki, T., Yamashita, M., Hara, Y., Ogonuki, N., and Ogura, A. (2005). Noninvasive visualization of molecular events in the mammalian zygote. Genes. N. Y. N 2000 *43*, 71–79.

Yang, H., Wang, H., Shivalila, C.S., Cheng, A.W., Shi, L., and Jaenisch, R. (2013). One-step generation of mice carrying reporter and conditional alleles by CRISPR/Cas-mediated genome engineering. Cell *154*, 1370–1379.

Yanik, M., Alzubi, J., Lahaye, T., Cathomen, T., Pingoud, A., and Wende, W. (2013). TALE-PvuII Fusion Proteins - Novel Tools for Gene Targeting. PloS One *8*, e82539.

Zhang, F., Cong, L., Lodato, S., Kosuri, S., Church, G.M., and Arlotta, P. (2011). Efficient construction of sequence-specific TAL effectors for modulating mammalian transcription. Nat. Biotechnol. *29*, 149–153.

8 Appendix

8.1 Abbreviations and acronyms

8.1.1 Abbreviations

A

A	Purine base/Adenine
amp	Ampicilin
ATG	Translational start site

B

BL6	C57BL/6

C

°C	Degree Celsius
C	Pyrimidine base cytosine
C. elegans	*Caenorhabditis elegans*
C9p21	Chromosome 9p21
CAG	chicken-actin promoter coupled with cytomegalovirus enhancer sequence
chr	Chromosome
CMV	Promotor of Cytomegalovirus
CO_2	carbon dioxide
C-terminal	Carboxy-terminal

D

Da	Dalton

DAPI	4',6-diamidino-2-phenylindole	
del	Deletion	
DH5α	*E.coli* strain DH5α	
DNA	Desoxyribonucleic acid	
dNTPS	Desoxyribonucleotide triphosphate	
DTT	1,4-dithiothreitol	
E		
E	Embryonic day	
E.coli	*Escherichia coli*	
e.g.	*exempli gratia*, for example	
EDTA	Ethylendiamintetraacetate	
EtOH	Ethanol	
F		
f	Female	
F	Forward primer	
fig.	Figure	
Fus or FUS	Fused in sarcoma	
G		
g	Acceleration of gravity (9.81 m/s2)	
g	Gramme	
G	Purinbase guanine	
G418	Geneticin	

H

HA	Hemagglutinin
HCl	Hydrochloric acid
Hist2h3c1	Histone cluster 2, H3c1
hr (s)	Hour (s)
HD	Histidine, aspartic acid

I

i.e.	*id est,* that is
i.p.	Intraperitoneal (injection)
ins	Insertion

K

kb	Kilo base pairs
KI	knockin
klenow fragment	Large fragment of E.coli DNA polymerase I
KO	knockout

L

l	Liter

M

m	Male
m	Metre
m	Milli (10^{-3})
M	molar (mol/L)
min	Minute (s)

mRNA	Messenger ribonucleic acid	
μ	micro (10^{-6})	
N		
n	nano (10^{-9})	
NaCl	Sodium chloride	
NaOAc	Sodium acetate	
NH_4OAc	Ammonium acetate	
no.	Number	
nt	Nucleotides	
Neo^R	Neomycin-resistance	
nm	Nanometre	
N-terminal	Amino-terminal	
O		
ODN (s)	Oligodesoxynucleotide (s)	
P		
PFA	Paraformaldehyde	
Psen2	Presenilin 2	
R		
R	Reverse primer	
RNA	Ribonucleic acid	
RNase	Ribonuclease	
S		
sgRNA	Single-guide RNAs	

	sec	Second
	SYQG	serine, tyrosine, glutamine, and glycine
	RGG	arginine/glycine/glycine
T		
	T	Pyrimidine base thymine
	Tab.	Table
	TE	Tris-EDTA
	temp.	Temperature
	tracrRNA	*trans*-activating crRNA
	Tris	trishydroxymethyl-aminoethane
U		
	U	Unit (s)
	UTR	untranslated region (of an mRNA)
	UV	Ultraviolet
V		
	V	Volt
	Vol.	volume or volumetric content
W		
	wt	wild type
	wt	weight
X		
	X	symbol for crosses between mouse lines
	X-Gal	5-bromo-4-chloro-3-indolyl-β-D-galactopyranoside

8.1.2 Acronyms

A

aa	Amino acid
ALS	Amyotrophic lateral sclerosis
APP	Amyloid beta (A4) precursor protein
ATM	Ataxia telangiectasia mutated
b.wt.	Body weight

B

BSA	Bovine serum albumin

C

Cas	CRISPR-associated
CdK1	Cyclin-dependent kinase 1
cDNA	Complementary DNA
CIP	Calf intestinal phosphatase
CND	*Clostridium* nuclease domain
CNS	Central nervous system
CODA	Context-dependent assembly
CRISPR	Clustered regularly interspaced short palindromic repeats

D

DENN	Differentially expressed in normal and neoplastic cell
DMEM	Dulbecco's modified eagle medium
DNA-PKcs	DNA-dependent protein kinase catalytic subunits

	DSB (s)	Double-strand break (s)
E		
	E	Exon
	ES (c)	Embryonic stem (cell)
	EWS	Ewing´s sarcoma
F		
	fALS	Familial amyotrophic lateral sclerosis
	FCS	Fetal calf serum
	FLASH	Fast ligation-based automatable solid-phase high throughput
	FTLD	Frontotemporal lobar degeneration
G		
	GEF	GDP/GTP exchange factor
	GFP	Green fluorescent protein
H		
	HCG	Human chorion gonadotropin
	HDR	Homology directed repair
	HEK293 cells	Human embryonic kidney 293 cells
	HR	Homologous recombination
	HRMA	High resolution melt analysis
I		
	ICA	Iterative cap assembly
	IVT	*In vitro* transcription
L		

	LB	Luria broth
M		
	MEFs	Mouse embryonic fibroblast cells
	MRN	MRE11-RAD50-NBS1
	MVA	Mosaic variegated aneuploidy
N		
	NHEJ	Non-homologous end joining
	NLS	Nuclear localisation sequence
O		
	OD	Optical density
	OPEN	Oligomerised pool engineering
	ORF	Open reading frame
	OS	off-target sites
P		
	PAM	Protospacer adjacent motif
	PBS	Phosphate buffered saline
	PCR	Polymerase chain reaction
	PDPs	Programmable DNA binding proteins
	PFA	Paraformaldehyde
	Pink1	PTEN induced putative kinase 1
	PMSG	Pregnant mare's serum gonadotropin
R		
	RFLP	Restriction fragment length polymorphism

RPM	Revolutions per minute	
RT	Room temperature	
RT	Reverse transcription	
RT-PCR	Reverse transcription-polymerase chain reaction	
RVD (s)	Repeat-variable di-residue (s)	

S

sALS	Sporadic amyotrophic lateral sclerosis	
SEM	Standard error of the mean	
SNP	Single-nucleotide polymorphism	
SPAST	spastin	
SSB	Single-strand break	

T

TAE	Tris acetate with EDTA	
TAF15	TATA-binding protein-associated factor 15	
TALE	Transcription activator-like effector	
TALENs	Transcription activator-like effector nucleases	
TBE	Tris borate with EDTA	
TDP-43	TAR DNA binding protein	
TIA-1	T-cell-restricted intracellular antigen-1	

U

UTR	untranslated region	

Z

ZFNs	Zinc finger nucleases	

8.2 Index of figures and tables

8.3 Supplementary data

8.3.1 Supplementary figures

Figure S1: PCR-RFLP analysis of Rik^{KO} mutants
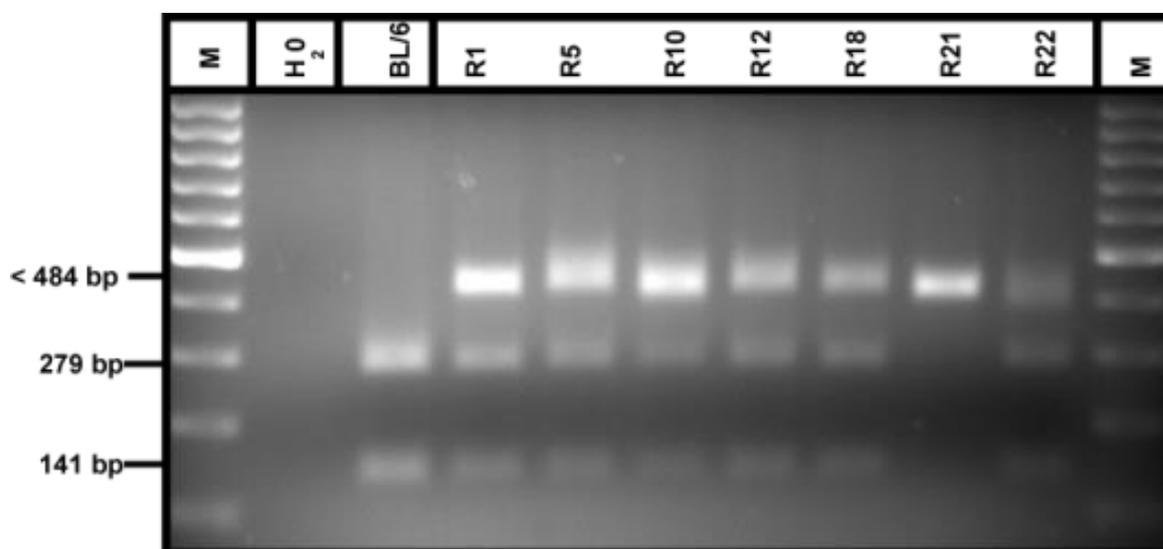
The 484 bp PCR amplified products from the tail DNA of founders derived from TALEN-Rik2 microinjection, are digested with BccI. Upon digestion with BccI, the wild-type control showed 141, 279 bp fragment, whereas knockout mutants revealed the resistant BccI fragment of size smaller than 418 bp (R1, R5, R10, R12, R18, R21, and R22). Interestingly, R22 founder did not show any wild type fragments, suggesting occurrence of a homozygous mutation.

Figure S2: Generation of *3110043O21Rik* knockout founders
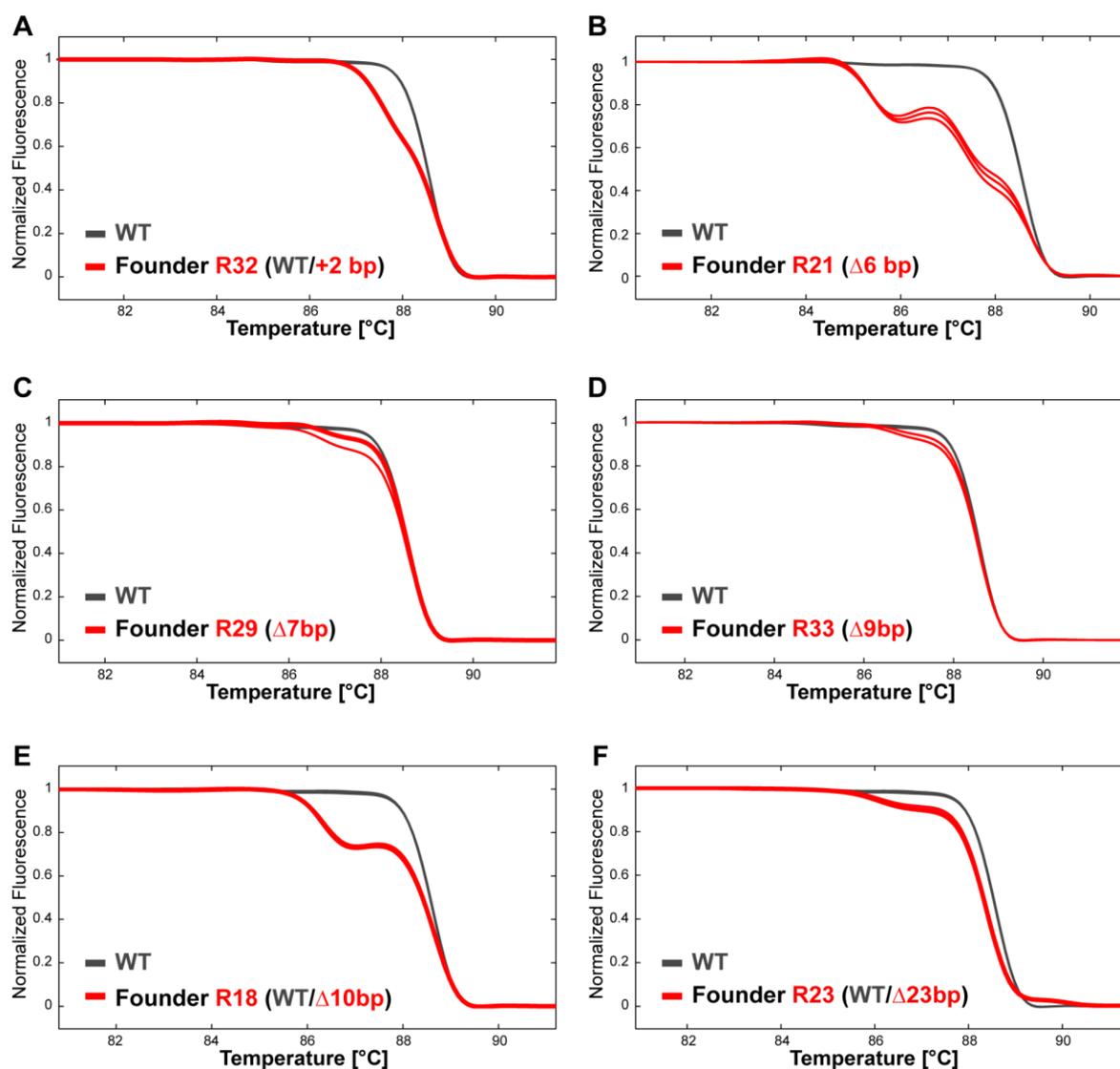
Melting analysis of PCR products amplified from the tail DNA of founder R32 **(A)**, R21 **(B)**, R29 **(C)**, R33 **(D)**, R18 **(E)**, and R23 **(F)** (red curves, overlayed) obtained from TALEN-Rik2 pronuclear microinjection or from a wild-type control (deep grey curves, overlayed). The genotype of mutant alleles is indicated in parentheses; see figure 14 for the allele sequences.

Figure S3: HRMA analysis of PCR products from founders generated by TALEN-Fus 15 and ssODN
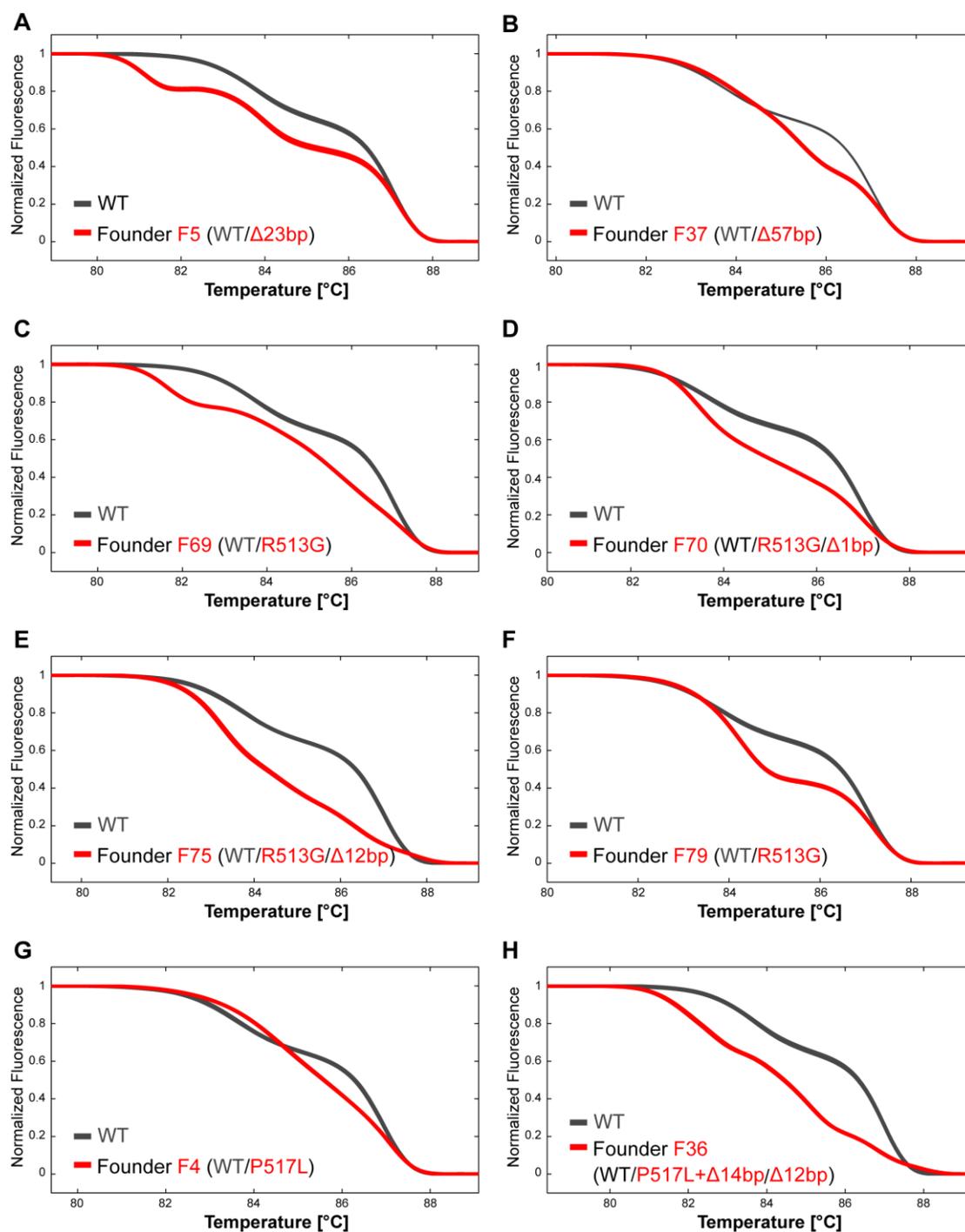
Melting analysis of PCR products amplified from the tail DNA of founder F5 **(A)**, F37 **(B)**, F69 **(C)**, F70 **(D)**, F75 **(E)** and F79 **(F)** produced from TALEN-Fus 15 and ODN^{R513G}, and of F4 **(G)**, F36 **(H)** by using TALEN-Fus15 and ODN^{P517L} pronuclear microinjection (red curves, overlayed) or from control mouse (deep grey curves, overlaid). The genotypes of mutant alleles are indicated in parentheses; see figure 17 for the allele sequences.

Figure S4: Generation of the Fus[511] mutant and germline transmission of the Fus[511] allele
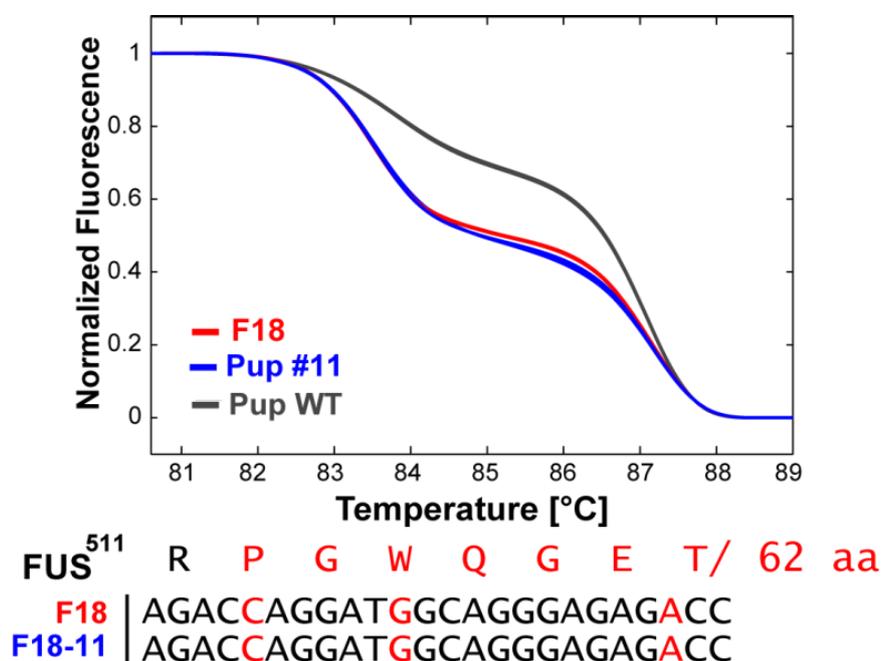
Melting analysis of duplicate tail-derived PCR products from founder F18 (ODN^{R513G}) **(C)** (red curves), its offspring F18-11 (blue curves) in comparison to wild-type controls (deep grey curves). Sequence analysis of the cloned PCR products from pup F18-11 confirmed the germline transmission of the Fus[511] allele.

Figure S5: Strain polymorphism at TALEN-Fus 15 off target sites
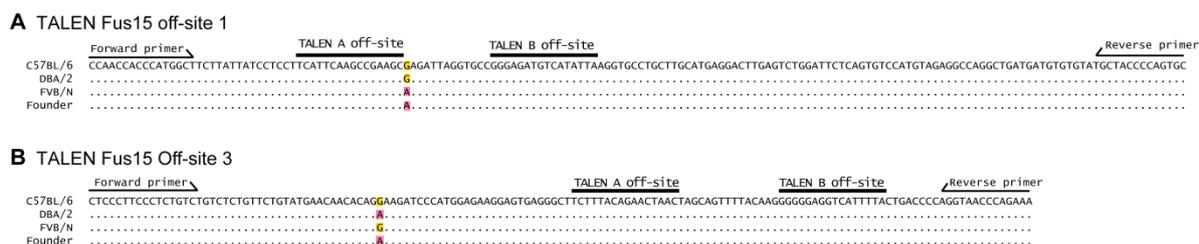
Upon sequence alignment of all TALEN Fus 15 off-sites, site 1 **(A)** and TALEN Fus 15 off-site 3 **(B)** revealed the presence of single-nucleotide polymorphisms in the inbred strains C57BL/6, DBA/2, and FVB/N. Nucleotide differences at specific positions are shown on pink background. Identical nucleotides are marked as dots. Predicted TALEN off-target binding sites and HRMA primer binding sites are indicated.

Figure S6: pCAG-TALEN expression vector
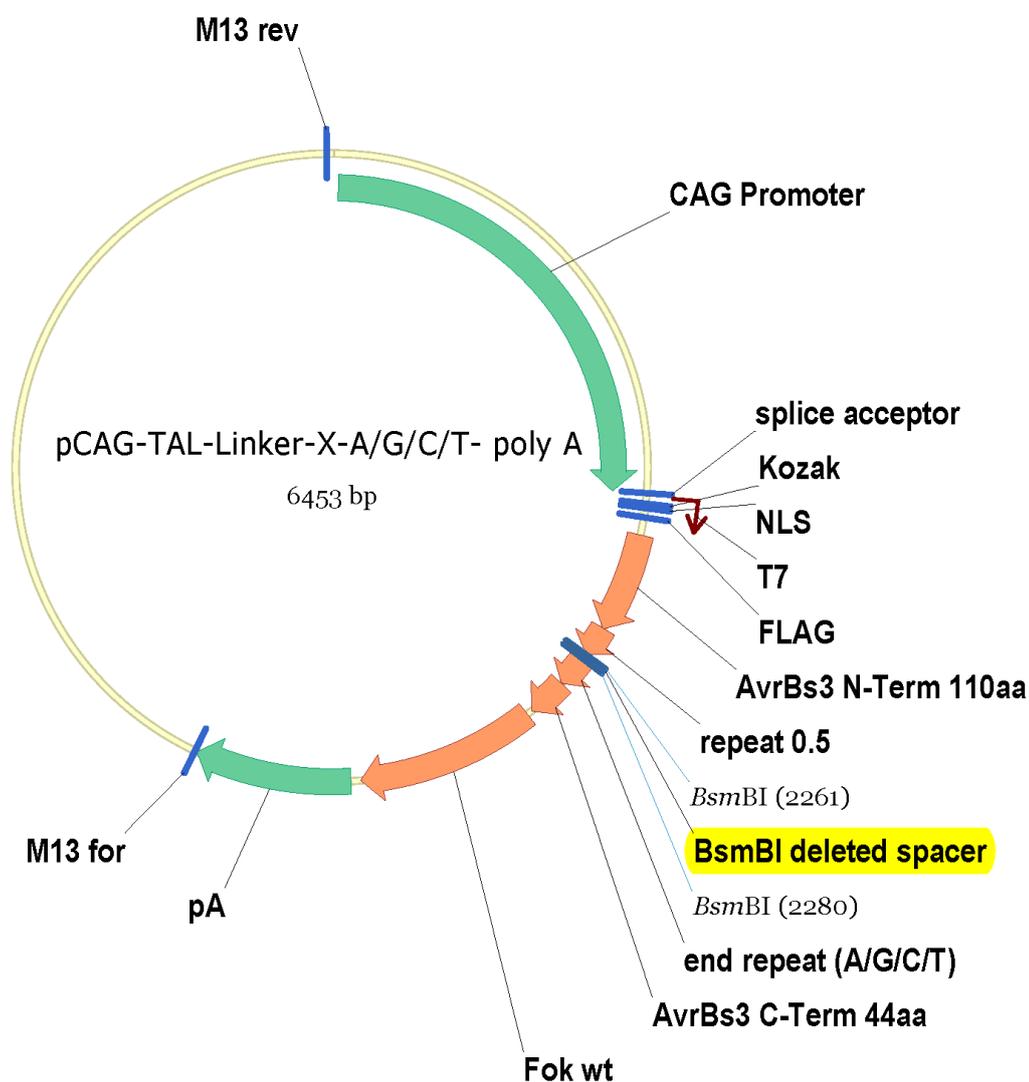
The N-terminal regions encompasses an ATG start codon, Kozak, a nuclear localisation sequence, a FLAG Tag sequence, a glycine rich linker sequence, a segment coding for 110 amino acids of the TAL protein AvrBs3, and the invariable N-terminal TAL repeat of the Hax3 TAL effector. Downstream of the central BsmBI sites, the transcriptional unit contains 78 codons including an invariable C-terminal TAL repeat and 44 residues derived from the TAL protein AvrBs3, followed by the coding sequence of the FokI nuclease domain, and a polyadenylation signal sequence. DNA segments coding for arrays of TAL repeats can be inserted into the BsmBI deleted spacer sites of pCAG-TALEN in frame with the up- and downstream coding regions to enable the expression of predesigned TAL-Fok nuclease proteins. The end repeat contains the DNA segments coding for arrays that recognise either A/G/C/T.

Figure S7: pbs-T7-sgRNA expression vector
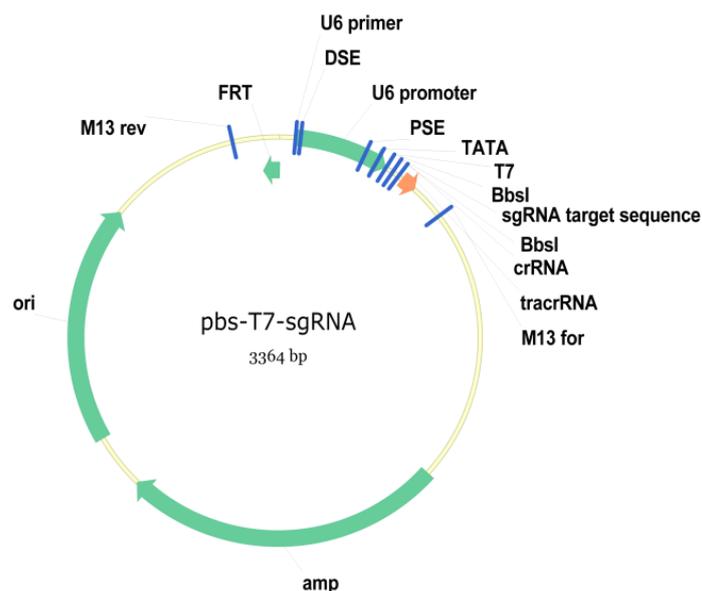
The 23 bp of sgRNA target sequence except the NGG sequence was cloned into the BbsI site pbS-T7-sgRNA expression vector harboring the U6 promoter, T7 promoter, crRNA and tracrRNA sequence.

Figure S8: pCMV-TALEN/CRISPR-Rep vector
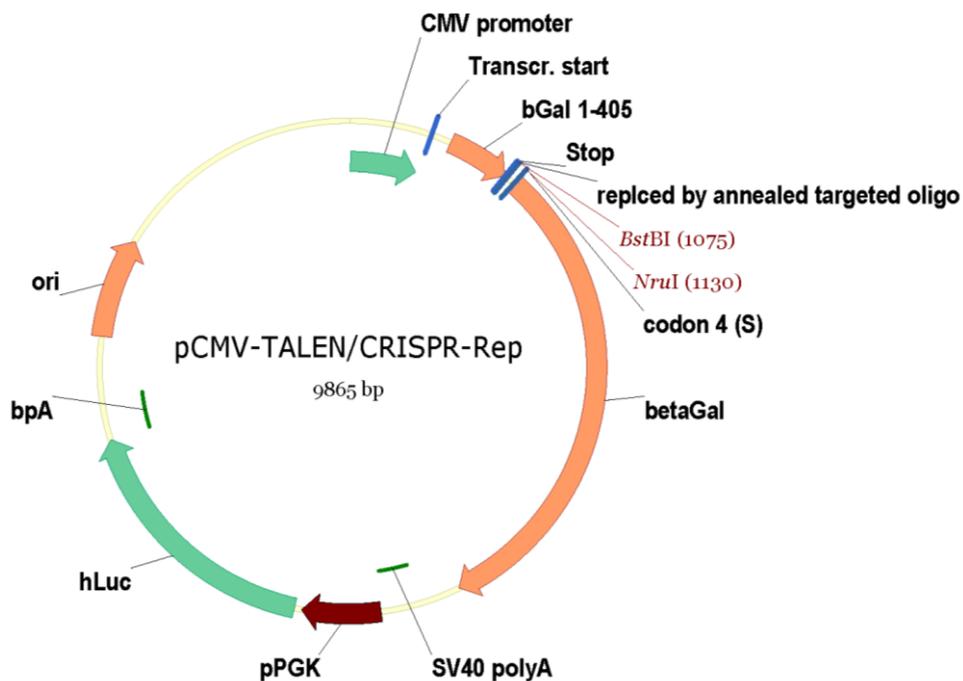
The annealed targeted oligos were cloned into the pCMV-TALEN/CRISPR-Rep. The 5' end of the vector encompasses CMV promoter, partial β-galactosidase sequence followed by stop codon to the inserted target sequence. The downstream of the target sequence harbored the original β-galactosidase and poly(A) sequences.

8.3.2 Supplementary tables

Table S1: Sequences of TALENs target regions

Number	Locus	TALEN-A (5'-3')	TALEN-B (5'-3')
		Mouse Model	
1	*Psen2*	CCCACCAGCT CTAC	CTCGGAGCCTCCGC
2	*Pink-1*	CTTCCTGGAGGGCA	TAGTAACTGGAGCA
3	*Pink-2*	CCTCCTCTCTTCCT	GGAGCACAGAGCCA
4	*Hist2h3c1*	GCGCCATCCACGCC	GGATGTCCTTGGGC
5	*Rik2*	GTCGACTATCTGCC	CTGTCTTGGCAACA
6	*Fus15*	CTTTCAGGGGCGAG	AATATGGCCTCTCC
7	*Fus14*	GACCGGGGCGGCTA	GAAGCCCCCACGGT
8	*Cdk1*	TAAGAAGATGTAGC	ACGACCAGCAGACA
		Cellular Model	
9	*CDK1*	CAGATTAAGAAGAT	AACATATGGAAACT
10	*APP*	CATAGCGACAGTGA	TTCTTCTTCAGCAT
11	*ROSA26-1*	GCAGGGCAACGCCC	TGCCTAGGCTTAAG
12	*ROSA26-2*	GACTAAGCTCCATT	CGAGGTTATTGTAA
13	*SPAST ERF 8/9*	CGCCGCATTAGCGG	ACAAACAGCGGGTA
14	*SPAST ERF 9/10*	GGCAAAAGATGCAG	CTTGTATACCTACC

Showing first one to eight TALENs are constructed for generating mouse models. Similarly, night to fourteen TALENs are constructed for generating the genetic cellular models. Each TALEN pair are designed to target 14 bp in the 5' to 3' direction having 15 bp spacer regions.

Table S2: Germline transmission of TALEN-Rik2 and TALEN-Fus 15 founders

Microinjection	Founder	Pups (n)	Positive (%)
TALEN-Rik2	R23	19	9 (47)
TALEN-Fus15 + ODN^{R513G}	F5	10	1 (10)
	F18	23	13 (56)
	F29	15	8 (53)
	F37	17	8 (47)
	F70	3	2 (67)
	F75	7	4 (57)
TALEN-Fus15 + ODN^{P517L}	F36	12	8 (67)

Table S3: Putative off-target genomic location of TALEN-Rik2 and TALEN-Fus 15

Locus	Chromosomal position	Target sequence A (5'-3')	Spacer length	Target sequence B (5'-3')	Dimer type
3110043O21Rik	*Chr4:35218811-35218854*	T CTGTCTTGGCAACAG	14	T GTCGACTATCTGCCC	A-B
Csmd1	*Chr8:16813743-16813785*	T CTAACTTGACAACAA	13	T CTATCTAATTAACAA	A-A
Intergenic	*Chr8:34491313-34491356*	T CTGTCTTCCCACCAG	14	T ATCAACTACATAACC	A-B
Gfra1	*Chr19:58314874-58314920*	T CTGTGTTCACAAAAG	17	T CTGTCCTGACCACAG	A-A
Intergenic	*Chr9:112015226-112015268*	T CTGCCTTGACAACCT	13	T TTCAACTATGTGCCC	A-B
Intergenic	*Chr19:4408724-4408766*	T CAGCCTTGGCAACAT	13	T CTCTCTTCCCAAAAG	A-A
Fus	*Chr7:127981783-127981827*	T CTTTCAGGGGCGAGC	15	T AATATGGCCTCTCCC	A-B
Intergenic	*Chr4:149785023-149785065*	T CATTCAAGCCGAAGC	13	T AATATGACATCTCCC	A-B
Zdhhc5	*Chr2:84705308-84705354*	T CTATCAAAGGCAACC	17	T AAGATGACCACTCCA	A-B
Sec23b	*Chr2:144575630-144575674*	T CTTTACAGAACTAAC	15	T AAAATGACCTCCCCC	A-B
AC122296.2-201	*Chr6:67120279-67120328*	T CTTCCACAACCAAGC	20	T CTTTCCGGCCCAAGC	A-A
Intergenic	*ChrX:35868551-35868598*	T CTTACAAAGCCAAAC	18	T CATATAACTTCTCCA	A-B

TALEN-Rik2 and TALEN-Fus 15 target sequences are shown in bold letters. Nucleotides of off-target sites matching the intended target sequence are shown in black, mismatches in off-target sites are shown in red. A-B: heterodimeric target sequence, A-A: homodimeric target sequence.

Table S4: Overview of pronuclear microinjection of TALEN-Fus 14 and ODN

Microinjection	TALEN Conc. (ng/µl)	Transferred Embryos (n)	No of Pups (%)	Males (n)	Females (n)	No. of Mutants (%)	Founder´s NHEJ (%)	Founder´s HR (%)
TALEN-Fus14 + ODN[R487X]	20	245	76 (31)	46	30	0 (0)	0 (0)	0 (0)
	90	182	48 (26.4)	23	25	0 (0)	0 (0)	0 (0)
TALEN-Fus14 ∑			124			0 (0)	0 (0)	0 (0)

Numbers of founder mice obtained from the microinjection of TALEN-Fus 14 together with mutagenic ODN[R487X] into the pronuclei of one-cell mouse embryos. The concentration of TALEN mRNAs and the number of pups (males and females) obtained from the transfer of manipulated embryos to pseudo-pregnant mice are shown.

Table S5: Putative off-target genomic sites of sgRNA[Rab#1]

Type	Locus	Strand	Chr. coordinates	Mismatches	Target sequence
sgRNA [Rab#2]	Chr:7	+	88430504:88430518		TCCTCGCACTACCGG
OS-1	Chr:1	+	177713308:177713322	1MM [8]	TCCTAGCACTACAGG
OS-2	Chr:1	-	182897435:182897449	1MM [15]	CCCTCGCACTACAGG
OS-3	Chr:3	-	86186255:86186269	2MM [1:15]	CCCTCGCACTACCGT

sgRNA[Rab#1] target seed and PAM sequences are shown in bold black and blue letters. The different nucleotide of alternative PAM sequence embedded in yellow, whereas the mismatch nucleotides of off-target sites are embedded in bright green. +/- denotes to the position of the sequence, which located either in sense or anti-sense strand of DNA. OS means off-target sites.

Curriculum Vitae

Personal Information

Date of birth	15.05.1983
Place of birth	Padmapur, Odisha, India
Marital Status	Single
Nationality	Indian

Professional Experience

Since 06/2011   **Helmholtz Zentrum München – German Research Centre for Environmental Health (Formly GSF)**, Institute of Developmental Genetics

PhD dissertation**:** "**Establishment of mouse disease models by using sequence specific nucleases**"

08/2010 to 05/2011   National Dairy Research Institute, Dairy Cattle Physiology Division, Karnal, India

Junior Research Fellow worked on the project: "Development of the plasma catecholamine assay for the evaluation of sympathetic neuronal function and milk production performance in heat stresses cows"

01/2008 to 06/2008   **Junior Veterinary Officer** in disease diagnostic laboratory, Odisha, India

Education

07/2008 to 07/2010   National Dairy Research Institute, Animal Biotechnology Centre, Karnal, India

Master of Veterinary Science in Animal Biotechnology, CGPA: **8.1**/10 (Distinction)

Master dissertation: "Efficient production of hand-guided cloned buffalo (*Bubalus bubalis*) embryos: Effects of an epigenetic modifier and cytoplasmic volume, and expression study of developmentally important genes"

06/2002 to 06/2007   Orissa University of Agricultural and Technology, Bhubaneswar, India

Bachelor of Veterinary Science and Animal Husbandry, OGPA: **8.15**/10 (Honours)

Internship

07/2007 to 12/2007   **Veterinary Dispensary**, Ramanaguda, India (As a medicine practitioner)

Workshops

2011 to 2013   At **Helmholtz Zentrum München**:

"Introduction to structural biology"

"Protein expression, purification and biophysical characterisation"

"Mass spectrometry in protein analytics"

"Proteomics for functional analysis of disease "

"Next generation sequencing"

"Project management"

"How to publish in peer-reviewed journals"

Computer Skills

Adobe Illustrator CS3

Endnote X6, Citavi and Zotero

Invitrogen VectorNTI 10

Microsoft Office, Windows XP, Vista, 7 and 8

SYSTAT and GraphPad Prism

Languages

German: Beginner

English: Fluent

Hindi: Fluent

Oriya: Native speaker

Awards and Achievements

2014   Awarded nerdiest talk in Interact, Munich

2011 to 2014   Indian Council of Agricultural Research (ICAR) - **International Fellowship**

2010   Qualified ICAR - **National Eligibility Test**

Excellent performance in post-graduate examination

2008   14th rank in ICAR - **Junior Research Fellowship** examination

2nd rank in **Combined Biotechnology** entrance examination

2002 to 2007   Monthly university **Scholarship** for outstanding academic performance

Publications

2013   1.   **Panda SK**, Wefers B, Ortiz O, Floss T, Schmid B, Haass C, Wurst W, Kühn R. Highly efficient targeted mutagenesis in mice using TALENs. **Genetics** [195(3):703-13. doi: 10.1534]

2.   Wefers B, **Panda SK**, Ortiz O, Brandl C, Hensler S, Hansen J, Wurst W, Kühn R. Targeted mutagenesis in mice by using TALENS. **Nature Protocols** [8(12):2355-79. doi: 10.1038]

3. Saha A, **Panda SK**, Chauhan MS, Manik RS, Palta P, Singla SK. Birth of cloned calves from vitrified-warmed zona-free buffalo (*Bubalus bubalis*) embryos produced by hand-made cloning. **Reproduction, Fertility and Development** [25(6):860-5. doi: 10.1071]

2012   4. **Panda SK**, George A, Saha A, Sharma R, Singh AK, Manik RS, Chauhan MS, Palta P, Singla SK. Effect of scriptaid, a histone deacetylase inhibitor, on the developmental competence of Handmade cloned buffalo (*Bubalus bubalis*) embryos. **Theriogenology** [77(1):195-200. doi: 10.1016]

5. Wefers B, Meyer M, Hensler S, **Panda S**, Ortiz O, Wurst W, Kühn R. Gene editing in one-cell embryos by zinc-finger and TAL nucleases. **Current Protocols in Mouse Biology** [2:347-64. doi: 10.1002]

2011   6. **Panda SK**, George A, Saha AP, Sharma R, Manik RS, Chauhan MS, Palta P, Singla SK. Effect of cytoplasmic volume on developmental competence of buffalo (*Bubalus bubalis*) embryos produced through hand-made cloning. **Cellular Reprogramming** [13(3):257-62. doi: 10.1089]

7. George A, Sharma R, Singh KP, **Panda SK**, Singla SK, Palta P, Manik RS, Chauhan MS. Production of cloned and transgenic embryos using buffalo (*Bubalus bubalis*) embryonic stem cell like cells isolated from *in vitro* fertilized and cloned blastocysts. **Cellular Reprogramming** [13(3):263-72. doi: 10.1089]

Conferences

2014   **Interact,** Munich, Germany: Oral presentation

2013   **Wellcome Trust Genome Campus**, Hinxton, Cambridge, UK.
Mouse Molecular Genetics: Oral and poster presentation

2012   **Frauenchiemse**, Germany.
TUM graduate school kick-off seminar: Poster presentation

2011   **National Dairy Research Institute**, Karnal, India.
Frontiers in reproductive biotechnology: Oral and poster presentation

2010   **Indian Veterinary Research Institute**, Izatnagar, India.
Physiological capacity building in livestock under changing climatic scenario: Oral presentation

University of Rajasthan, Jaipur, India.
International conference on reproductive health: Poster presentation

2009   **CCS Haryana Agricultural University,** Hisar, India.
XV Annual convention and national symposium on recent approaches in veterinary immunology and biotechnology for animal health and production: Poster presentation

---

Oberschleißheim, September 4th, 2014

Sudeepta kumar Panda

Sudeepta Kumar Panda

Highly Efficient Targeted Mutagenesis in Mice Using TALENs

Sudeepta Kumar Panda,*,†,1 **Benedikt Wefers,***,1 **Oskar Ortiz,*** **Thomas Floss,*** **Bettina Schmid,**‡,§
Christian Haass,‡,§ **Wolfgang Wurst,***,†,‡,** **and Ralf Kühn***,†,2

*Institute of Developmental Genetics, Helmholtz Zentrum München, German Research Center for Environmental Health, 85764
Munich, Germany, †Technische Universität München, 85350 Freising-Weihenstephan, Germany, ‡Deutsches Zentrum für
Neurodegenerative Erkrankungen e. V., 80336 Munich, Germany, §Biochemistry and Munich Cluster for Systems Neurology,
Adolf Butenandt Institute, Ludwig Maximilians University, 80336 Munich, Germany, and **Max-Planck-Institute of
Psychiatry, 80804 Munich, Germany

ABSTRACT Targeted mouse mutants are instrumental for the analysis of gene function in health and disease. We recently provided proof-of-principle for the fast-track mutagenesis of the mouse genome, using transcription activator-like effector nucleases (TALENs) in one-cell embryos. Here we report a routine procedure for the efficient production of disease-related knockin and knockout mutants, using improved TALEN mRNAs that include a plasmid-coded poly(A) tail (TALEN-95A), circumventing the problematic *in vitro* poly-adenylation step. To knock out the *C9orf72* gene as a model of frontotemporal lobar degeneration, TALEN-95A mutagenesis induced sequence deletions in 41% of pups derived from microinjected embryos. Using TALENs together with mutagenic oligodeoxynucleo-tides, we introduced amyotrophic lateral sclerosis patient-derived missense mutations in the fused in sarcoma (*Fus*) gene at a rate of 6.8%. For the simple identification of TALEN-induced mutants and their progeny we validate high-resolution melt analysis (HRMA) of PCR products as a sensitive and universal genotyping tool. Furthermore, HRMA of off-target sites in mutant founder mice revealed no evidence for undesired TALEN-mediated processing of related genomic sequences. The combination of TALEN-95A mRNAs for enhanced mutagenesis and of HRMA for simplified genotyping enables the accelerated, routine production of new mouse models for the study of genetic disease mechanisms.

GENETIC engineering of cells and organisms to create targeted mutants is a key technology for genetics and biotechnology. The ascent of the mouse as a mammalian genetic model is based on gene targeting through homolo-gous recombination (HR) in embryonic stem (ES) cells (Capecchi 2005). Classical gene targeting via ES cells is a time- and labor-intense procedure that proceeds in the steps of vector construction, ES cell mutagenesis, chimera generation, and the transmission of mutant alleles through the germline (Hasty *et al.* 2000). Since the frequency of spontaneous HR in ES cells is low, it was a key finding that double-strand breaks (DSBs), created by sequence-specific

nucleases, enhance local DNA repair by several orders of magnitude (Rouet *et al.* 1994). DSBs may be repaired through HR, using the sister chromosome as template or using gene targeting vectors that provide sequence homol-ogy regions flanking a desired genetic modification (Court *et al.* 2002; San Filippo *et al.* 2008). Alternatively, DSBs can be sealed by the nonhomologous end-joining (NHEJ) path-way that religates open ends without a repair template (Lieber 2010). By this means the DNA ends are frequently edited through the loss of multiple nucleotides, causing frameshift (knockout) mutations within coding regions. Tar-geted DSBs were first induced by zinc-finger nuclease (ZFN) fusion proteins that combine a DNA-binding domain made of zinc-finger motifs with the nuclease domain of *Fok*I (Porteus and Carroll 2005). The application of ZFNs in one-cell em-bryos provided proof-of-principle for the direct mutagene-sis of the mouse, rat, and rabbit genome in a single step (Geurts *et al.* 2009; Carbery *et al.* 2010; Meyer *et al.* 2010; Flisikowska *et al.* 2011). Nevertheless, ZFNs do not provide a universal tool since the available code for the recognition

of nucleotide triplets is incomplete and multiple elements cannot be combined in a simple modular fashion. In contrast, the DNA-binding code of the transcription activator-like (TAL) proteins of *Xanthomonas* is based on the recognition of single nucleotides by individual peptide motifs, such that combinations of just four basic modules can be combined into domains that bind any target sequence (Boch *et al.* 2009; Moscou and Bogdanove 2009). Based on extensive experience with ZFNs, the TAL system could be readily adapted for gene editing by the fusion of DNA-binding modules with *Fok*I into TAL effector nucleases (TALENs) (Cermak *et al.* 2011; Miller *et al.* 2011). Taking advantage of its modular nature, a variety of cloning protocols enable us to assemble TALEN coding regions within a short time (Cermak *et al.* 2011; Reyon *et al.* 2012).

We recently reported that TALEN target sites are distributed in the mouse genome at an average spacing of 14 bp, enabling genome-wide targeted mutagenesis at high precision. In particular, we provided proof-of-principle that TALENs and oligodeoxynucleotides (ODNs) can be applied in one-cell embryos to introduce targeted mutations (Wefers *et al.* 2013). For HR- and NHEJ-mediated gene modifications, we achieved rates of 2% and 6%, respectively, using experimental conditions that were not yet optimized. Higher rates of NHEJ-mediated nucleotide deletions (>40%) were obtained upon the microinjection of TALEN mRNAs into the cytoplasm of one-cell embryos, tolerating larger injection volumes (Sung *et al.* 2013). Nevertheless, for the creation of targeted mutations it is instrumental to deliver DNA templates for HR together with TALEN mRNAs directly into the pronucleus, tolerating only minimal injection volumes. To set up an efficient routine procedure for mutagenesis we enhanced the activity of TALEN mRNAs to optimize nuclease expression upon pronuclear delivery, such that one or more knockin or knockout alleles are obtained among a group of mice derived from a single microinjection experiment. Upon the establishment of a mutant by embryo manipulation, the genotyping of breeding colonies imposes a constant workload. PCR-based protocols for the detection of subtle mutations often require the digestion of PCR products and gel electrophoresis. To minimize these efforts we validated whether high-resolution melt analysis (HRMA) represents a reliable and simplified tool for the genotyping of mouse mutants. HRMA identifies mutant PCR products by their specific denaturation profile (Liew *et al.* 2004) and requires no restriction digestion and size separation of PCR products.

We applied this streamlined procedure to introduce targeted and knockout mutations into the *Fus* and *C9orf72* genes to create disease models for inherited amyotrophic lateral sclerosis (ALS) and frontotemporal lobar degeneration (FTLD). Mutations disrupting the C-terminal nuclear localization sequence (NLS) of *FUS* have been identified in ALS patients (Kwiatkowski *et al.* 2009), whereas a hexanucleotide repeat expansion in the first intron of the *C9orf72* gene was found in patients representing ALS, FTLD, or both diseases (DeJesus-Hernandez *et al.* 2011; Renton *et al.* 2011). In the

Fus gene dominant mutations within the NLS disrupt the nuclear import of FUS and lead to its cytoplasmic deposition in the brain and spinal cord of patients (Bosco *et al.* 2010; Gal *et al.* 2011; Ito *et al.* 2011; Kino *et al.* 2011; Dormann and Haass 2013). This defect is a key to pathogenesis since mutations that severely impair nuclear import, such as the P525L replacement, lead to an early onset and rapid progression of the disease. Since FUS is involved in multiple steps of gene expression, including transcription, pre-mRNA splicing, and mRNA transport, neurodegeneration may be caused by the loss of essential nuclear functions and/or the gain of a toxic function in the cytosol. Depletion of FUS in zebrafish and fruit flies causes a motoneuron phenotype but is perinatal lethal in mice (Hicks *et al.* 2000; Kabashi *et al.* 2011; Sasayama *et al.* 2012). To faithfully mimic the human codon replacements R521G and P525L, we targeted the analogous positions R513 and P517 of the mouse *Fus* gene, using TALENs and ODNs. As a cause of *C9orf72*-associated pathogenesis, the intronic repeat expansion may be deleterious through RNA-mediated toxicity or by the translation of repeat sequences, causing the production and aggregation of dipeptide repeat proteins (Ash *et al.* 2013; Mori *et al.* 2013) or both (Taylor 2013). To clarify whether *C9orf72* loss-of-function also contributes to the FTLD phenotype and to decipher its cellular function, we disrupted the mouse homolog of the *C9orf72* gene, *3110043O21Rik*, by the creation of TALEN-induced frameshift mutations.

Using our advanced TALEN mutagenesis procedure we obtained recombined *Fus* alleles in 6.8% and nucleotide deletions within *C9orf72* in 41% of mice derived from pronuclear embryo injections, validating this approach for the expedited recapitulation of disease-associated alleles. The established *Fus* codon replacement and *C9orf72* knockout mutants will be instrumental to studying genetic ALS and FTLD disease mechanisms.

Materials and Methods

TALEN target sites

For the selection of TALEN target sequences we used the "TALEN*designer*" (www.talen-design.de) as described in Wefers *et al.* (2013). Selected target sites cover two recognition sequences of 15 bp preceded by a T, separated by a spacer of 14–15 bp. To minimize off-target recognition, potential sites were analyzed using the "Paired Target Finder" (https://tale-nt.cac.cornell.edu) (settings: spacer length 13–20 bp, cutoff 3.0) (Doyle *et al.* 2012).

TALEN construction and expression

Details on the construction of TALEN coding regions, expression vectors, and TALEN sequences are given in Supporting Information, File S1. For the expression of TALENs in mammalian cells we used the expression vector pCAG-TALEN-pA as described in Wefers *et al.* (2013). pT7-TALEN-95A was derived from pCAG-TALEN-pA by replacement

of the poly(A) signal sequence with a segment of 95 adenine residues derived from a mouse *Oct4* cDNA clone.

Oligodeoxynucleotides

The oligodeoxynucleotides ODN[R513G] (5′-TGGGTAGGG TAGTTCAGTAACACGTAATCTAACATAACTTTTTCTTTCAG GGGCGAGCACAGACAGGAT**G**GCAGGGAGAG<u>A</u>CCATATTAG CCTGGCTCCTGAAGTTCTGGAACTCTTCCTGTACCCAGTGT TACCCTTGT-3′) and ODN[P517L] (5′- TCAGTAACACGTAATC TAACATAACTTTTTCTTTCAGGGGCGAGCACAGACAGGATC GCAGGGAGAG**A**C<u>T</u>ATATTAGCCTGGCTCCTGAAGTTCTGG AACTCTTCCTGTACCCAGTGTTACCCTTGTTATTTTGTAA ACT-3′) were synthesized and HPLC purified by Metabion (Martinsried, Germany), each having a length of 140 nt, including the targeted mutation (shown in boldface type) and a silent replacement (underlined), covering 70 bp upstream and downstream of the targeted codon.

Microinjection of one-cell embryos

The injection of TALEN mRNA and targeting molecules (ODNs) was performed as described in Wefers *et al.* (2012, 2013), except that injections were done only into pronuclei. Briefly, capped TALEN mRNA was prepared in a single step by *in vitro* transcription from pT7-TALEN-95A plasmid DNA linearized with *Xba*I and *Ale*I (New England Biolabs, Frankfurt, Germany), using the mMessage mMachine T7 Ultra kit (omitting the polyadenylation step) and the MEGAclear kit (Life Technologies, Carlsbad, CA). The quality of synthesized mRNAs was controlled by agarose gel electrophoresis under denaturing conditions, using the NorthernMax-Gly system and the RNA Millenium size marker (Life Technologies). Each TALEN mRNA was then diluted in injection buffer (10 mM Tris, 0.1 mM EDTA, pH 7.2) to a working concentration of 90 ng/µl TALEN-Rik2 mRNA or 20 ng/µl TALEN-Fus15 mRNA. The targeting oligodeoxynucleotides were dissolved in water and diluted with injection buffer to a working concentration of 15 ng/µl. For microinjections, one-cell embryos were obtained by mating of (DBA/2 × C57BL/6)F$_1$ males with superovulated FVB/N females (Charles River, Sulzbach, Germany). One-cell embryos were injected with either only TALEN-Rik2 mRNA or a mixture of TALEN-Fus15 mRNA and the targeting oligodeoxynucleotides (15 ng/µl) (ODN[R513G] and ODN[P517L]) into the larger pronucleus, but not into the cytoplasm. Test experiments showed that microinjections of Venus mRNA (90 ng/µl), using pronuclear capillaries, led to green fluorescence in all embryos, but the direct delivery of the same volume into the cytoplasm is less effective and labels only ∼10% of embryos. Injected zygotes were transferred into pseudopregnant CD1 female mice to obtain live pups. All mice showed normal development and appeared healthy. Mice were handled according to institutional guidelines approved by the animal welfare and use committee of the government of Upper Bavaria and housed in standard cages in a specific pathogen-free facility on a 12-h light/dark cycle with *ad libitum* access to food and water.

Isolation of genomic DNA

Genomic DNA was isolated from tail tips of founder mice and their progeny, using the Wizard Genomic DNA Purification Kit (Promega, Mannheim, Germany), following the manufacturer's instructions.

HRMA

For the screening of TALEN-induced mutations, the TALEN target regions of *C9orf72* and *Fus* (amplicon size 140 and 133 bp, respectively) were amplified in a 10-µl PCR reaction containing 40 ng lyophilized genomic DNA, 1 µl LC Green Plus+ Dye (Bioké, Leiden, The Netherlands), 200 nM of each dNTP, 250 nM each forward and reverse primers (Table S3), and 0.2 µl Phire Hot Start II DNA Polymerase (Thermo Scientific, Dreieich, Germany). PCR reaction protocols for mutagenic detection were 98°, 30 sec; 40 cycles of [98°, 5 sec; 62° (*C9orf72*)/66° (*Fus*), 5 sec; 72°, 5 sec]; 72°, 1 min; denaturation at 98°, 1 min; and rapid cool down to 25° for heteroduplex formation. Following the PCR, samples were analyzed with a LightScanner (BioFire Diagnostics, Salt Lake City) over a 65°–95° range. PCR products that contained mutant alleles were purified using the Qiaquick PCR purification kit (QIAGEN, Hilden, Germany), subcloned using the StrataClone Blunt PCR Cloning Kit (Agilent, Waldbronn, Germany), and sequenced (GATC Biotech, Konstanz, Germany). Sequences were compared to wild type, using the Vector NTI Advance 11.5 software suite (Life Technologies). To determine the detection limit of HRMA, cloned mutant PCR products from *C9orf72* founders R5 and R12 were diluted with wild-type PCR product. The melting curves of three replicates of each test sample were analyzed and compared to wild-type controls, using the LightScanner software with Call-IT 2.0 (BioFire Diagnostics).

Off-target analysis

To assess potential TALEN off-target activity, the five highest-scored off-target sites (Table S2) were analyzed by HRMA in duplicate reactions, using locus-specific PCR primer pairs (see Table S3: *Fus* OS1–OS5 and Rik OS1–OS5). Four *Fus* and two *C9orf72* founders were compared to a C57BL/6 wild-type control. Founder-derived PCR products amplified from the *Fus* off-sites 1 and 3 were subcloned and sequenced. These sequences were compared to the respective genomic sequences of the C57BL/6, DBA/2, and FVB/N mouse strains (Ensembl Resequencing database, http://www.ensembl.org, release 71, April 2013).

Results

### Optimized expression of TALENs in one-cell mouse embryos

To target the *Fus* and the *C9orf72* genes, we constructed TALEN pairs recognizing sequences within exon 15 and exon 2, respectively, using our TALEN*designer* algorithm and modular construction protocol (Wefers *et al.* 2013). The TALEN

coding regions were inserted into the mammalian expression vector pCAG-TALEN-pA, providing a CAG promoter and a poly-adenylation signal sequence (Figure 1A). For the assessment of TALEN activity, expression vectors were cotransfected with customized nuclease reporter plasmids into HEK 293 cells as described in Wefers *et al.* (2013) and found to exhibit specific nuclease activity (Figure S1). For the expression of TALENs in one-cell embryos, the coding regions can be transcribed *in vitro* by T7 polymerase from linearized pCAG-TALEN-pA plasmids, followed by the polyadenylation of the coding RNA with poly(A) polymerase. Using this two-step protocol, we frequently noted an inconsistent production of single-species TALEN mRNAs, resulting in a smeared appearance of transcripts upon the polyadenylation step [Figure 1C, TALEN-poly(A)]. This effect occurred for TALEN but not for shorter, *e.g.*, ZFN RNAs, possibly because the transcription of the 3-kb TALEN coding region leads to a larger fraction of truncated products, contaminating the polyadenylation reaction. To enable the reliable production of TALEN mRNAs, for optimal nuclease expression upon pronuclear injection, we inserted the TALEN coding regions into pT7-95A (Figure 1B). This vector provides a T7 promoter and a region of 95 adenine (A) residues located downstream of the TALEN coding region for the production of polyadenylated (TALEN-95A) mRNAs in a single step. Using pT7-TALEN-95A vectors for *in vitro* transcription, we reproducibly obtain full-length TALEN mRNAs of the expected size of 2948 nucleotides (Figure 1C, TALEN-95A). To determine the RNA concentration that supports efficient translation upon pronuclear microinjection, we used a 95A RNA encoding the Venus reporter. We found green fluorescence in all embryos microinjected with Venus-95A RNA at 90 ng/µl, upon culture to the two-cell stage (Figure 1D). To assess the potency of TALEN-95A RNAs for the mutagenesis of the *C9orf72* and *Fus* genes we used concentrations of 90 ng/µl and 20 ng/µl, respectively.

Generation of C9orf72 knockout mice

To induce frameshift mutations within the mouse homolog of *C9orf72* we designed a TALEN pair (TALEN-Rik2) targeting a sequence downstream of the start codon located within the second exon of the murine *3110043O21Rik* gene (Figure 2A and Figure 3, A and C).

From pronuclear microinjections of TALEN-Rik2 mRNAs (95A type, 90 ng/ul), we obtained 51 pups (Table 1) that were screened for the presence of mutant alleles by HRMA of PCR products covering the targeted exon. Twenty-one of these mice (41%) were identified as founders harboring mutant *C9orf72* alleles, confirming that the pronuclear delivery of 95A-type mRNAs leads to a high mutagenesis rate. Representative HRMA results from 8 founders are shown in Figure 2 and Figure S2, exhibiting melting curves that deviate from the wild-type control. We selected 11 founders for the further characterization of modified *C9orf72* alleles by subcloning and sequence analysis of PCR products. Among founders R5–R32 we identified 12 mutant alleles (Figure 3A) that exhibit deletions of 1–36 nucleotides or a 2-bp insertion
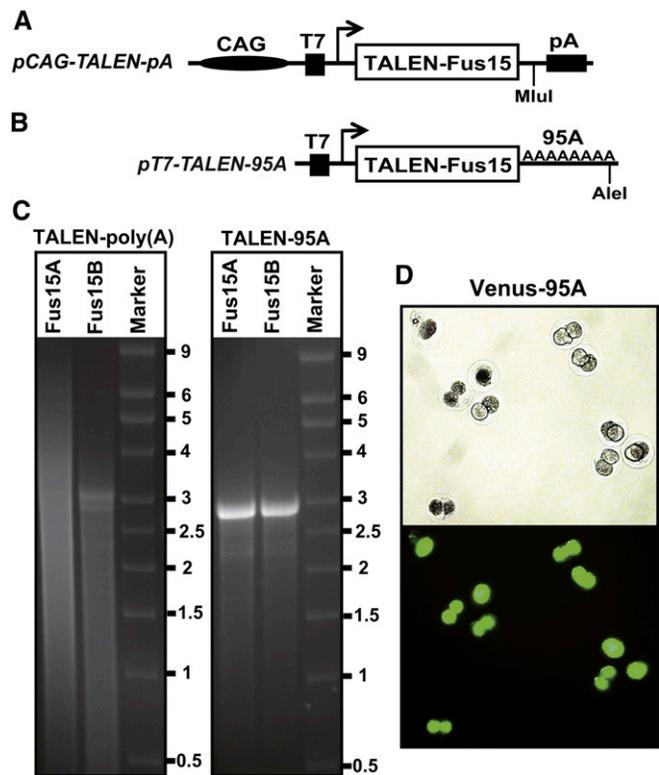
Figure 1 Production of TALEN mRNAs for embryo microinjection. (A) Plasmid pCAG-TALEN-Fus15-pA provides a CAG promoter (CAG) and a poly(A) signal sequence (pA) for expression of TALEN-Fus15 proteins in mammalian cells. TALEN mRNA can be produced *in vitro* from *Mlu*I-linearized plasmid DNA in a two-step procedure, using T7 polymerase for transcription and poly(A) polymerase for polyadenylation. (B) Plasmid pT7-TALEN-Fus15-95A provides a T7 promoter (T7) and a region of 95 adenine (95A) nucleotides, followed by an *Ale*I site. TALEN RNA, including a plasmid-coded poly(A) sequence, can be produced in a single step, using T7 polymerase and *Ale*I-linearized plasmid DNA. T7: T7 promoter region. (C) Agarose gel electrophoresis of reaction products transcribed with T7 polymerase from *Mlu*I-linearized pCAG-TALEN-Fus15-pA plasmids, followed by polyadenylation with poly(A) polymerase [left gel, TALEN-poly(A)], or produced in a single step with T7 polymerase from *Ale*I-linearized pT7-TALEN-Fus15-95A plasmids (right gel, TALEN-95A). The size of full-length TALEN-95A transcripts is expected at 2948 nt. Marker: RNA size marker (×1000 nucleotides). (D) Microinjection of *in vitro*-produced Venus-95A RNA (90 ng/µl) into pronuclei of one-cell mouse embryos. The manipulated embryos were cultured to the two-cell stage and analyzed for Venus expression by fluorescence microscopy. Top, white light; bottom, green fluorescence.

within the TALEN target region. Seven of these deletions disrupt the *C9orf72* reading frame in between codons 6–9 and are predicted for the translation of 8–11 additional amino acids (Figure 3B). For the establishment of a mutant breeding colony, founder R23 was mated to wild-type mice and its progeny genotyped by PCR and HRMA. Seven of 15 pups derived from R23 showed melting curves distinguished from the wild-type control and the sequencing of PCR products from pup R23-15 confirmed the germline transmission of the parental *C9orf72* allele (Figure 3C).

Founders obtained from microinjections of TALENs or ZFNs are frequently mosaics, harboring a mutation only in
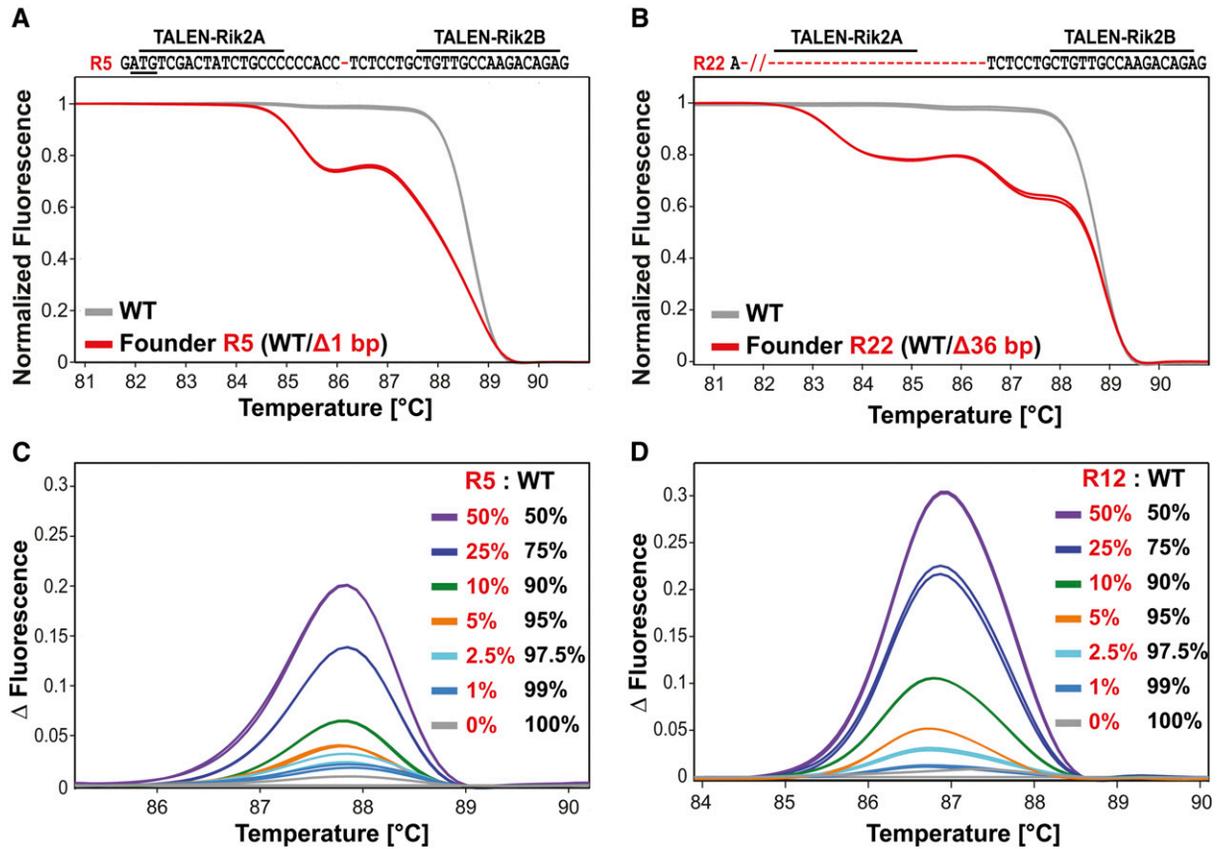
Figure 2 Identification of *C9orf72* mutants by HRMA. (A and B) Melting analysis of PCR products amplified in duplicate from tail DNA of founder R5 (A) and of founder R22 (B) (red curves, overlaid) in comparison to wild-type controls (gray curves, overlaid). The TALEN-Rik2 target sequences within exon 2 are shown (start codon underlined); nucleotides deleted in mutant alleles are shown as red dashes and genotypes are given in parentheses. (C and D) The sensitivity of HRMA for mutant detection was determined by analyzing HRMA samples prepared with varying amounts of wild-type or mutant PCR products from founder R5 (1-bp deletion, C) and founder R12 (6-bp deletion, D). The limit to detect the R5 allele is at 5% for the mutant product (orange curve) and at 2.5% for the R12 allele (light blue curve).

some of the somatic cells, if gene editing occurred after genome replication (Wefers *et al.* 2013). To assess whether mosaic mutant genotypes can be identified by HRMA, we performed control experiments to establish its detection limits. For this purpose we prepared HRMA test samples containing 1–50% of cloned, mutant *C9orf72* PCR product (allele R5, 1-bp deletion; or R12, 6-bp deletion) and 99–50% of wild-type PCR product. In comparison to the wild-type controls, the presence of mutant alleles could be reliably detected in samples containing 5% (1-bp deletion) or 2.5% (6-bp deletion) of mutant DNA (Figure 2, C and D). These results indicate that mosaic founders harboring even a minor fraction of mutant cells can be recognized by melting analysis and validate HRMA as a simple and sensitive tool for the identification of mutants derived from embryo microinjection of TALENs.

Generation of Fus^{R513G} and Fus^{P517L} codon replacement mutants

To recapitulate the patient-derived codon replacements R521G and P525L in the mouse *Fus* gene, we targeted the analogous positions R513 and P517, using synthetic oligodeoxynucleotides as template for TALEN-induced HR. We

designed a TALEN pair (TALEN-Fus15) recognizing the C-terminal coding sequence located within exon 15 (Figure 4A). The oligonucleotides ODN^{R513G} and ODN^{P517L} cover 140 nt centered on exon 15 and include nucleotide replacements that redefine the codons 513 and 517 into glycine (R513G) or leucine (P517L), respectively. To exclude the potential reprocessing of recombined alleles by TALENs, each ODN included an additional, silent nucleotide replacement within the TALEN-Fus15B recognition sequence. TALEN-Fus15 mRNAs (95A type, 20 ng/μl) were co-injected with ODN^{R513G} or ODN^{P517L} into the pronuclei of one-cell embryos. We obtained 83 pups from the injections of ODN^{R513G} and 50 pups from ODN^{P517L} (Table 1), which were screened for mutations by HRMA of PCR products covering exon 15. The samples from 8 mice from ODN^{R513G} (9.6%) and 2 mice from ODN^{P517L} (4%) injections showed melting curves distinguished from the wild-type control (Figure S3) and were further analyzed by the subcloning and sequencing of each of the five PCR products. The founders derived from ODN^{R513G} injections harbored 14 modified *Fus* alleles (Figure 4A). Four founders contained the desired R513G replacement together with (F69, F70) or without (F29, F37) the silent replacement within the TALEN-Fus15B binding region. Three

Figure 3

A

```
              TALEN-Rik2A                    TALEN-Rik2B
C9orf72  GGATGTCGACTATCTGCCCCCCCACCATCTCCTGCTGTTGCCAAGACAGAGA
```

Founder	Sequence	Genotype
R10	GGATGTCGACTATCTGCCCCCCACC-TCTCCTGCTGTTGCCAAGACAGAGA	Δ1bp
R12a	GGATGTCGACTATCTGCCCCCCACC-TCTCCTGCTGTTGCCAAGACAGAGA	Δ1bp
R12b	GGATGTCGACTATCTGCCCCCCAC------CTGCTGTTGCCAAGACAGAGA	Δ6bp
R5	GGATGTCGACTATCTGCCCCCCCACCA-CTCCTGCTGTTGCCAAGACAGAGA	Δ1bp
R21	GGATGTCGACTATCTGCCCCCCAC------CTGCTGTTGCCAAGACAGAGA	Δ6bp
R24	GGATGTCGACTATCTGCCCCCCAC------CTGCTGTTGCCAAGACAGAGA	Δ6bp
R29	GGATGTCGACTATCTGCCCCC-A------CCTGCTGTTGCCAAGACAGAGA	Δ8/+1bp
R33	GGATGTCGACTATCTGCCCCCC---------TGCTGTTGCCAAGACAGAGA	Δ9bp
R18	GGATGTCGACTATCTGCCCCCCA----------CTGTTGCCAAGACAGAGA	Δ10bp
R23	GGATGTCGACTATCTGCC--------------------AAGACAGAGA	Δ23bp
R22	------------//-------------------TGTTGCCAAGACAGAGA	Δ36bp
R32	GGATGTCGACTATCTGCCCCCCCACCATTTCTCCTGCTGTTGCCAAGACAGA	+2bp

B

```
C9ORF72  MSTICPPPSPAVAKTEIALSG/456 aa/LMTF*  481aa
```

Founder	Predicted protein	
R10	MSTICPPPLLLLPRQRLL*	8 + 10 aa
R12a	MSTICPPPLLLLPRQRLL*	8 + 10 aa
R12b	MSTICPPP--AVAKTEIALSG/456 aa/LMTF*	Δ S9, P10 / 479 aa
R5	MSTICPPPLLLLPRQRLL*	8 + 10 aa
R21	MSTICPPP--AVAKTEIALSG/456 aa/LMTF*	Δ S9, P10 / 479 aa
R24	MSTICPPP--AVAKTEIALSG/456 aa/LMTF*	Δ S9, P10 / 479 aa
R29	MSTICPHLLLPRQRLL*	6 + 10 aa
R33	MSTICPP---AVAKTEIALSG/456 aa/LMTF*	Δ P8, S9, P10 / 478 aa
R18	MSTICPPLLPRQRLL*	7 + 8 aa
R23	MSTICQDRDCFKW*	5 + 8 aa
R22	--------------------/332 aa/LMTF*	Δ M1 - W145 /336 aa
R32	MSTICPPPFLLLLPRQRLL*	8 + 11 aa

C


```
             TALEN-Rik2A              TALEN-Rik2B
R23    GGATGTCGACTATCTGCC--------------------AAGACAGAGA
R23-15 GGATGTCGACTATCTGCC--------------------AAGACAGAGA
```

Figure 3 TALEN-induced *C9orf72* alleles. (A) Sequence comparison of the TALEN-Rik2 target region within exon 2 of *C9orf72* in comparison to mutant alleles amplified by PCR from tail DNA of the indicated founders. The start codon of *C9orf72* is underlined and the recognition sequences of TALENs are indicated. Nucleotide deletions and insertions are shown as red dashes and red letters, respectively. The genotype classifies mutant alleles as products of NHEJ-associated deletion (Δ) or insertion (+); alleles exhibiting reading frameshifts are shown in red. Founder R12 contained two mutant alleles showing the deletion of 1 or 6 bp, respectively. (B) Predicted protein sequences of TALEN-induced *C9orf72* alleles (start codon underlined). Upon the translation of the first five to eight wild-type codons, the mutant alleles R10, R12a, R5, R29, R18, R23, and R32 exhibit a reading frameshift, followed by a nonsense sequence of 8–11 residues (red letters) and a stop codon (asterisk). Allele R22 lost the start codon (Δ ATG) and may result in the complete loss of translation or in translational initiation at the downstream ATG codon 146 and the production of a truncated protein. The alleles R12b, R21, R24, and R33 show only deletions of codons 8–10 or 9–10 and preserve the downstream reading frame of *C9orf72*. (C) Melting analysis of triplicate PCR products from founder R23 (red curves, overlaid), its pup R23-15 (blue curves), and a wild-type C57BL/6 control (gray curves). The sequence analysis of cloned PCR products confirmed the germline transmission of the R23 allele.

founders (F18, F75, and F79) showed recombined R513G *Fus* alleles that included unintended single-nucleotide alterations (Figure 4A), likely resulting from ODN synthesis errors. Indeed, we noted that our ODN^{R513G} synthesis used for microinjection contained a substantial fraction (~1/3) of variant molecules, as determined by PCR, subcloning, and sequencing (data not shown). Furthermore, four of the founders harbored additional modified *Fus* alleles that underwent nucleotide deletions (F37b, F70b, F75d, and F5) or showed an unexpected nucleotide replacement within codon 512 (F69b). From the microinjection of ODN^{P517L} both founders harbored recombined *Fus* alleles, including the P517L and adjacent silent replacements (F4, F36a, Figure 4B). Founder F36 was mosaic for another recombined allele, including a 14-bp deletion (F36b) and a deletion allele that lost 12 bp (F36c).

For the establishment of *Fus* mutant lines we mated founders F29 (*Fus^{R513G}*, Figure 4C) and F36 (*Fus^{P517L}*, Figure 4D) to wild-type mice and genotyped their offspring by PCR and HRMA. Eight of 15 pups derived from F29 and 8 of 12 pups from F36 showed melting curves differing from the wild-type control and the cloning and sequencing of PCR products confirmed the germline transmission of the parental *Fus^{R513G}* (pup F29-24, Figure 4C) and *Fus^{P517L}* alleles (pup F36-13, Figure 4D). Five additional founders were mated to wild-type mice and transmitted modified *Fus* loci to their offspring, as confirmed by HRMA (Table S1).

These results show that TALENs and ODNs created recombined *Fus* loci in 6.8% of mice derived from microinjections (1 recombined founder per 15 pups, Table 1) and that mutations identified in the founders' tail DNA were faithfully transmitted through the germline. To further confirm the

Table 1 TALEN-mediated gene editing events

Microinjection experiment	TALEN mRNA concentration (ng/μl)	No. pups	No. mutant founders (%)	Founders' NHEJ events (%)	Founders' HR events (%)
1. TALEN-Rik2	90	51	21 (41.2)	21 (41.2)	—
2. TALEN-Fus15 + ODN^{R513G}	20	83	8 (9.6)	8 (9.6)	7 (8.4)
3. TALEN-Fus15 + ODN^{P517L}	20	50	2 (4)	2 (4)	2 (4)
TALEN-Fus15 $\sum$ =		133	10 (7.5)	10 (7.5)	9 (6.8)

Shown are mutant founder mice and mutant alleles obtained from the microinjection of Rik TALENs or Fus TALENs together with mutagenic ODNs into the pronuclei of one-cell embryos. The concentration of TALEN mRNAs and the number of pups obtained from embryo transfers are shown. Within these groups the overall frequency of TALEN-induced gene editing is indicated by the number of mice harboring mutant alleles (mutant founders), modified either by NHEJ or by HR events. Half of the founders derived from experiments 2 and 3 were mosaics, containing more than one modified allele. Therefore, the combined number of mice exhibiting alleles modified by NHEJ or HR exceeds the total number of mutant founders.

integrity of the targeted Fus^{R513G} locus we amplified genomic sequences covering 3.4 kb upstream of codon 513 and 3.2 kb of the downstream region, using tail DNA of the heterozygous Fus^{R513G} pup F29-24. The direct sequencing of both PCR products, representing molecules derived from the wild type and the Fus^{R513G} allele, revealed a uniform reading pattern of the *Fus* wild-type sequence, except for the C to G replacement within codon 513 that showed a mixed G/C peak (Figure S5). This result proves the genomic integrity of the Fus^{R513G} allele within a region of 6.6 kb centered on codon 513. To further analyze the functionality and transcription of the Fus^{R513G} allele we isolated mRNA from the tail of pup F29-24, prepared *Fus* cDNA, and PCR amplified a 341-bp region of the *Fus* transcript covering exons 14 and 15. The sequence analysis of cloned PCR products revealed spliced cDNA sequences including the R513G replacement, confirming the functionality of the Fus^{R513G} allele (Figure S4).

Analysis of TALEN off-target activity

TALENs may recognize genomic (off-target) sites, which are similar to the intended target sequence and cause undesired genetic modifications. To assess the frequency of such off-target events in mutants derived from TALEN microinjections, we analyzed for each pair of our TALENs five off-target sites (Table S2) (Doyle *et al.* 2012), using tail DNA from four *Fus* and two *C9orf72* founder mutants. PCR products covering these regions were analyzed by HRMA in comparison to a C57BL/6 wild-type control (Figure 5). Whereas the melting curves of all TALEN-Rik2 and of three TALEN-Fus15 off-target sites were identical to the controls, the PCR products from the *Fus* off-sites 1 and 3 were distinguished from the control. These PCR products were subcloned and the analysis of five sequences per sample revealed single-nucleotide substitutions that represent known polymorphisms in the genome of the inbred strains (Figure S6) we used for embryo production. Hence, we found no evidence for the presence of off-target mutations in founders derived from microinjections of our TALENs.

Discussion

Single-nucleotide polymorphisms leading to codon replacements within human genes are increasingly identified as disease-related mutations by high-throughput genomic analy-

sis such as exome sequencing. Genetic mouse models that recapitulate such mutations will be instrumental to studying the underlying disease mechanisms and to developing therapeutic interventions. We recently provided proof-of-principle that nucleotide and codon replacements can be directly introduced into the mouse genome by microinjection of TALEN mRNAs (15 ng/μl) and ODNs into the pronuclei of one-cell embryos (Wefers *et al.* 2013). For the *Rab38* locus we achieved a rate of 1.8% for targeted replacements and of 4.8% for NHEJ-mediated deletions, using as yet nonoptimized conditions. To enable the routine production of targeted mouse models at high efficiency, we aimed to enhance gene editing by increasing the incidence of TALEN-induced DSBs upon pronuclear delivery. High rates (>40%) of NHEJ-mediated deletions have been achieved by the microinjection of TALEN mRNAs into the embryonic cytoplasm (Sung *et al.* 2013), tolerating large volumes, but this route provides no option for the codelivery of DNA templates into the nucleus. Since pronuclei tolerate only minimal volumes and narrow injection capillaries, restricted for the delivery of a few picoliters, we sought to optimize the activity and concentration of the co-injected TALEN mRNAs. To this end we used mRNAs with template-coded poly(A) regions (95A) and found that pronuclear delivery at 90 ng/μl leads to the effective translation of a fluorescent reporter. As a validation of this protocol we found that deletions in *C9orf72* were induced in 41% of pups derived from injections of TALEN mRNAs at 90 ng/μl. For the targeting of *Fus* we used TALEN-95A mRNAs at a lower concentration (20 ng/μl) together with ODNs, comparable to the earlier targeting of *Rab38*, and found targeted replacements to occur at a rate of 6.8%. These rates of gene editing are four- to eightfold higher compared to our previous results from *Rab38*, suggesting that TALEN-95A mRNAs lead to enhanced mutagenesis. At these rates one or more targeted alleles can be obtained from a single day of microinjection, typically resulting in ∼25 pups if FVB-derived embryos are used for microinjection. TALENs have been further used to induce knockout mutations in embryos of the C57BL/6 inbred strains upon cytoplasmic delivery (Davies *et al.* 2013; Sung *et al.* 2013; Qiu *et al.* 2013). Therefore we are confident that it will be also possible to generate targeted mutations by the delivery of TALEN-95A mRNAs and targeting DNA molecules into the pronuclei of C57BL/6 embryos. Nevertheless, the number of live births from C57BL/6 embryos is about half compared to

A

Exon 15

FUS | G E H R Q D R R E R P Y *

TALEN-Fus15A   TALEN-Fus15B

Fus   TTTCTTTCAGGGGCGAGCACAGACAGGAT**C**GCAGGGGAGAG**G**CCATATTAGCC

ODN^{R513G} TTTCTTTCAGGGGCGAGCACAGACAGGAT**GG**CAGGGGAGAGA**A**CCATATTAGCC

R513G

Founder		Genotype
F29	TTTCTTTCAGGGGCGAGCACAGACAGGATGGCAGGGGAGAGGCCATATTAGCC	HR
F37a	TTTCTTTCAGGGGCGAGCACAGACAGGATGGCAGGGGAGAGGCCATATTAGCC	HR
F37b	------------------------------GGAGAGGCCATATTAGCC	Δ57bp
F69a	TTTCTTTCAGGGGCGAGCACAGACAGGATGGCAGGGGAGAGACCATATTAGCC	HR
F69b	TTTCTTTCAGGGGCGAGCACAGACAGGCTGGCAGGGGAGAGACCATATTAGCC	HR
F70a	TTTCTTTCAGGGGCGAGCACAGACAGGATGGCAGGGGAGAGACCATATTAGCC	HR
F70b	TTTCTTTCAGGGGCGAGCACAGACA-GATCGCAGGGGAGAGGCCATATTAGCC	Δ1bp
F75a	TTTCTTTCAGGGGCGAGCACAGACAGGATGGAAGGGGAGAGGCCATATTAGCC	HR
F75b	TTTTCTTTCAGGGGCGAGCACAG-CAGGATGGCAGGGGAGAGGCCATATTAGCC	HR
F75c	TTTCTTTCAGGGGCGAGCACAGACAAGGATGGAAGGGGAGAGGCCATATTAGCC	HR
F75d	TTTCTTTCAGGGGCGAGCA------------CAGGGGAGAGGCCATATTAGCC	Δ12bp
F18	TTTCTTTCAGGGGCGAGCACAGACCAGGATGGCAGGGGAGAGACCATATTAGCC	HR
F79	TTTCTTTCAGGGGCGAGCACA-ACAGGATGGCAGGGGAGAGGCCATATTAGCC	HR
F5	TTTCTTTCAGGGGCGAGCA--------------------CATATTAGCC	Δ23bp

B

P517L

ODN^{P517L} TTTCTTTCAGGGGCGAGCACAGACAGGATCGCAGGGGAGAG**ACT**ATATTAGCC

F4	TTTCTTTCAGGGGCGAGCACAGACAGGATCGCAGGGGAGAGACTATATTAGCC	HR
F36a	TTTCTTTCAGGGGCGAGCACAGACAGGATCGCAGGGGAGAGACTATATTAGCC	HR
F36b	TTTCTTTCAGGGGCGAGCA-------------GGGAGAGACTATATTAGCC	HR/Δ14bp
F36c	TTTCTTTCAGGGGCGAGCAC-----------AGGGAGAGGCCATATTAGCC	Δ12bp

C

Normalized Fluorescence vs Temperature [°C]
- F29 (red)
- F29-24 (blue)
- F29-25 (WT) (gray)

F29 | AGACAGGAT**G**GCAGGGGAGAGGCCATATTAG
F29-24 | AGACAGGAT**G**GCAGGGGAGAGGCCATATTAG
FUS^{R513G} | R Q D **G** R E R P Y *

D

Normalized Fluorescence vs Temperature [°C]
- F36 (red)
- F36-13 (blue)
- F36-12 (WT) (gray)

F36a | CACAGACAGGATCGCAGGGGAGAG**ACT**ATATTAG
F36-13 | CACAGACAGGATCGCAGGGGAGAG**ACT**ATATTAG
FUS^{P517L} | H R Q D G R E R **L** Y *

Figure 4 Generation of *Fus^{R513G}* and *Fus^{P517L}* mutants. (A and B) Sequence comparison of the TALEN target region covering the *Fus* exon 15, of ODN^{R513G}, ODN^{P517L}, and cloned PCR products amplified from tail DNA of ODN^{R513G} (A) and ODN^{P517L} (B) founder mutants, identified by HRMA. The exon 15 coded FUS sequence, the TALEN binding sites, and codons 513 and 517 are indicated; nucleotides deviating from wild type (green background) are shown in red on a yellow background. Nucleotide deletions or insertions are shown as red dashes or red letters. The genotype describes the mutant alleles as a product of homologous recombination (HR) or NHEJ-associated deletion (Δ) or insertion (+). (C and D) Melting analysis of duplicate PCR products from founder F29 (ODN^{R513G}) (C) (red curves) its pup F29-24 (blue curves) and founder F36 (ODN^{P517L}) (D) (red curves) and its pup F36-13 in comparison to wild-type controls (gray curves). The sequence analysis of cloned PCR products from pups F29-24 and F36-13 confirmed the germline transmission of the *Fus^{R513G}* and *Fus^{P517L}* alleles.

that from the FVB strain such that 2 days of microinjection will be required to recover 25 pups.

Several *Fus* founders recombined with the 140-nt ODN^{R513G} showed unintended nucleotide insertions, deletions, or replacements. These alterations likely result from the error-prone synthesis of oligonucleotides and identify ODN quality and length as important factors to optimize the net rate of correctly modified alleles. Since the synthesis of shorter ODNs correlates with an increased fraction of correct molecules, it will be of future interest to determine the *in vivo* recombination rate of ODNs in relation to the molecules' length. In mammalian cell lines it has been shown that a minimum of 50 bp of homology is sufficient to achieve a high recombination rate (Chen *et al.* 2011).

As previously observed for ZFN- and TALEN-induced mutagenesis, a part of our *Fus* and *C9orf72* founders were mosaic for one or more modified alleles, resulting from mul-tiple, independent editing events that may occur before or after the first or second cycle of genome replication. Since modified loci are first identified in the founder's tail DNA, it is essential that the same alleles are present in the germ cell population to establish breeding colonies. Each of eight mated founders transmitted mutant alleles to 10–67% of its progeny, thereby confirming the contribution of mutant cells to the germline. Furthermore, the resequencing of *Fus* and *C9orf72* alleles from heterozygous pups confirmed the identity to the parental loci, indicating that the analysis of tail DNA is predictive of the mutational spectrum in the germline.

At present little is known about the potential processing of sites that are similar to the intended TALEN target sequence and which degree of sequence divergence is necessary to exclude off-target recognition. Using tail DNA from *Fus* and *C9orf72* founders we analyzed five potential off-target sites
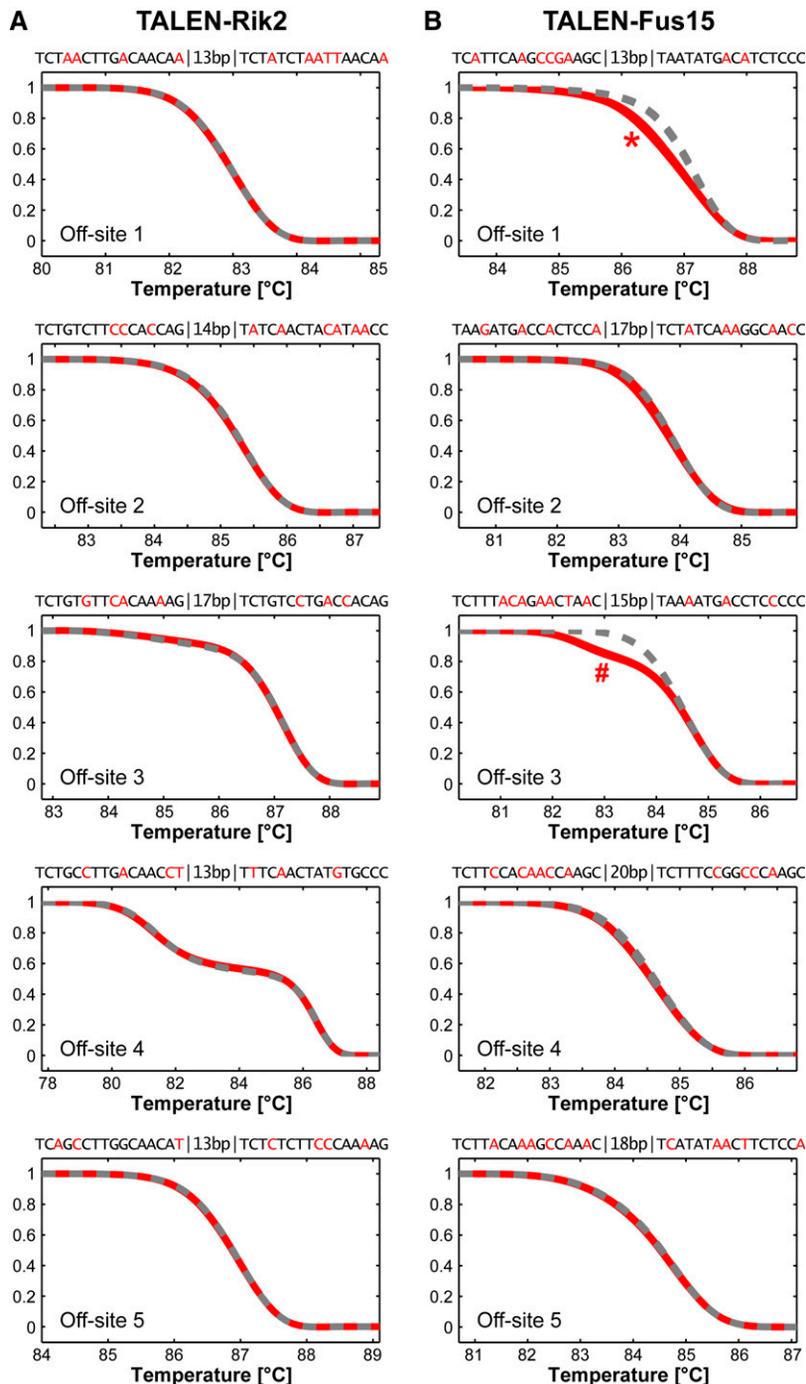
Figure 5 Genome-wide off-target analysis of TALEN-Rik2 and TALEN-Fus15. (A and B) Melting analysis of predicted off-target sites of TALEN-Rik2 (A) and TALEN-Fus15 (B) in wild-type and mutant founder mice (R5, R23 and F5, F29, F4, F36). The potential TALEN target sequences, spacer length, and mismatches (red letters) to the *Fus* and *C9orf72* target sites are indicated. HRMA revealed no differences from the C57BL/6 wild-type control (dashed gray curves) and founder-derived PCR products (red curves), except for the *Fus*15 off sites 1 (*) and 3 (#), which were identified as polymorphisms present in the different genetic backgrounds. Details on these polymorphisms are shown in Figure S6.

by HRMA and found no indication for processing at these sites. Since for TALEN-Fus15 and Rik2 the closest genomic off sites are distinguished by seven or more nucleotide substitutions, our results suggest that under this condition TALENs do not cause modifications at sites that are predictable with the known binding code. Whether TALENs also recognize other, presently unpredictable target sites requires further clarification by whole-genome sequencing.

Besides the one-time generation of mutant alleles by embryo manipulation, the genotyping of mutant offspring adds a constant workload to the maintenance of breeding colonies. Mutant alleles harboring nucleotide replacements cannot be identified through the mere size of PCR products. Therefore, present PCR genotyping protocols require differentiating between wild-type and mutant alleles by digestion with restriction enzymes and gel electrophoresis. This rationale often requires the incorporation of additional, undesired nucleotide substitutions to create or delete enzyme recognition sites. All of these drawbacks are relieved by automated HRMA that requires just the melting analysis of PCR reactions. Our characterization of mutant *Fus* and *C9orf72* founders and their offspring validated HRMA as a universal

and sensitive tool for the identification and genotyping of TALEN-induced nucleotide replacements and deletions. By the inclusion of wild-type control DNA it will be further possible to differentiate heterozygous and homozygous mutant genotypes by HRMA.

Taken together, our advanced TALEN mutagenesis and analysis procedure enables the accelerated, routine production of new genetic mouse models. Since TALENs combined with ODNs allow genome-wide targeting at high precision, this technology supports expedited *in vivo* analysis of newly discovered disease-associated mutations.

Acknowledgments

Literature Cited

Ash, P. E. A., K. F. Bieniek, T. F. Gendron, T. Caulfield, W.-L. Lin *et al.*, 2013 Unconventional translation of C9ORF72 GGGGCC expansion generates insoluble polypeptides specific to c9FTD/ALS. Neuron 77: 639–646.

Boch, J., H. Scholze, S. Schornack, A. Landgraf, S. Hahn *et al.*, 2009 Breaking the code of DNA binding specificity of TAL-type III effectors. Science 326: 1509–1512.

Bosco, D. A., N. Lemay, H. K. Ko, H. Zhou, C. Burke *et al.*, 2010 Mutant FUS proteins that cause amyotrophic lateral sclerosis incorporate into stress granules. Hum. Mol. Genet. 19: 4160–4175.

Capecchi, M. R., 2005 Gene targeting in mice: Functional analysis of the mammalian genome for the twenty-first century. Nat. Rev. Genet. 6: 507–512.

Carbery, I. D., D. Ji, A. Harrington, V. Brown, E. J. Weinstein *et al.*, 2010 Targeted genome modification in mice using zinc-finger nucleases. Genetics 186: 451–459.

Cermak, T., E. L. Doyle, M. Christian, L. Wang, Y. Zhang *et al.*, 2011 Efficient design and assembly of custom TALEN and other TAL effector-based constructs for DNA targeting. Nucleic Acids Res. 39: e82.

Chen, F., S. M. Pruett-Miller, Y. Huang, M. Gjoka, K. Duda *et al.*, 2011 High-frequency genome editing using ssDNA oligonucleotides with zinc-finger nucleases. Nat. Methods 8: 753–755.

Court, D. L., J. A. Sawitzke, and L. C. Thomason, 2002 Genetic engineering using homologous recombination. Annu. Rev. Genet. 36: 361–388.

Davies, B., G. Davies, C. Preece, R. Puliyadi, D. Szumska *et al.*, 2013 Site specific mutation of the Zic2 locus by microinjection of TALEN mRNA in mouse CD1, C3H and C57BL/6J oocytes. PLoS ONE 8: e60216.

DeJesus-Hernandez, M., I. R. Mackenzie, B. F. Boeve, A. L. Boxer, M. Baker *et al.*, 2011 Expanded GGGGCC hexanucleotide repeat in noncoding region of C9ORF72 causes chromosome 9p-linked FTD and ALS. Neuron 72: 245–256.

Dormann, D., and C. Haass, 2013 Fused in sarcoma (FUS): an oncogene goes awry in neurodegeneration. Mol. Cell. Neurosci. DOI: 10.1016/j.mcn.2013.03.006.

Doyle, E. L., N. J. Booher, D. S. Standage, D. F. Voytas, V. P. Brendel *et al.*, 2012 TAL Effector-Nucleotide Targeter (TALE-NT) 2.0: tools for TAL effector design and target prediction. Nucleic Acids Res. 40: W117–W122.

Flisikowska, T., I. S. Thorey, S. Offner, F. Ros, V. Lifke *et al.*, 2011 Efficient immunoglobulin gene disruption and targeted replacement in rabbit using zinc finger nucleases. PLoS ONE 6: e21045.

Gal, J., J. Zhang, D. M. Kwinter, J. Zhai, H. Jia *et al.*, 2011 Nuclear localization sequence of FUS and induction of stress granules by ALS mutants. Neurobiol. Aging 32: 2323.e27–40.

Geurts, A. M., G. J. Cost, Y. Freyvert, B. Zeitler, J. C. Miller *et al.*, 2009 Knockout rats via embryo microinjection of zinc-finger nucleases. Science 325: 433.

Hasty, P., A. Abuin, and A. Bradley, 2000 Gene targeting, principles, and practice in mammalian cells, pp. 1–35 in *Gene Targeting: A Practical Approach*, *The Practical Approach Series*, edited by A. Joyner. Oxford University Press, Oxford.

Hicks, G. G., N. Singh, A. Nashabi, S. Mai, G. Bozek *et al.*, 2000 Fus deficiency in mice results in defective B-lymphocyte development and activation, high levels of chromosomal instability and perinatal death. Nat. Genet. 24: 175–179.

Ito, D., M. Seki, Y. Tsunoda, H. Uchiyama, and N. Suzuki, 2011 Nuclear transport impairment of amyotrophic lateral sclerosis-linked mutations in FUS/TLS. Ann. Neurol. 69: 152–162.

Kabashi, E., V. Bercier, A. Lissouba, M. Liao, E. Brustein *et al.*, 2011 FUS and TARDBP but not SOD1 interact in genetic models of amyotrophic lateral sclerosis. PLoS Genet. 7: e1002214.

Kino, Y., C. Washizu, E. Aquilanti, M. Okuno, M. Kurosawa *et al.*, 2011 Intracellular localization and splicing regulation of FUS/TLS are variably affected by amyotrophic lateral sclerosis-linked mutations. Nucleic Acids Res. 39: 2781–2798.

Kwiatkowski, Jr., T. J., D. A. Bosco, A. L. Leclerc, E. Tamrazian, C. R. Vanderburg *et al.*, 2009 Mutations in the FUS/TLS gene on chromosome 16 cause familial amyotrophic lateral sclerosis. Science 323: 1205–1208.

Lieber, M. R., 2010 The mechanism of double-strand DNA break repair by the nonhomologous DNA end-joining pathway. Annu. Rev. Biochem. 79: 181–211.

Liew, M., R. Pryor, R. Palais, C. Meadows, M. Erali *et al.*, 2004 Genotyping of single-nucleotide polymorphisms by high-resolution melting of small amplicons. Clin. Chem. 50: 1156–1164.

Meyer, M., M. H. de Angelis, W. Wurst, and R. Kuhn, 2010 Gene targeting by homologous recombination in mouse zygotes mediated by zinc-finger nucleases. Proc. Natl. Acad. Sci. USA 107: 15022–15026.

Miller, J. C., S. Tan, G. Qiao, K. A. Barlow, J. Wang *et al.*, 2011 A TALE nuclease architecture for efficient genome editing. Nat. Biotechnol. 29: 143–148.

Mori, K., S.-M. Weng, T. Arzberger, S. May, K. Rentzsch *et al.*, 2013 The C9orf72 GGGGCC repeat is translated into aggregating dipeptide-repeat proteins in FTLD/ALS. Science 339: 1335–1338.

Moscou, M. J., and A. J. Bogdanove, 2009   A simple cipher governs DNA recognition by TAL effectors. Science 326: 1501.

Porteus, M. H., and D. Carroll, 2005   Gene targeting using zinc finger nucleases. Nat. Biotechnol. 23: 967–973.

Qiu, Z., M. Liu, Z. Chen, Y. Shao, H. Pan *et al.*, 2013   High-efficiency and heritable gene targeting in mouse by transcription activator-like effector nucleases. Nucleic Acids Res. 41: e120.

Renton, A. E., E. Majounie, A. Waite, J. Simón-Sánchez, S. Rollinson *et al.*, 2011   A hexanucleotide repeat expansion in C9ORF72 is the cause of chromosome 9p21-linked ALS-FTD. Neuron 72: 257–268.

Reyon, D., S. Q. Tsai, C. Khayter, J. A. Foden, J. D. Sander *et al.*, 2012   FLASH assembly of TALENs for high-throughput genome editing. Nat. Biotechnol. 30: 460–465.

Rouet, P., F. Smih, and M. Jasin, 1994   Expression of a site-specific endonuclease stimulates homologous recombination in mammalian cells. Proc. Natl. Acad. Sci. USA 91: 6064–6068.

San Filippo, J., P. Sung, and H. Klein, 2008   Mechanism of eukaryotic homologous recombination. Annu. Rev. Biochem. 77: 229–257.

Sasayama, H., M. Shimamura, T. Tokuda, Y. Azuma, T. Yoshida *et al.*, 2012   Knockdown of the Drosophila fused in sarcoma (FUS) homologue causes deficient locomotive behavior and shortening of motoneuron terminal branches. PLoS ONE 7: e39483.

Sung, Y. H., I.-J. Baek, D. H. Kim, J. Jeon, J. Lee *et al.*, 2013   Knockout mice created by TALEN-mediated gene targeting. Nat. Biotechnol. 31: 23–24.

Taylor, J. P., 2013   Neuroscience. RNA that gets RAN in neurodegeneration. Science 339: 1282–1283.

Wefers, B., M. Meyer, S. Hensler, S. Panda, O. Ortiz *et al.*, 2012   Gene editing in one-cell embryos by zinc-finger and TAL nucleases. Curr. Protoc. Mouse Biol. 2: 347–364.

Wefers, B., M. Meyer, O. Ortiz, M. Hrabé de Angelis, J. Hansen *et al.*, 2013   Direct production of mouse disease models by embryo microinjection of TALENs and oligodeoxynucleotides. Proc. Natl. Acad. Sci. USA 110: 3782–3787.

Communicating editor: D. Voytas

Generation of targeted mouse mutants by embryo microinjection of TALEN mRNA

Benedikt Wefers[1], Sudeepta K Panda[1,2], Oskar Ortiz[1], Christina Brandl[1,2], Svenja Hensler[1,2], Jens Hansen[1], Wolfgang Wurst[1–4] & Ralf Kühn[1,2]

[1]Institute of Developmental Genetics, Helmholtz Zentrum München, German Research Center for Environmental Health, Munich, Germany. [2]Technische Universität München, Freising-Weihenstephan, Germany. [3]Deutsches Zentrum für Neurodegenerative Erkrankungen (DZNE), Munich, Germany. [4]Max Planck Institute of Psychiatry, Munich, Germany. Correspondence should be addressed to R.K. (ralf.kuehn@helmholtz-muenchen.de).

Genetically engineered mice are instrumental for the analysis of mammalian gene function in health and disease. As classical gene targeting, which is performed in embryonic stem (ES) cell cultures and generates chimeric mice, is a time-consuming and labor-intensive procedure, we recently used transcription activator–like (TAL) effector nucleases (TALENs) for mutagenesis of the mouse genome directly in one-cell embryos. Here we describe a stepwise protocol for the generation of knock-in and knockout mice, including the selection of TALEN-binding sites, the design and construction of TALEN coding regions and of mutagenic oligodeoxynucleotides (ODNs) and targeting vectors, mRNA production, embryo microinjection and the identification of modified alleles in founder mutants and their progeny. After a setup time of 2–3 weeks of hands-on work for TALEN construction, investigators can obtain first founder mutants for genes of choice within 7 weeks after embryo microinjections.

INTRODUCTION

Mice are the prime mammalian model for studying gene function *in vivo*, on the basis of the creation of targeted knockout or knock-in mutations by homologous recombination (HR) in ES cells[1]. As ES cell–based gene targeting and the generation of germ-line chimeras is a time- and labor-intensive procedure, we sought a fast and simple alternative for introducing mutations directly into the genome of one-cell embryos with the assistance of sequence-specific nucleases. Double-strand breaks (DSBs) induced by such nucleases at selected target sites increase the rate of HR by several orders of magnitude[2,3]. Initially, we provided evidence for this approach by using zinc-finger nucleases (ZFNs) together with gene targeting vectors or synthetic ODNs[4,5]. However, highly active ZFNs are hard to build and cannot address every target sequence; in comparison, DNA recognition by TAL effector proteins and the design of customized TALENs (refs. 6,7; **Fig. 1a**) provide a versatile alternative for targeting the mouse genome. The modular nature of the TAL DNA-binding code enables the simple construction of TALEN-coding regions and the production of synthetic mRNAs within 2 weeks. When mRNAs are microinjected together with targeting DNA molecules into the pronuclei of one-cell embryos, TALENs are translated, creating DSBs in the target genes that lead to their modification through DNA repair mechanisms (**Fig. 1b**). Mice obtained after 7 weeks from the reimplanted embryos are genotyped to identify individual founders harboring the desired mutation. These founders are further mated for the germ-line transmission of the mutant allele, enabling the establishment of mutant strains. By following the step-by-step procedures of this protocol, researchers can generate knockout or knock-in mutants for their genes of interest rapidly and efficiently, without the use of ES cells.

Gene editing in mouse embryos using TALENs

Natural TAL effector proteins are bacterial transcriptional activators that bind to promoter regions of their host plant cells via a central repeat domain, enabling the recognition of specific DNA sequences. Each repeat motif comprises 34 highly conserved amino acids, except for the repeat variable di-residues (RVDs) at positions 12 and 13 (**Fig. 1a**; refs. 8–10). The di-residues of each repeat mediate the recognition of a single, specified nucleotide of a DNA target sequence, according to the four-RVD code shown in **Figure 1a** (refs. 6,7,11,12). TAL repeat domains are flanked by an invariable N-terminal half repeat (repeat 0.5) positioned toward a thymidine that defines the first nucleotide of each target sequence. The assembly of TAL repeats into a functional DNA-binding domain requires an additional C-terminal half repeat, as well as flanking N- and C-terminal TAL effector–derived sequences[13]. According to the four-RVD code, these elements can be assembled into new repeat arrays that recognize any target sequence preceded by a thymidine, enabling the simple construction of vectors coding for customized DNA-binding proteins[6,13,14]. On the basis of previous experience with ZFNs, TAL effectors could be readily adapted into TALENs for gene editing by fusion with the FokI nuclease domain[13–15]. The bipartite target regions include two TALEN recognition sequences located on opposite DNA strands to enable the dimerization of two FokI nuclease domains, leading to DSB formation (**Fig. 1b**).

To achieve gene editing in mice, we transcribe *in vitro* TALEN mRNAs from the coding vectors and introduce them by microinjection into the pronuclei of one-cell embryos (**Fig. 1b**). Upon the translation of TALEN mRNAs into proteins, the induction of DSBs enforces the repair of target sites by HR or by the nonhomologous end joining (NHEJ) pathway (**Fig. 1c**). Targeted gene modifications are obtained through HR[16] with co-injected ODNs or gene targeting vectors that include homology sequences and serve as repair templates. Alternatively, DSBs can be closed by template-free NHEJ repair[17] that is frequently associated with the loss of nucleotides, causing frameshift (knockout) mutations within coding regions. Both repair mechanisms are not mutually exclusive in the microinjected nucleus, and alleles harboring both knock-in and knockout mutations are found within a group of microinjected embryos. Upon the transfer of microinjected embryos into foster mothers, 25–50 pups are obtained that must

Gene Editing in One-Cell Embryos by Zinc-Finger and TAL Nucleases

Benedikt Wefers,[1] Melanie Meyer,[1,2] Svenja Hensler,[1,2] Sudeepta Panda,[1,2] Oskar Ortiz,[1] Wolfgang Wurst,[1,2,3,4] and Ralf Kühn[1,2]

[1]Helmholtz Center Munich, Institute for Developmental Genetics Munich, Germany
[2]Chair for Developmental Genetics, Technische Universität München, Munich, Germany
[3]Max Planck Institute of Psychiatry, Molecular Neurogenetics, Munich, Germany
[4]Deutsches Zentrum für Neurodegenerative Erkrankungen, Standort München, Munich, Germany

ABSTRACT

Gene targeting by sequence-specific nucleases in one-cell embryos provides an expedited mutagenesis approach in rodents. This technology has been recently established to create knockout and knockin mutants through sequence deletion or sequence insertion. This article provides protocols for the preparation and microinjection of nuclease mRNA and targeting vector DNA into fertilized mouse eggs. Furthermore, we provide guidelines for genotyping the desired mouse mutants. *Curr. Protoc. Mouse Biol.* 2:347-364 © 2012 by John Wiley & Sons, Inc.

Keywords: pronucleus injection • gene targeting • mouse mutant • zinc-finger nuclease • TAL nuclease • homologous recombination

INTRODUCTION

This article describes the microinjection of gene-specific nuclease mRNA and targeting vector DNA into one-cell mouse embryos. This technique makes it possible to produce targeted mouse mutants in a single step by stimulating homologous recombination with the paternal or maternal pronuclear genomes. We provide step-by-step protocols for the preparation of injection buffer (Basic Protocol 1), nuclease mRNA (Basic Protocol 2), and targeting vector DNA (Basic Protocol 3), and the setup of these components into aliquots for microinjection (Basic Protocol 4). These are followed by protocols for the microinjection of one-cell embryos (Basic Protocol 5) and for genotyping of nuclease-induced mutants (Basic Protocol 6). The protocol section is preceded by an introduction to nuclease technology and followed by a discussion of strategies for genotyping offspring to identify the desired mutants.

Strategic Planning and Experimental Design

Gene targeting is routinely applied in embryonic stem (ES) cells to modify the mouse genome, and has established the mouse as the most commonly used genetic animal model (Capecchi, 2005). Gene targeting in ES cells relies on spontaneously occurring homologous recombination (HR) of a gene-targeting vector with its chromosomal counterpart. The absolute frequency of these events in ES cells is low, and spontaneous HR is antagonized by the more frequent event of random vector integration. Therefore, gene targeting in ES cells requires the inclusion of selection marker genes in targeting vectors and the isolation of drug-resistant ES cell clones. Usually, genotyping of several hundred colonies is required to identify a few recombined ES cell clones among the majority of clones harboring random vector integrations. Recombined ES cells are subsequently